

MICROCOPY RESOLUTION TEST CHART
NATIONAL BUREAU OF STANDARDS-1963-A

2

NAVAL POSTGRADUATE SCHOOL Monterey, California



AD-A 150 784

THESIS

THE IMPLICIT FINITE-DIFFERENCE (IFD)
ACOUSTIC MODEL
IN A SHALLOW WATER ENVIRONMENT

by

Mark E. Kosnik

June 1984

Thesis Co-advisors:

J.V. Sanders
C.R. Dunlap

Approved for public release; distribution unlimited

DTIC
ELECTE
MAR 4 1985

S
D

DTIC FILE COPY

85 : 02 19 079

UNCLASSIFIED

SECURITY CLASSIFICATION OF THIS PAGE (When Data Entered)

REPORT DOCUMENTATION PAGE		READ INSTRUCTIONS BEFORE COMPLETING FORM
1. REPORT NUMBER	2. GOVT ACCESSION NO.	3. RECIPIENT'S CATALOG NUMBER
4. TITLE (and Subtitle) The Implicit Finite-Difference (IFD) Acoustic Model in a Shallow Water Environment		5. TYPE OF REPORT & PERIOD COVERED Master's Thesis June 1984
7. AUTHOR(s) Mark E. Kosnik		6. PERFORMING ORG. REPORT NUMBER
9. PERFORMING ORGANIZATION NAME AND ADDRESS Naval Postgraduate School Monterey, California 93943		8. CONTRACT OR GRANT NUMBER(s)
11. CONTROLLING OFFICE NAME AND ADDRESS Naval Postgraduate School Monterey, California 93943		10. PROGRAM ELEMENT, PROJECT, TASK AREA & WORK UNIT NUMBERS
14. MONITORING AGENCY NAME & ADDRESS (if different from Controlling Office)		12. REPORT DATE June 1984
		13. NUMBER OF PAGES 128
		15. SECURITY CLASS. (of this report)
		15a. DECLASSIFICATION/DOWNGRADING SCHEDULE
16. DISTRIBUTION STATEMENT (of this Report) Approved for public release; distribution unlimited		
17. DISTRIBUTION STATEMENT (of the abstract entered in Block 20, if different from Report)		
18. SUPPLEMENTARY NOTES (48 1472E)		
19. KEY WORDS (Continue on reverse side if necessary and identify by block number) Pressure Amplitude, Trapped Normal Mode Propagation, Shallow Water Acoustics, and Ocean Modeling.		
20. ABSTRACT (Continue on reverse side if necessary and identify by block number) In this thesis An implicit finite-difference (IFD) computer model was developed by Jaeger to solve the parabolic equation. The model preserves continuity of pressure and the normal component of particle velocity at the ocean bottom where there is an interface between media with different sound speeds and densities. This feature was implemented to make the model more accurate.		

Accession For	
NTIS GRA&I	<input checked="" type="checkbox"/>
DTIC TAB	<input type="checkbox"/>
Unannounced	<input type="checkbox"/>
Justification	
By _____	
Distribution/	
Availability Codes	
Dist	Avail and/or Special
A-1	

copy inspected

DD FORM 1 JAN 73 1473

EDITION OF 1 NOV 69 IS OBSOLETE
S/N 0102-LF-014-6601

UNCLASSIFIED
SECURITY CLASSIFICATION OF THIS PAGE (When Data Entered)

(cont.)

in a shallow water environment. The IFD performance in a shallow water environment is analyzed. The IFD results are compared with those of two other models and analyzed in light of basic physical reasoning. In addition, a single sloping ocean bottom is modeled in an experimental tank so that the measured pressure field can also be compared to IFD model results. Originator - Supplied keywords include:

(to 1473A)

B

Approved for public release; distribution unlimited.

The Implicit Finite-Difference (IFD)
Acoustic Model
in a Shallow Water Environment

by

Mark E. Kcsnik
Lieutenant, United States Navy
E.B.A., University of Notre Dame, 1973

Submitted in partial fulfillment of the
requirements for the degree of

MASTER OF SCIENCE IN METEOROLOGY AND OCEANOGRAPHY

from the

NAVAL POSTGRADUATE SCHOOL
June 1984

Author:

Mark E. Kcsnik

Approved by:

James V. Saunders

Thesis Co-Advisor

Calvin L. Dunlap

Thesis Co-Advisor

Christopher G. McIvor

Chairman, Department of Oceanography

J. H. Dyer

Dean of Science and Engineering

ABSTRACT

An implicit finite-difference (IFD) computer model was developed by Jaeger to solve the parabolic equation. The model preserves continuity of pressure and the normal component of particle velocity at the ocean bottom where there is an interface between media with different sound speeds and densities. This feature was implemented to make the model more accurate in a shallow water environment. The IFD performance in a shallow water environment is analyzed. The IFD results are compared with those of two other models and analyzed in light of basic physical reasoning. In addition, a simple sloping ocean bottom is modeled in an experimental tank so that the measured pressure field can also be compared to IFD model results.

TABLE OF CONTENTS

I. INTRODUCTION 10

II. THE IFD COMPUTER MODEL 12

 A. BACKGROUND 12

 B. THE COMPUTER MODEL 13

 C. MODEL PRELIMS/MODIFICATIONS 14

 D. MODEL VERIFICATION 18

 1. Comparison with Jaeger Model Run 18

 2. Comparison with Jensen and Kuperman
 Model Run 19

 3. Comparison with Coppens, Humphries and
 Sanders Model Run 28

 4. Comparison with Physical Reasoning 30

 5. Verification Summary 40

III. LABORATORY MEASUREMENTS 42

 A. BACKGROUND 42

 B. EXPERIMENTAL DESIGN 42

 1. The Tark 42

 2. Signal Generating/Receiving Equipment 44

 C. MEASUREMENT PROCEDURES 47

IV. MODEL RESULT COMPARISONS WITH LABORATORY
MEASUREMENTS 53

 A. INTRODUCTION 53

 B. THE GENERAL ANALYSIS 53

 C. THE DETAILED ANALYSIS 64

V. CONCLUSIONS/RECOMMENDATIONS 75

 A. CONCLUSIONS 75

1. Performance of the IFD Model	75
2. Modeling/Measurement Procedures	76
B. RECOMMENDATIONS	76
APPENDIX A: REVISED IFD PROGRAM LISTING	78
APPENDIX B: TL CONTCUR PLOT PROGRAM LISTING	113
APPENDIX C: RUNNING THE CONTCUR PLOT ON THE NPS COMPUTER	115
A. INTRODUCTION	115
B. COPYING THE FILE FOR USE	115
C. RUNNING THE PROGRAM	115
APPENDIX D: SOURCE DEPTH SENSITIVITY ANALYSIS	117
BIBLIOGRAPHY	125
INITIAL DISTRIBUTION LIST	127

LIST OF FIGURES

2.1	Jaeger's Deep-to-Shallow Water Case	19
2.2	Jensen and Kuperman Sloping Bottom Case	20
2.3	IFL and JKM Comparison at a Range of 2.5 Km	22
2.4	IFL and JKM Comparison at a Range of 5.0 Km	23
2.5	IFL and JKM Comparison at a Range of 7.5 Km	24
2.6	IFL and JKM Comparison at a Range of 10.0 Km	25
2.7	IFL and JKM Comparison at a Range of 12.5 Km	26
2.8	10 Degree Simple Sloping Bottom Case	29
2.9	IFL and CHSM Comparison at the Apex	31
2.10	IFL TL Contours (db) from the Source to 604 Meters	33
2.11	IFL TL Contours (db) from 600 to 1350 Meters	34
2.12	IFL TL Contours (db) from 1350 to 2100 Meters	35
2.13	IFL TL Contours (db) from 1550 to 2300 Meters	36
2.14	Normal Mode Propagation in a Wedge Shaped Ocean	39
3.1	Experimental Tank Set Up	43
3.2	Electronic Equipment Schematic	46
3.3	Pulse Length Analysis at 3.0X	49
3.4	Pulse Length Analysis at 10.4X	50
3.5	Pulse Length Analysis at 10.4X	51
4.1	Comparison of Results at 1.0X	54
4.2	Comparison of Results at 2.1X	55
4.3	Comparison of Results at 3.1X	56
4.4	Comparison of Results at 4.2X	57
4.5	Comparison of Results at 5.2X	59
4.6	Comparison of Results at 6.2X	59
4.7	Comparison of Results at 7.3X	60

4.8	Comparison of Results at 8.3X	61
4.9	Comparison of Results at 9.4X	62
4.10	Comparison of Results at 10.4X	63
4.11	Comparison of Results at 0.7X	65
4.12	Comparison of Results at 0.8X	66
4.13	Comparison of Results at 1.0X	67
4.14	Comparison of Results at 1.3X	68
4.15	Comparison of Results at 1.5X	69
4.16	Comparison of Results at 1.7X	70
4.17	Comparison of Results at 1.9X	71
4.18	Comparison of Results at 2.1X	72
4.19	Comparison of Results at 2.3X	73
E.1	Source Sensitivity Analysis at 1.0X	119
E.2	Measurements with Source Depth of 5, 7, and 9 Cm	120
E.3	Measurements with Source Depth of 11, 13, and 15 Cm	121
E.4	Measurements with Source Depth of 17, 19, and 21 Cm	122
E.5	Measurements with Source Depth of 23, 25, and 27 Cm	123
E.6	Measurements with Source Depth of 29 and 31 Cm	124

ACKNOWLEDGEMENTS

The author thanks LCDR James Nelson, USN, for his advice and assistance in developing many of the graphics plotting programs. Appreciation is also due LT Patrick LeSesne, USCG, for his many long hours spent assisting in the laboratory while compiling the experimental data. Thanks are also due to Professor Calvin Dunlap for his review of the thesis.

The author also expresses his appreciation to Dr. Alan E. Coppens for his advice and clarification given to the theoretical aspects of the thesis. Finally, the author thanks Dr. James V. Sanders for his time and effort in assisting in all aspects of research and thesis preparation. Without the knowledge, patience, and advice of the Coppens and Sanders team this thesis would not have been possible.

I. INTRODUCTION

A variety of acoustic models exist to predict transmission loss. Each of these models contain inherent strengths and weaknesses. All have shown poor results in a shallow water environment due to difficulties at the ocean bottom where there is an interface between media of different sound speeds and densities.

Since its introduction (Hardin and Tappert, 1973), the parabolic wave equation has been a widely accepted means of solution for acoustic propagation. The earliest programs used a split-step Fourier transform algorithm to solve the parabolic equation (PE). Several other solution techniques have been developed primarily to overcome difficulties that occur when the Fourier transform encounters an interface between different media (Lee and Botseas, 1982 and McDaniel and Lee, 1982).

An alternative solution technique that uses an implicit finite-difference (IFF) algorithm was developed by Lee and Papadakis (1979). This method incorporates appropriate interface conditions and allows solutions in shallow water. Starting with the IFF algorithm, Jaeger (1983) developed a computer model to predict transmission loss and acoustic pressure based on user specified bottom topography and a single sound speed profile. This computer model uses the mathematical treatment of the horizontal and sloping interfaces developed by McDaniel and Lee (1982) and Lee and McDaniel (1983). It also utilizes several design features and methods incorporated in an earlier computer program developed by Lee and Botseas (1982), and a PE computer model developed by Brock (1978).

The IFD program preserves continuity of pressure and continuity of the normal component of particle velocity at an interface between media having different sound speeds and densities. This feature makes the program unconditionally stable and better able to handle the bottom boundary condition.

Since its development, the IFD program has not been rigorously tested. This thesis analyzes the program's performance in an idealized shallow water environment. The environment includes a simple sloping sand bottom beneath an isospeed water field. The analysis begins by comparing the IFD's predictions with predictions from Jensen and Kupersman's (1980) FE model and Coppens, Humphries and Sander's (1984) image model. The analysis also includes a comparison of the model's estimated transmission loss contours with expectations based on simple physical reasoning. Finally, the thesis describes an attempt to model a shallow sloping bottom in an experimental tank. The tank contains a sand bottom sculptured with a ten degree slope. Laboratory measurements of the pressure field are taken at a frequency of 100 kHz for comparison to the predicted pressure field generated by the IFD. These comparisons of the IFD predictions with other model estimates, theory, and laboratory measurements give an indication of the IFD's performance in a shallow water environment.

II. THE IFD COMPUTER MODEL

A. BACKGROUND

An implicit finite-difference solution technique to the parabolic equation has been studied and refined by many authors. The history of this development is explained in detail by Jaeger (1983), but merits review in order to gain a perspective on an analysis of the IFD computer model. The parabolic equation is an approximation to the elliptical wave equation. The first means of solving the PE used a split-step fast Fourier transform method as developed by Tappert and Hardin (1973). This method requires periodic boundary conditions in depth because of the finite Fourier transform and handles this constraint by introducing an artificial horizontal pressure release bottom below the actual physical bottom. This method of implementing an artificial bottom was incorporated into the earliest PE models developed by Jenson and Krol (1975) and Brock (1976).

Errors in this split-step Fourier transform method were found to be proportional to the horizontal range step and the second derivative of the index of refraction. The second derivative of the index of refraction tends to be large across the ocean bottom interface. Another problem with the split-step method is that it does not consider density differences between two different media at an interface, which influences the reflection coefficient. For these reasons the split-step Fourier transform method proved to be poorly suited for a shallow water environment.

The IFD solution method was introduced by Lee and Papadakis (1979) as an alternative to the split-step method. The IFD method employs a second order central difference

formula to solve the FE in the form of a tridiagonal matrix. Although the first version of the IFD did handle discontinuities in the sound speed profile, it did not consider density discontinuities. In 1982 McDaniel and Lee introduced a method to handle a horizontal interface of different densities. In 1983, they extended their treatment to include a sloping interface. It is this version of the IFD that is used in Jaeger's computer program.

E. THE COMPUTER MODEL

The IFD computer program consists of a main program and twenty subroutines. The program utilizes a modular construction so that each of the various subroutines are called from the main program to complete a specific calculation or function when required. The IFD is run interactively from a user generated input file that contains values for frequency, one sound speed profile, a bottom profile, source/receiver depths, attenuation coefficients for both the water and the bottom, and several other input parameters that tell the program where to obtain a solution within the field. The program initiates the calculations assuming an initial Gaussian pressure field and an artificial pressure release surface at a user specified depth.

Attenuation in both the water and the sediment is handled as complex indices of refraction. An artificial attenuation layer is established beneath the sediment to introduce attenuation above the artificial pressure release surface. The actual magnitude of this enhanced attenuation is calculated using an equation derived by Brock (1978) for use in his FE computer model.

The IFD program steps along the specified bottom profile and makes calculations down through the water/sediment column at each user specified horizontal range. The program

requires that the bottom intersect exactly at a vertical grid point. As a result, for a sloping bottom the program automatically calculates the range step to fulfill this requirement. This computer generated range step is always less than or equal to the user provided range step. As the slope of the bottom increases, the range step must decrease and more calculations and computer time are required to solve the entire pressure field. In some situations an actual modification of the user inputted bottom is required. This occurs with a very gently sloping bottom when the required range step exceeds the user specified range step. Here, the program automatically models the bottom as a series of level and sloping sections in order to ensure the user generated range step is not exceeded. This modification of the bottom is always less than or equal to one-half the vertical grid spacing and the model issues a warning to the user of the modification.

Both printed and graphical output are provided by the IFD. The printed output provides transmission loss and the real and imaginary components of the pressure field at each depth for a specified horizontal range. The graphical output is a plot of transmission loss versus range at the user specified receiver depth.

C. MODEL PROBLEMS/MODIFICATIONS

As this study of the IFD program progressed, it became necessary to modify certain aspects of the model. Most of these modifications were necessary to alter the program output into a more desirable form, but a few were implemented to correct programming deficiencies. Although this section of the thesis discusses the earliest model runs, these results are not presented in detail, but only discussed in general terms because they were obtained before

the computer model was fully modified. All modifications were made only after careful analysis of multiple model runs. It is important to realize that all results generated for comparison to other models and laboratory measurements came from a fully modified version of the IFD.

Since the ultimate objective of this study was to compare IFD model results with laboratory measurements the program was first run with input parameters which exactly modeled conditions in the tank. The experimental set up, explained later in great detail, consisted of a tank that is approximately two meters in length, one meter in depth, with a ten degree sloping sand bottom and a maximum water depth of 35 centimeters (cm). Based on a test case run by Jaeger (1983) of a simple sloping bottom, and by results shown by Jensen and Kuperman (1980) for propagation in a wedge-shaped ocean, it was expected that there would be certain recognizable patterns in the predicted propagation patterns. Specifically, since the speed of sound in the bottom exceeds that in the water (fast bottom), the simple sloping bottom supports trapped normal mode propagation (Coppens and Sanders, 1981). As the acoustic energy travels upslope toward the apex, successively lower modes are cut off and the energy contained in these modes is transmitted into the bottom. The range from the apex at which energy of the lowest mode is transmitted into the bottom is referred to as the dump distance and is a function of wavelength, wedge angle, and the ratio of sound speed in the water to the sound speed in the sediment. An empirical equation that defines this dump distance was derived by Coppens, Sanders, Ioannou, and Kawamura (1978); and was used to identify the expected ranges of these dump distances for the given scenario described above.

The initial unmodified IFD run used the parameters taken from the tank and showed no recognizable patterns in the

acoustic field. There was no observable decrease in transmission loss at the various dump distances as expected. Rather, results indicated widely fluctuating patterns in the acoustic field that appeared inconsistent with both previous studies and simple physical reasoning. Upon closer analysis, it was discovered that although the program was designed to be independent of scale there are several logic statements that are not implemented if the user provided range step is less than one meter. Because the logic statements aren't satisfied, the NEWSEG and NEWMAT subroutines (Jaeger, 1983) are not called correctly. The NEWSEG subroutine initializes the bottom slope and the NEWMAT subroutine computes matrix elements for the program. Obviously, errors in these two program functions seriously distort results. Because of this systematic error in the program it became necessary to scale up all tank parameters. All distances were scaled up by a factor of 1000, and frequency was scaled down by a factor of 1000. Careful analysis reveals that all input parameters are a function of either distance or frequency, so this scaling produces results that model those expected in the tank.

The second modification of the IFD was required to provide a three dimensional graphics display. As discussed earlier, the IFD provides a transmission loss plot versus range at a single depth. However, to study the model predictions in greater detail it was felt that a two dimensional analysis of the model estimates would be more meaningful. As a result a transmission loss contouring program was developed. The program (Appendix B) displays transmission loss contours for range versus depth. Use of the contour plot requires that transmission loss values generated by the IFD be sent to a data disk used by the contour routine. To facilitate this transfer a dummy variable (LIFD) was established in the PRINT2 subroutine to store the transmission loss values and then these values are written to the data disk at the end of the main program.

Another modification of the IFD output was required to change the real and imaginary components of the pressure to a single pressure amplitude magnitude. It was felt that dealing with the pressure magnitude was easier and more meaningful than with the real and imaginary components of the pressure field. This conversion was done in the PRINT2 subroutine and established a new variable (PRMAG) to represent the pressure magnitude.

A final modification in the computer program was made due to a suspected error in the computation of the attenuation in the artificial layer. Physical reasoning dictates that proper implementation of the artificial attenuation would result in a steady drop off in acoustic pressure with depth throughout the artificial layer, with pressure dropping to zero at the pressure release surface. IFD model results on the other hand showed wide fluctuations in pressure with depth in the layer and then only a minimal fall off at the pressure release surface. The equation in the IFD that actually computes the magnitude of the attenuation in the artificial layer was taken directly from Erck's (1978) EE model (Jaeger, 1983). However, Brock's equation was derived with feet as the unit of measurement while Jaeger's model is derived with meters as the unit of measurement. With this in mind, Jaeger's equation should be approximately a factor of three larger than Brock's equation to correct for the difference in units. To correct for this error the equation to calculate attenuation (ATT(I)) in the NEWMAT subroutine was increased by a factor of three. When this correction was implemented, the large fluctuations in pressure with depth were eliminated. The expected drop off in pressure with depth and the fall off of pressure to zero at the pressure release surface were noted.

A listing of the revised IFD computer program with all modifications can be seen in Appendix A.

L. MODEL VERIFICATION

1. Comparison with Jaeger Model Run

In light of the modifications to the IFD computer program just discussed, it was necessary to ensure that the changes themselves did not introduce errors into the model. So as a first step the modified IFD program was run for one of the test cases used by Jaeger in his original work. This case analyzes propagation in an environment that moves from deep to shallow water. This particular environment is depicted in Figure 2.1 and was chosen because it was very similar to the simple sloping bottom in the tank experiment. A solution is obtained for a bottom with an upslope of 8.5 degrees. An isospeed water field is used with sound speed set at 1500 m/s. Source frequency is 25 Hz. The scenario has a maximum depth of 350 meters and a range of 40 kilometers. Both the source and the receiver are set at 25 meters.

The results using the modified IFD program were the same as Jaeger's for this test case above the artificial attenuation layer. As explained earlier, the program was modified to reflect higher attenuation in the artificial layer, so as to properly reflect the effect of attenuation in this region. The modified program results did not show the large fluctuations in pressure with depth in the artificial layer but rather the gradual decline in pressure towards a value of zero at the pressure release surface. But above the artificial layer the modified program results were identical with those achieved by Jaeger with the original program. Apparently, the minor changes in the program designed to improve on the form of the program output does not hinder the model's ability to achieve a solution in the upper sediment and water column.

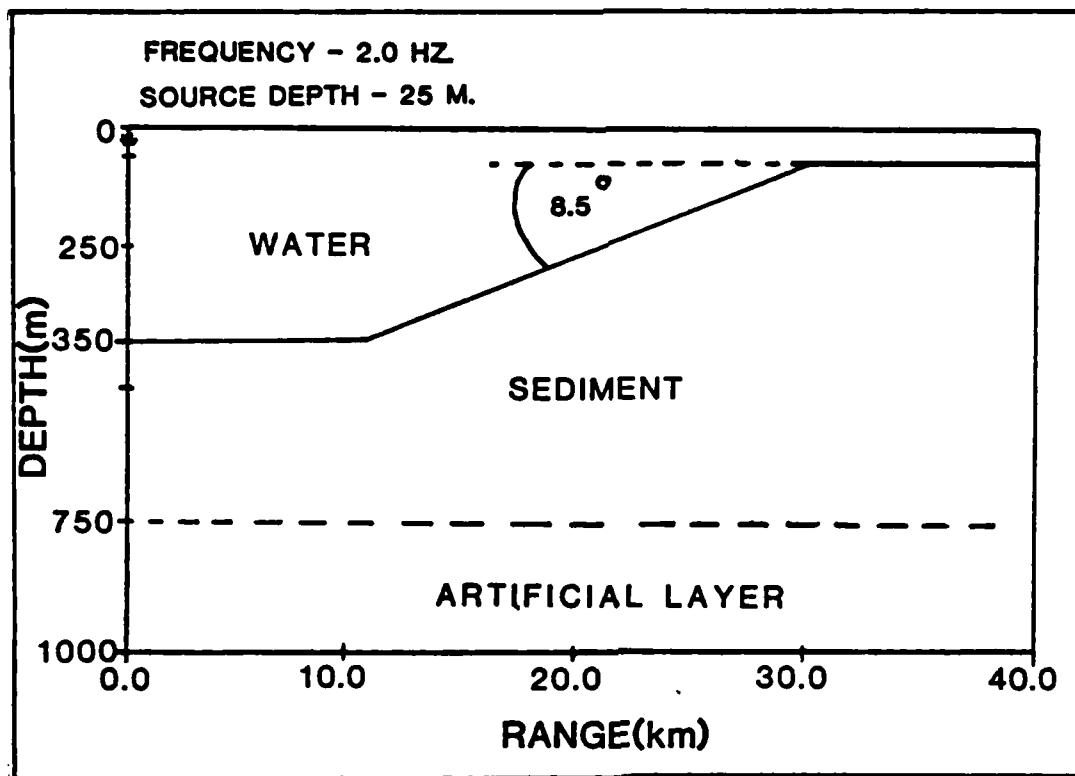


Figure 2.1 Jaeger's Deep-to-Shallow Water Case.

2. Comparison with Jensen and Kuperman Model Run

The second attempt at verifying the IFL model involved a comparison of model results with those achieved with a FE model designed by Jensen and Kuperman (1980). The Jensen and Kuperman Model (JKM) uses a split-step solution technique. Comparison with this particular model was chosen because it is one of the few that obtains a solution in two dimensions. Most acoustic models obtain a solution at only a single depth. In addition, Jensen and Kuperman made their model runs in a simple sloping ocean bottom environment very similar to the scenario of interest modeled in the task. This environment is depicted in Figure 2.2 and features a gently sloping bottom of 2.2 degrees. The water column has a

uniform speed of 1500 m/s. The source is placed just below the midpoint in the channel at 112 meters and is driven at a frequency of 25 Hz. The maximum depth in this scenario is 200 meters and has a maximum range of 12.5 kilometers.

The Jensen and Kuperman results were expressed as

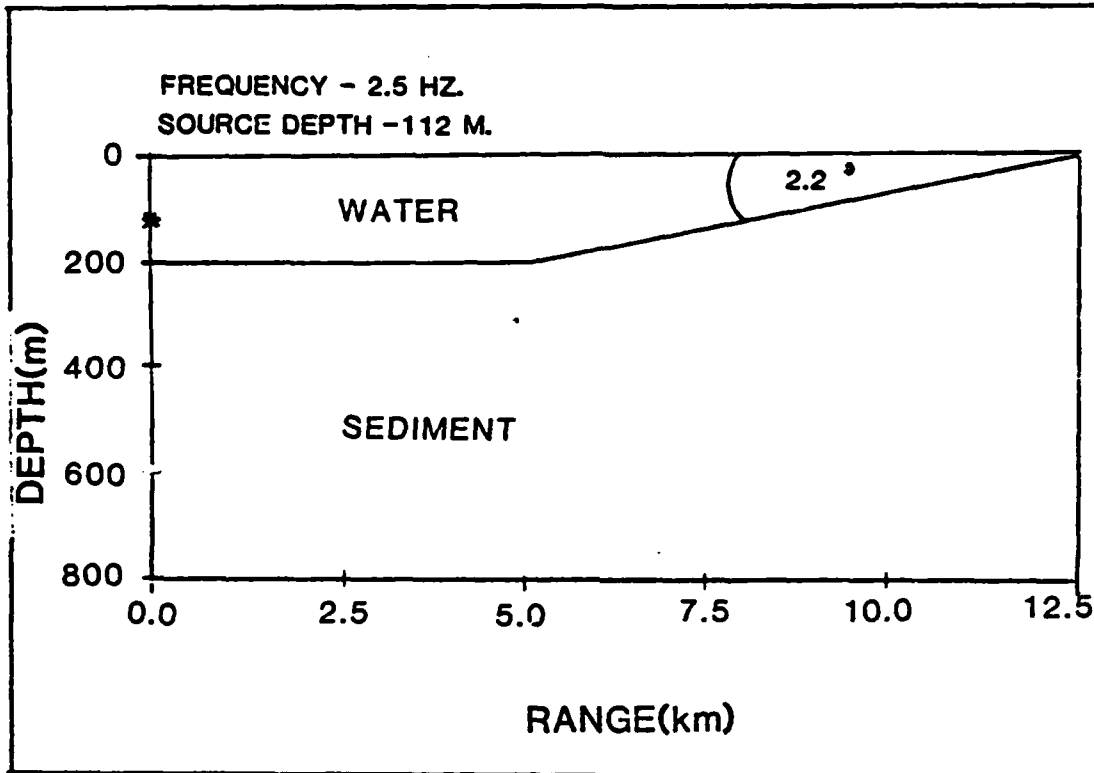


Figure 2.2 Jensen and Kuperman Sloping Bottom Case.

transmission loss contours for range versus depth. Their study concentrated on transmission loss patterns in the sediment, but results were obtained both in the sediment and in the water. These results are compared to the IFD results at ranges of 2.5, 5.0, 7.5, 10.0, and 12.5 kilometers. These ranges were chosen for analysis because the JKM results showed the greatest variation in transmission loss with

depth and thus, makes for a more meaningful comparison with the IFD results.

The IFD and JKM results can be seen in Figure 2.3 through Figure 2.7. In all the figures, the IFD estimates are shown as a solid curve while the Jensen and Kuperman results are depicted as circular points. The first analysis is at a range of 2.5 kilometers. From Figure 2.2, it can be seen that the depth at this range is 200 meters and is in a flat bottom region. From the results shown in Figure 2.3, it is obvious that both models obtained almost identical results from the surface down to a depth of about 300 meters. There are differences between the two sets of predictions from the ocean bottom to a depth of 100 meters below this point. Below 300 meters the Jensen and Kuperman results show a very slight increase in transmission loss (TL) with depth. The IFD also shows an overall increase in transmission loss with depth but with several fluctuations in transmission loss and a marked peak at about 300 meters. So in general, the results from the two models have the same general tendencies although the IFD appears to show greater detail in results near the water/sediment boundary.

Figure 2.4 shows results at 5.0 km in range. Here, the water depth is still 300 meters and marks the very beginning of the sloping bottom section. For this range the JKM predictions are only available to a depth of 300 meters. The results are nearly identical with those obtained by the IFD. Both models show a relative minimum in transmission loss at a depth of 100 meters and then a gentle increase in TL with depth.

The model results at a range of 7.5 km are seen in Figure 2.5. At this range the bottom depth is about 150 meters and the bottom is sloping. The models show the greatest difference at this range. Both models produce nearly identical results in the water column, but beneath

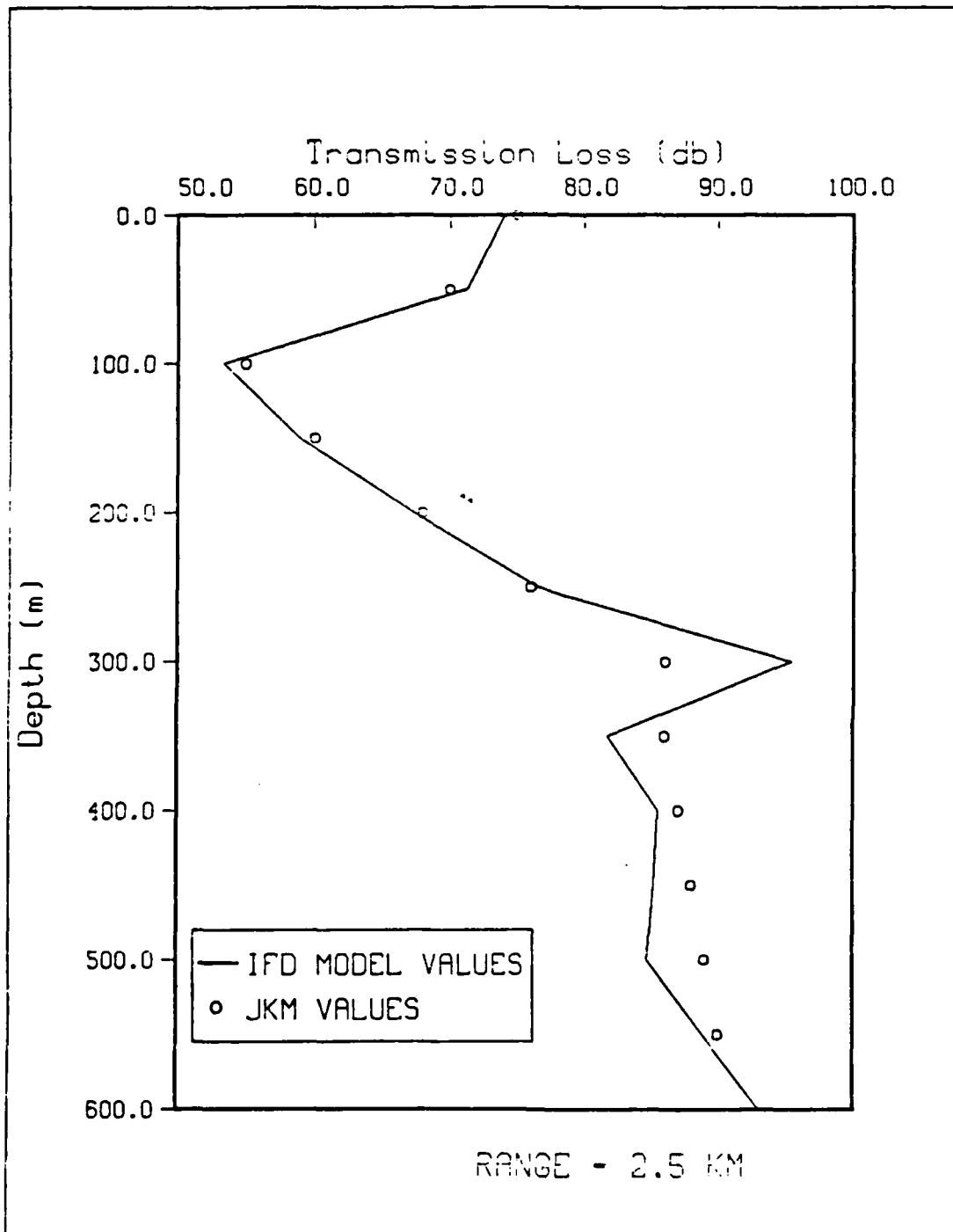


Figure 2.3 IFD and JKM Comparison at a Range of 2.5 Km.

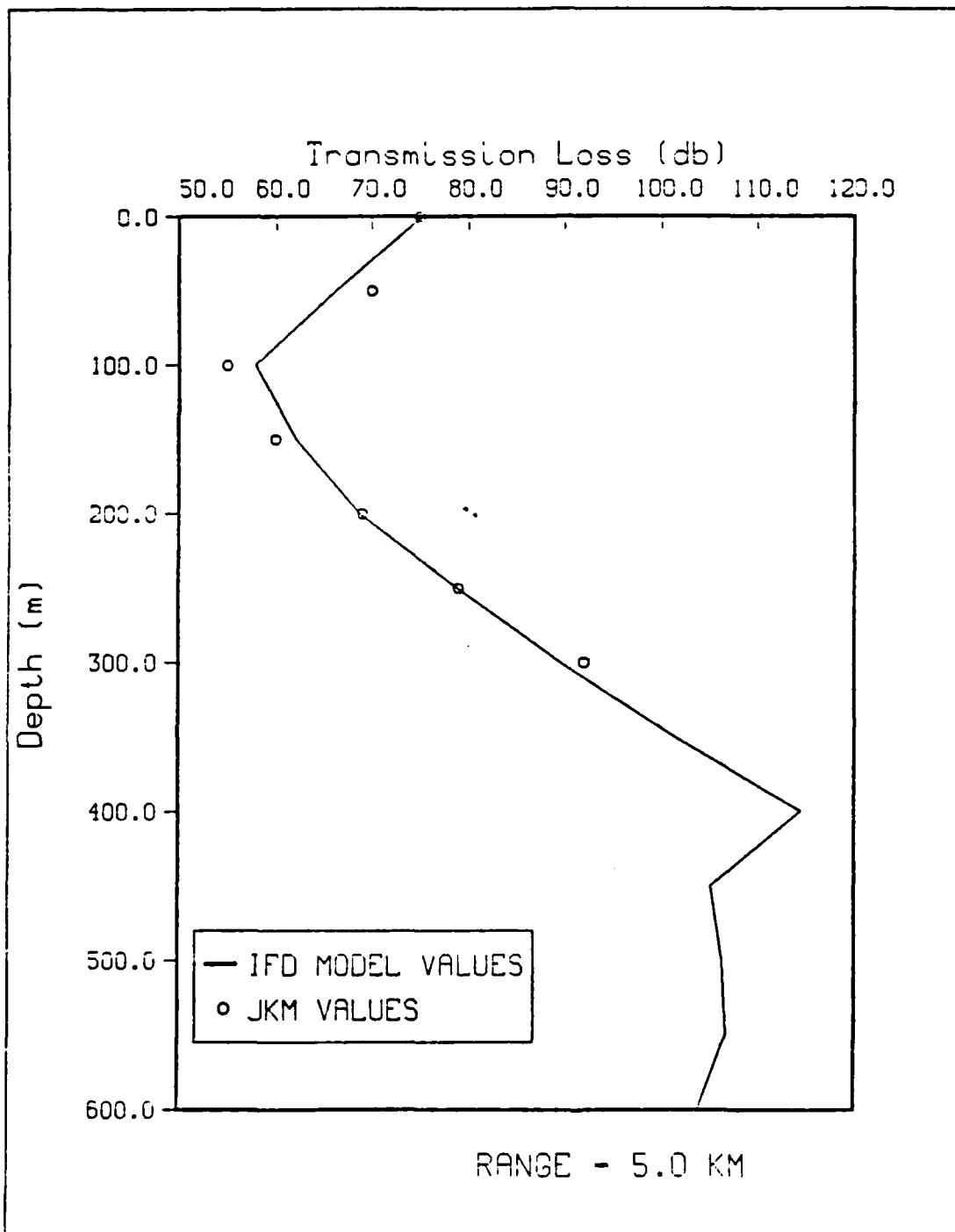


Figure 2.4 IPD and JKM Comparison at a Range of 5.0 Km.

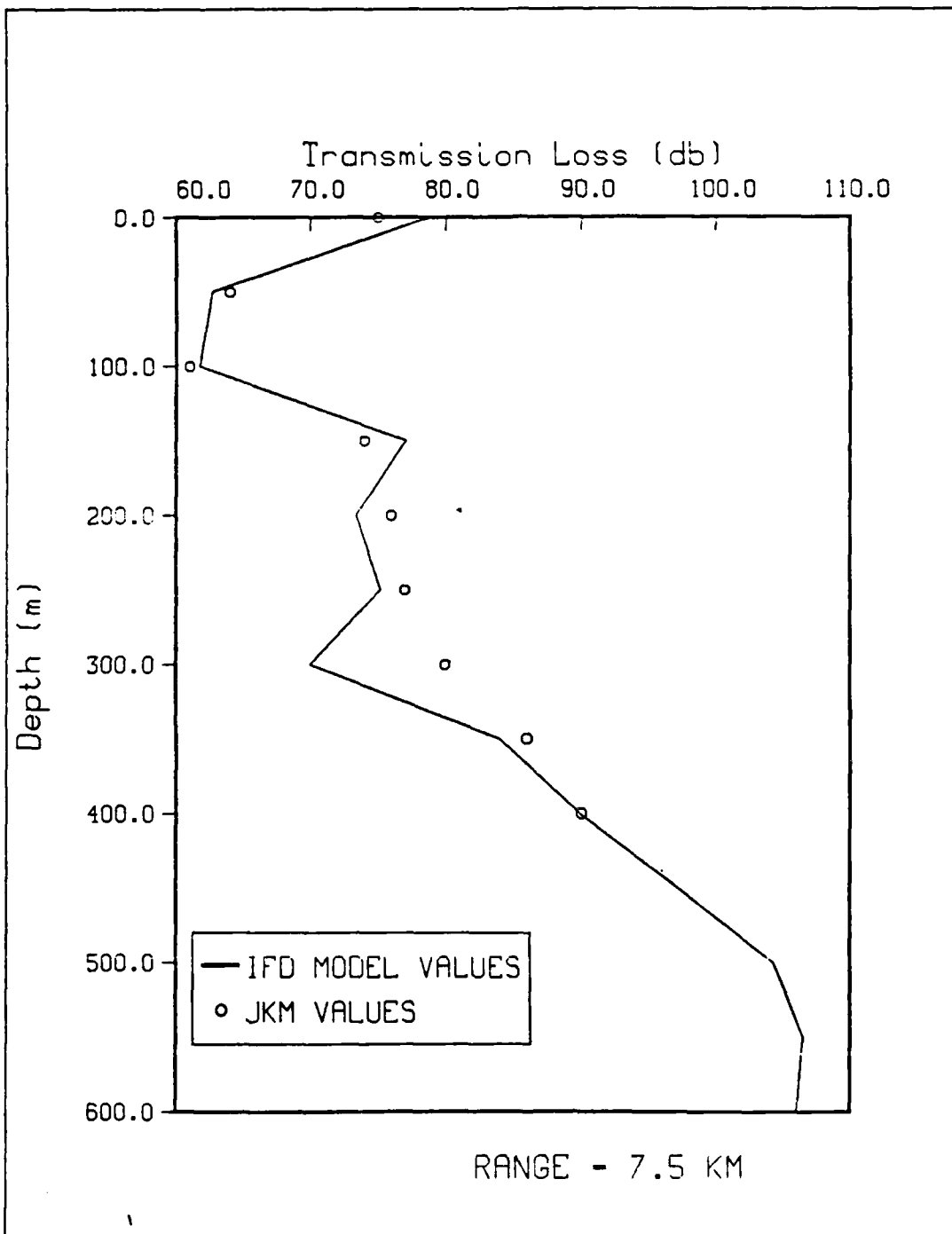


Figure 2.5 IFD and JKM Comparison at a Range of 7.5 Km.

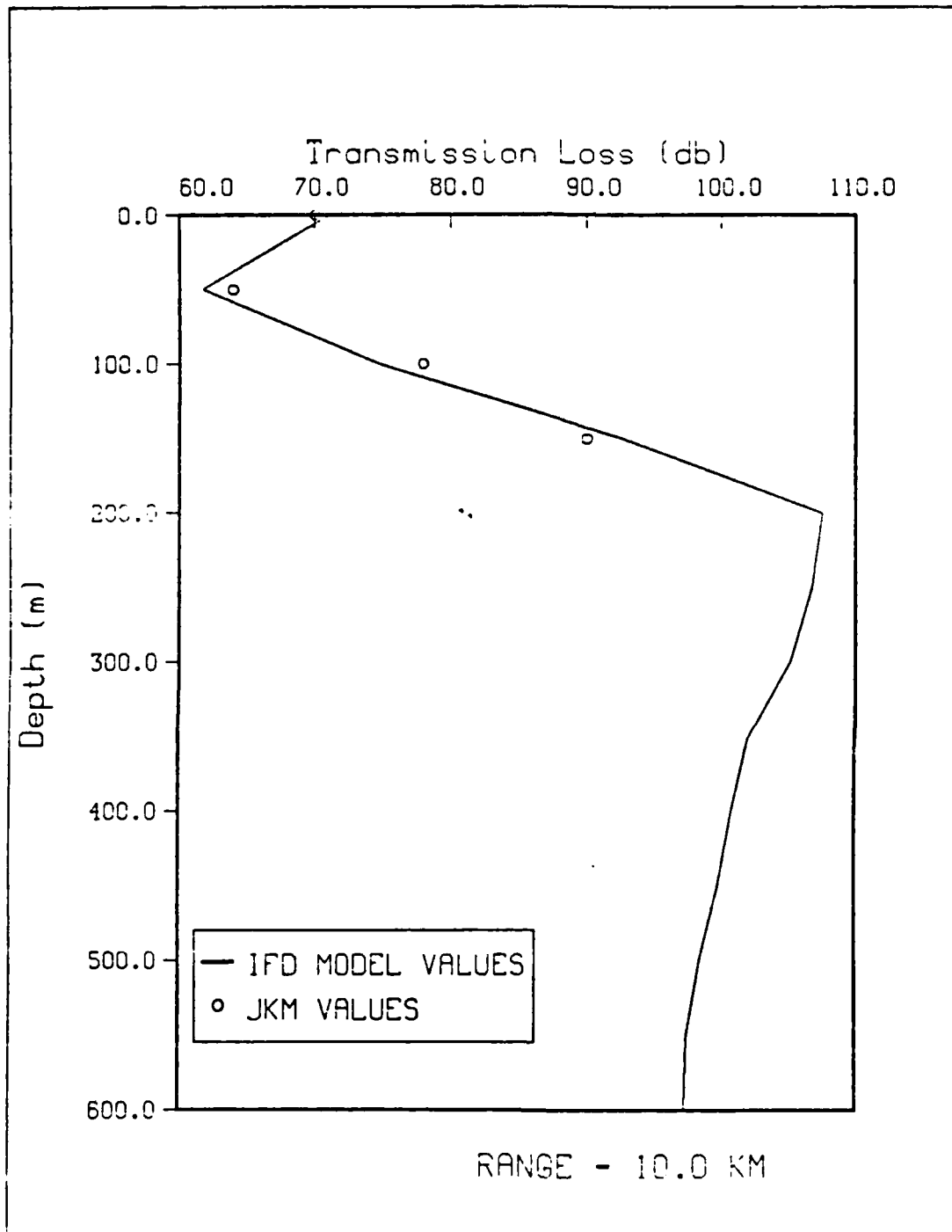


Figure 2.6 IFD and JKM Comparison at a Range of 10.0 Km.

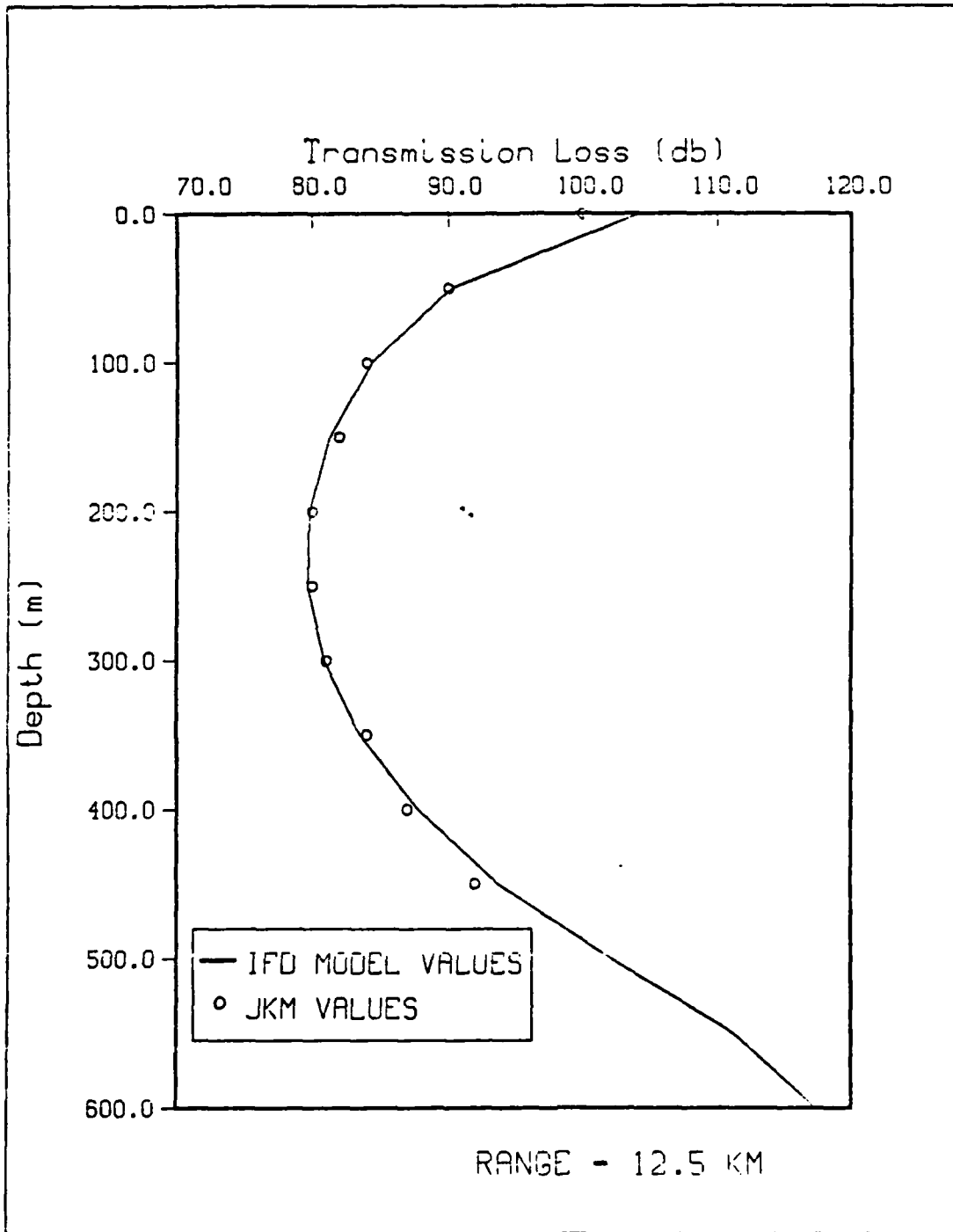


Figure 2.7 IPD and JKM Comparison at a Range of 12.5 Km.

150 meters in depth the model estimates begin to show differences. The Jensen and Kuperman results show a gradual increase in TL with depth below the ocean bottom. The IFD results on the other hand, show a gradual decrease in transmission loss from 150 meters to 300 meters, with a relative minimum at 300 meters and then an increase in TL beneath this depth. Although there are some differences in model estimates near the boundary in the flat bottom sections previously discussed, the differences appear to be greater at the boundary in this sloping bottom case. In these regions away from the boundary in either the water column or in the sediment, however, both models produce similar results. The JKM's difficulty in obtaining an accurate solution at the sediment boundary is not totally unexpected. The model uses a variation of the straight split-step solution technique similar to Brock's computer model (Jensen and Kuperman, 1980), that has characteristically been unsuccessful in obtaining a reliable solution near a boundary.

The results at a range of 10.0 km are seen in Figure 2.6. At this range the water depth is approximately 100 meters and the bottom is again in a sloping region. At this range Jensen and Kuperman results are only available to about 150 meters in depth. For the data available, the models produce nearly identical results. Both models predict a minimum at about 50 meters in depth and then an almost linear increase in TL with depth. The IFD results also reflect a transmission loss maximum at about 200 meters, and then a slight decrease of TL beneath this depth. Data at these depths are not available from the Jensen and Kuperman run. In light of the results obtained at 7.5 km for a sloping bottom case one might expect that the results for the two models would show differences near the ocean bottom. However, since there is only one Jensen and Kuperman prediction available near the bottom for this range, it is

difficult to make any definite conclusions regarding differences in model performance at the boundary.

Results at the apex (range equal to 12.5 km) can be seen in Figure 2.7. Since all estimates are made in the sediment at this range, there is no boundary to contend with. At this range the two models show the best agreement. Both models show a gradual decrease in transmission loss to a depth of about 300 meters and then a gradual increase of TL with depth.

In general, there appears to be good agreement between the IFD and the JKM model results in regions not influenced by a boundary. In both the water and the deep sediment the two models produce similar results. Although this is not conclusive evidence, these similarities suggest that the IFD can successfully model acoustic propagation in these regions. Near the water/sediment boundary however, the Jensen and Kuperman and IFD predictions show marked differences. These differences appear to intensify as the bottom becomes more sophisticated. In general, the Jensen and Kuperman results do not seem to show the detail the IFD results do. Considering the different solution techniques employed by the two models, these differences in results are expected.

3. Comparison with Coppens, Humphries and Sanders Model Run

The third attempt at verifying the IFD performance was done by comparing results with an image theory model derived by Coppens, Humphries, and Sanders (1984). This Coppens, Humphries, and Sanders Model (CHSM) uses a saddle point approximation to an image model to solve for the acoustic field. Both programs were run for the scaled scenario modeled in the tank experiment. This scenario is depicted in Figure 2.8 and features a ten degree sloping

bottom. The maximum water depth for the run is 350 meters and the maximum range is two kilometers. The source generates a 100 Hz signal and is set at a depth of 175 meters.

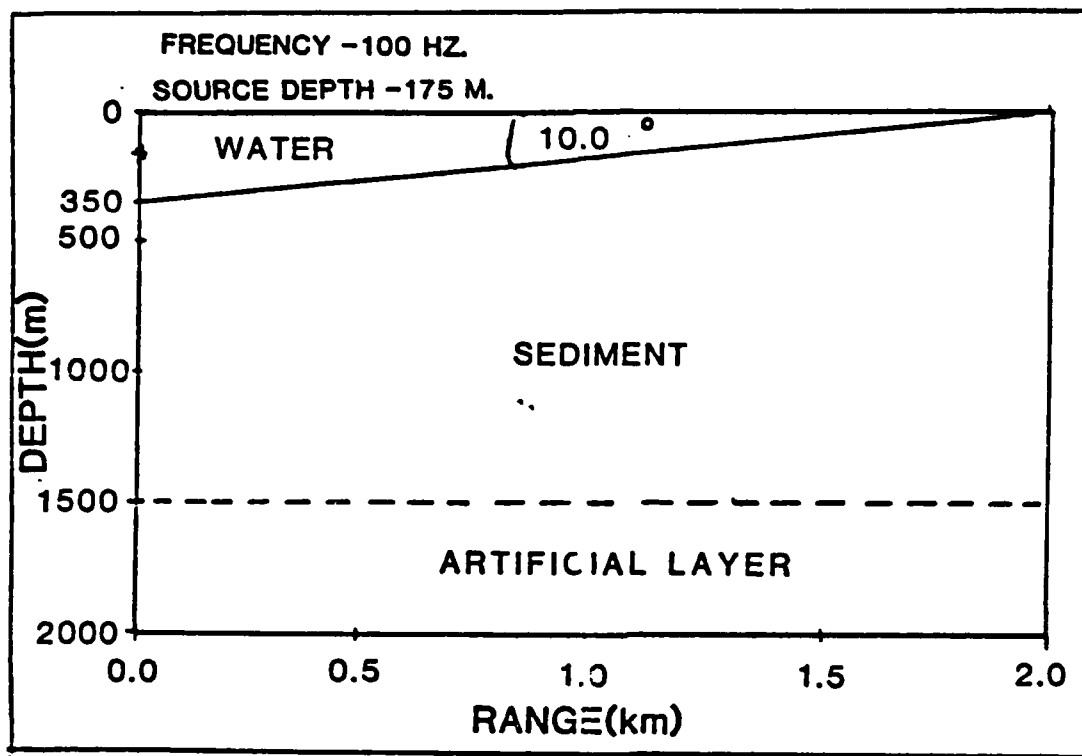


Figure 2.8 10 Degree Simple Sloping Bottom Case.

The image model provides solutions only at the apex. The comparison of predictions at the apex (range equal to 2 kilometers), can be seen in Figure 2.9. In the Figure, the IFD values are plotted as the solid curve while the image model values are shown as circular points. The predictions are shown as values of normalized pressure amplitude for a given depth. The different models produce pressure amplitude values in different units, and thus, had to be normalized to make a comparison of values possible. This normalization was

done for each model by dividing the pressure amplitude by the maximum amplitude predicted by the model.

The results suggest that even though the models predict similar large scale trends in pressure amplitude with depth, there are several differences in detail. The plot shows that both the IFD and the image model predict an almost linear increase in amplitude with depth down to a specific maximum and then a slow decrease in amplitude beneath this maximum. The IFD however, shows the maximum at about 15.5 meters in depth while the image model maximum is deeper at 19 meters. Beneath this maximum the IFD shows a much steeper decrease in amplitude than the image model. The trend in the image model data appears smooth, while the IFD curve reflects several small scale fluctuations.

It appears that both models predict similar large scale trends in pressure amplitude for this scenario. It is difficult, if not impossible, to account for the differences in detail. As a minimum, however, this comparison indicates that the two sets of predictions are consistent with one another and can be considered reasonable in this shallow water environment.

4. Comparison with Physical Reasoning

From model comparisons it appears that the IFD at least makes a reasonable estimation of acoustic fields in a shallow water environment. IFD results are also analyzed in comparison with basic physical reasoning and theory as a fourth attempt at model verification. This analysis examines IFD transmission loss contours for the simple ten degree sloping ocean scenario seen in Figure 2.8. The scenario is two kilometers in range with a maximum depth of 350 meters. The source generates a signal at 100 Hz and is placed at 175 meters in depth.

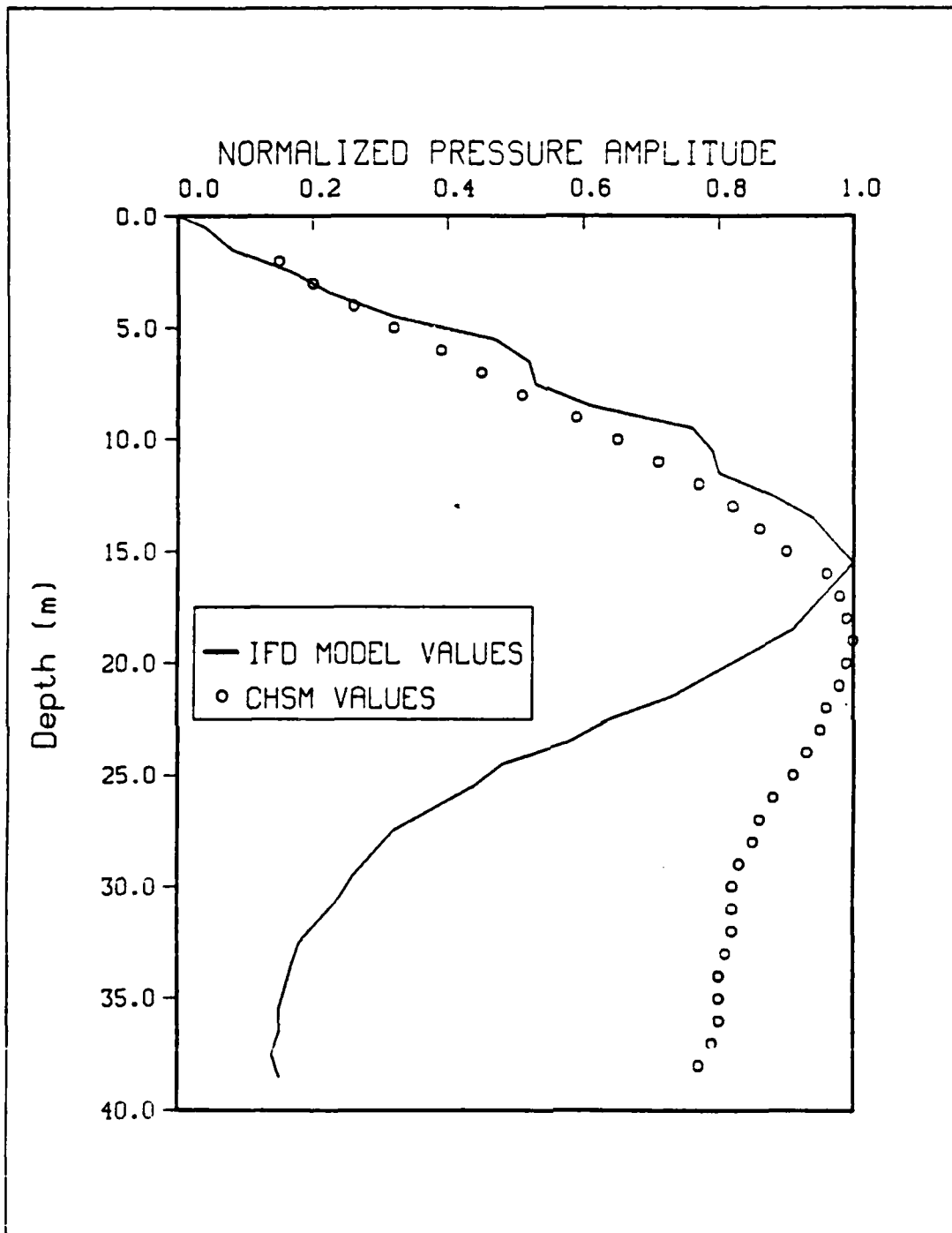


Figure 2.9 IFI and CHSM Comparison at the Apex.

Transmission loss contour plots are displayed in Figure 2.10 through Figure 2.13. All TL contours are expressed in decibels(db) and are shown as a function of depth versus range. In all figures, the ten degree sloping bottom is shown as a solid unlabeled line. The contour plots are displayed over four range subsections due to computer graphics limitations and to emphasize different significant features in the field.

The first figure shows transmission loss contours from the source to a range of 600 meters. The contours in the first 250 meters appear very symmetric, increasing outward from the source in a pattern that resembles spherical spreading. Since the IFD program assumes a Gaussian starting field this early pattern is expected.

From a range of about 300 meters to 600 meters the field in the water appears to be dominated by a surface reflection pattern. From the spotty appearance of the TL contours in this region there is an indication of an interaction of surface reflection and bottom reflection on the contours. It is possible to compare transmission loss maxima with nodes in the surface interference pattern. Based on surface interference theory these nodes should occur where (Kinsler, Frey, Coppers, and Sanders, 1982):

$$\text{SIN}(khd/r) = 0$$

or in other words;

$$khd/r = n\pi$$

where:

$$n = 0, 1, 2 \dots$$

$$r = \text{Range}$$

$$k = \text{Wavenumber}(2\pi/\lambda)$$

$$d = \text{Source Depth}$$

$$h = \text{Depth of Node}$$

$$\lambda = \text{Wavelength.}$$

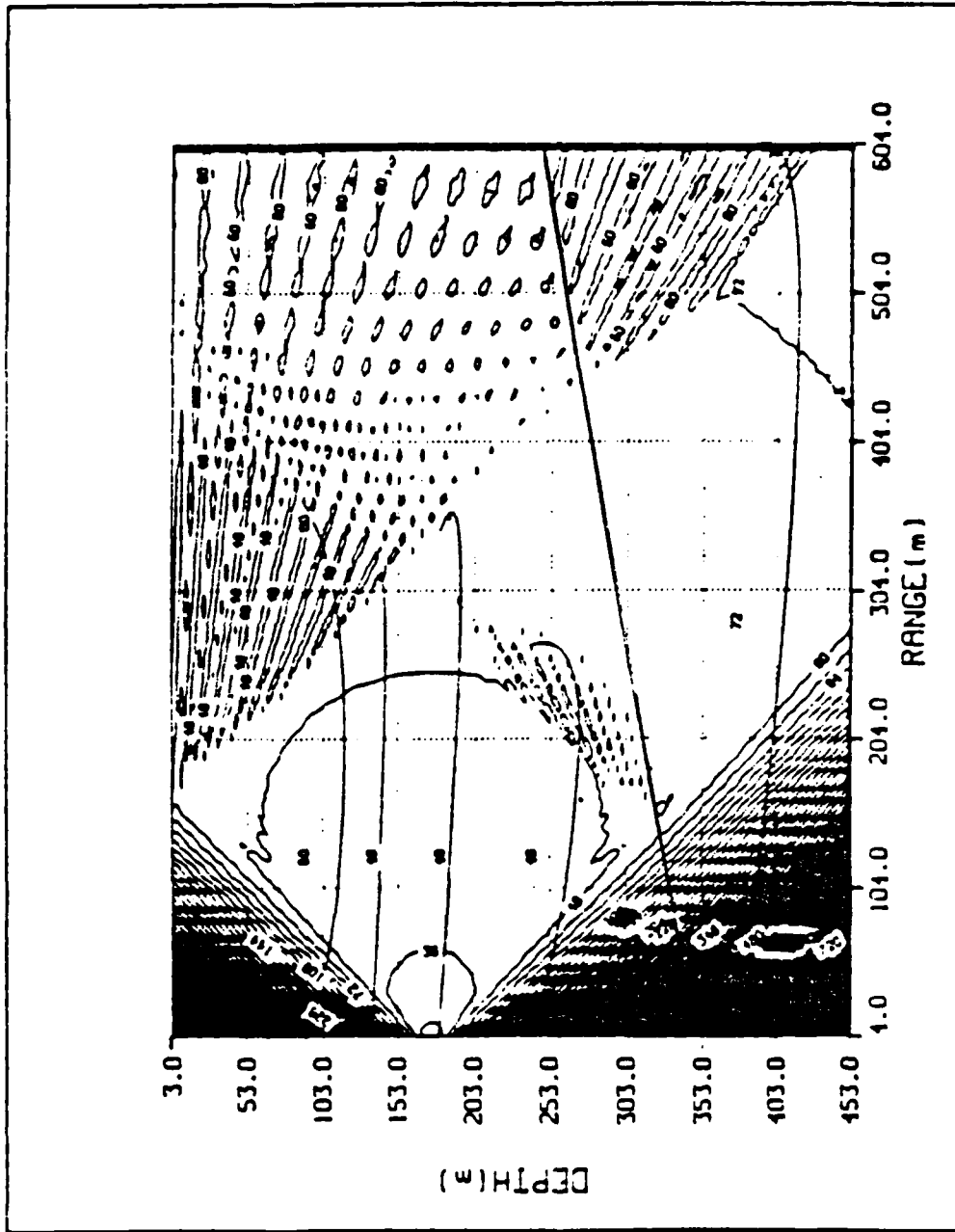


Figure 2.10 IFD TL Contours (dB) from the Source to 604 Meters

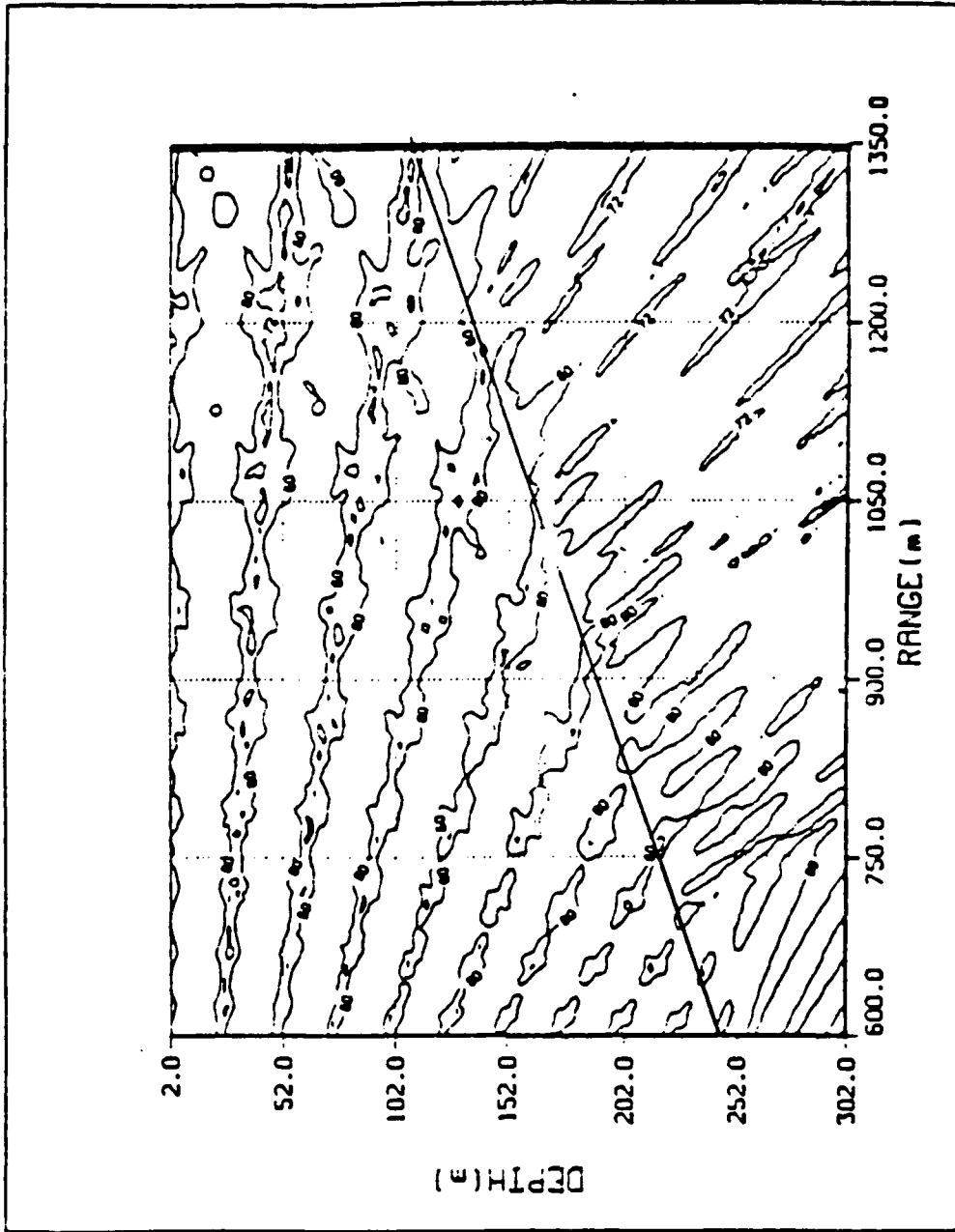


Figure 2.11 IPD TL Contours (db) from 600 to 1350 Meters.

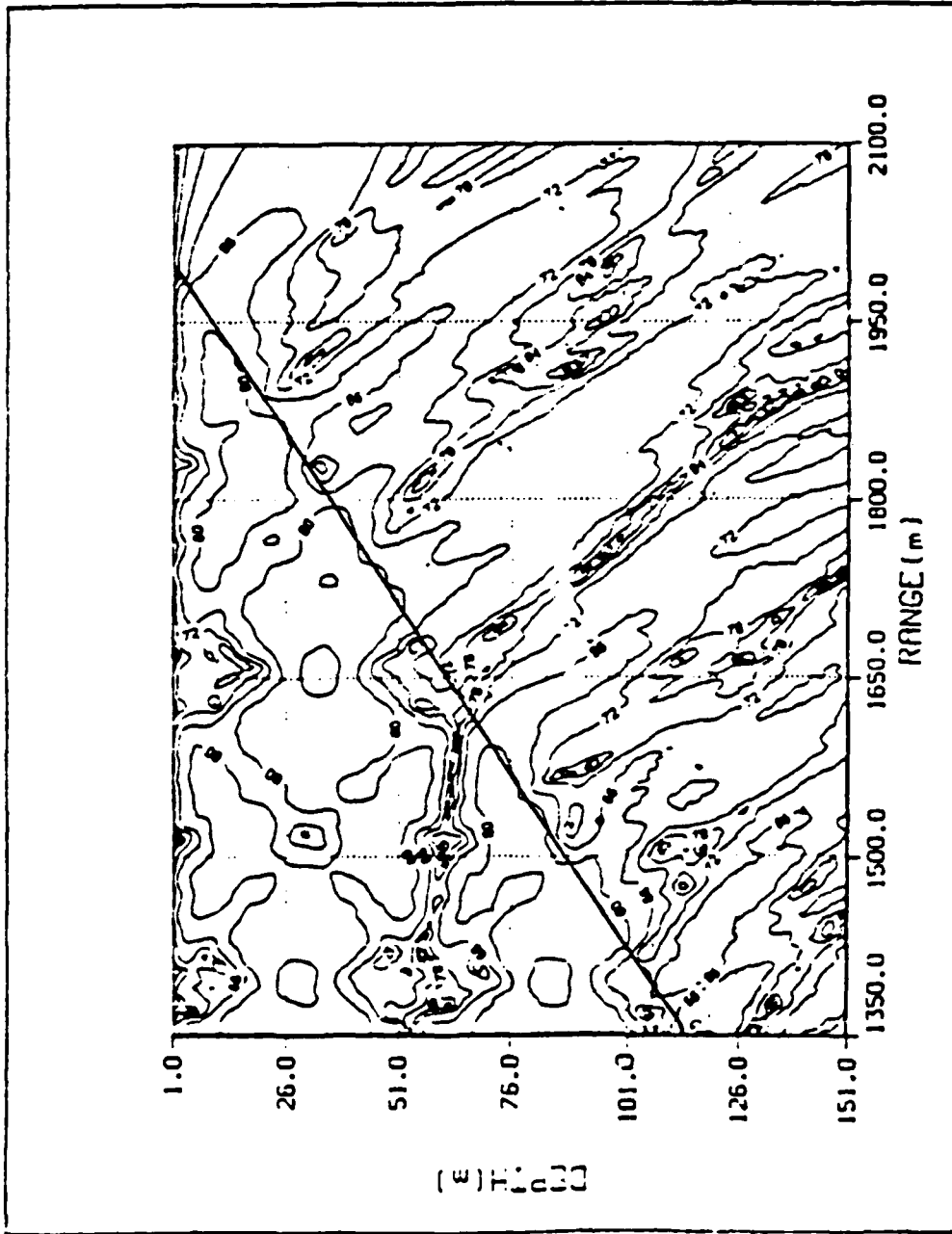


Figure 2.12 IFD TL Contours (db) from 1350 to 2100 Meters.

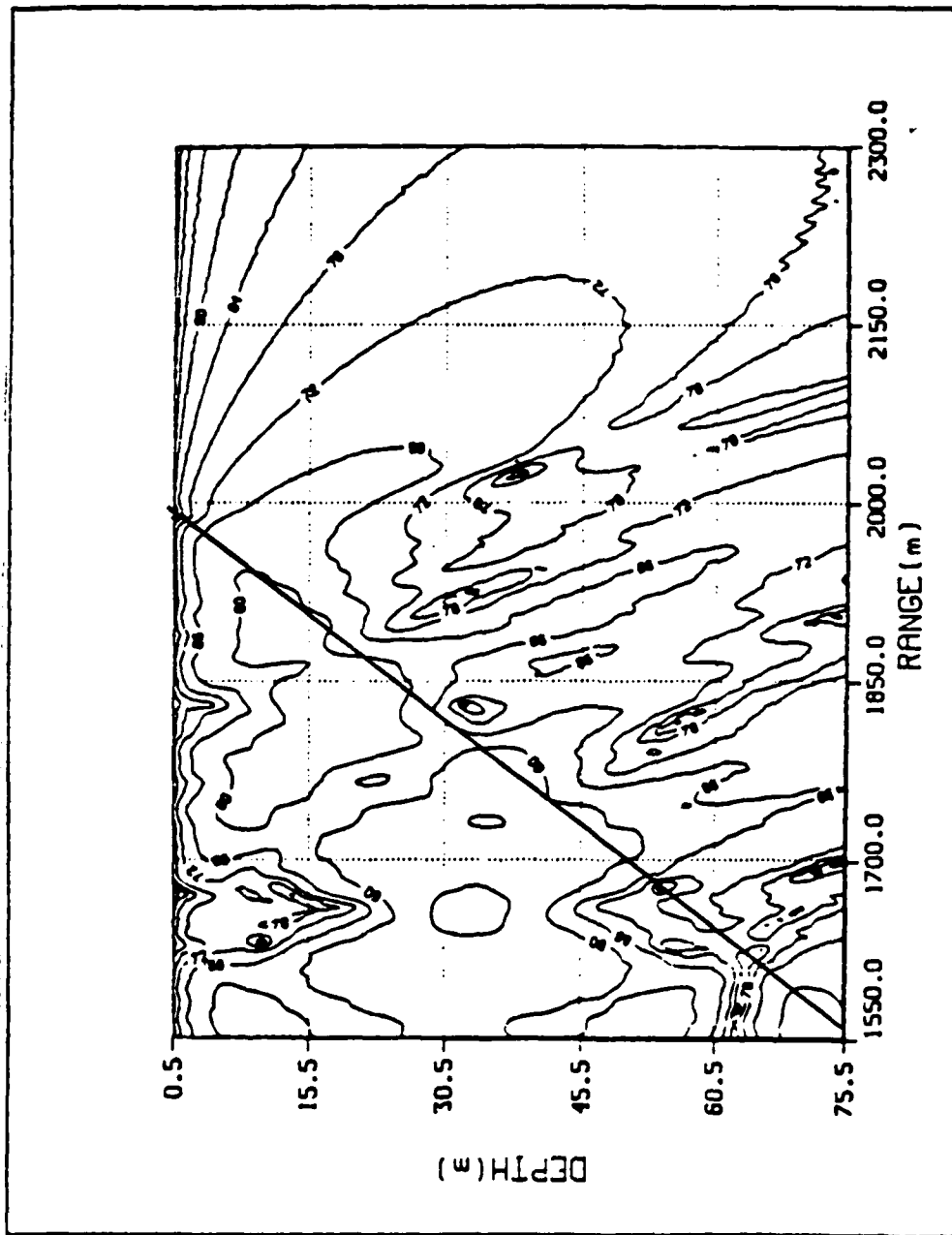


Figure 2.13 IFD TL Contours (db) from 1550 to 2300 Meters.

By manipulating the above equation it is possible to solve for the depth at which the nodes should be observed. For this particular scenario at a range of 604 meters, nodes should occur at integer multiples of 25 meters in depth ($25n$). Figure 2.10 shows that these transmission loss maxima do exist as expected, every 25 meters in depth at the stated range.

Based on simple physical reasoning one would expect refractive bending along the ocean bottom due to density differences between the water and the sediment. The contour plot reflects a change in basic pattern at the interface. There is a bending of the TL contours that suggest a refractive influence.

Figure 2.11 shows transmission loss contours from a range of 600 meters to 1350 meters. Again in this region the water appears to be dominated by surface reflection. Solving for the nodes in this surface interference pattern at a range of 1350 meters, it is found that these nodes should appear every 55 meters in depth. From the figure it is again seen that TL maxima do occur every 55 meters in depth as anticipated. As in the first figure there is a change in the basic TL pattern at the ocean bottom. The bending appears more accentuated than in the previous figure, but still suggests the influence of refraction at the ocean bottom.

Figure 2.12 displays transmission loss from 1350 meters to past the apex at a range of 2100 meters. In this figure, the dominance of the surface reflection mechanism is less obvious and the TL patterns become more complicated. It is in this region that the influence of trapped normal mode propagation can be seen. As discussed earlier, as acoustic energy travels up the slope toward the apex, normal modes are cut off and energy is transmitted into the bottom. According to adiabatic normal mode theory, modal separation

is range dependent (Graves, Nagel, Uberall, and Zaur, 1975 and Coppens and Sanders, 1980). The range from the apex at which the lowest mode is transmitted into the bottom, can be calculated using the following equation (Coppens, Sanders, Icanncu, and Kawamura, 1978):

$$X = \lambda/4 \sin\theta_c \tan\beta$$

where:

X = Dump Distance Of The Lowest Mode

λ = Wavelength

θ_c = Critical Angle

β = Wedge Angle.

According to adiabatic normal mode theory (Kinsler, Frey, Coppens, and Sanders, 1982), in deep water (near the source) the lower normal modes are far above cutoff and the adiabatic eigenfunctions consist of an integer number of half sine waves with zero pressure at both the top and bottom surfaces. At the cutoff of each mode, the pressure at the bottom must be maximized, resulting in an adiabatic eigenfunction that contains 1/4, 3/4, and 5/4 wavelengths at the respective cutoff distances of 1X, 3X, and 5X for the three lowest modes. From Figure 2.14 it can be seen that as the normal modes travel up the sloping bottom, successive modes are forced into the bottom at distances where a particular mode reaches a depth at which it can not longer propagate. Also from the figure it is obvious that a source set at mid-depth can not excite the second mode. Since this particular geometry is present in the tank scenario it is expected that the energy associated with this second mode should not be seen. Based on this line of physical reasoning, modes should be dumped into the sediment at the first dump distance, fifth dump distance, ninth dump distance and so on. If these modes are dumped as described

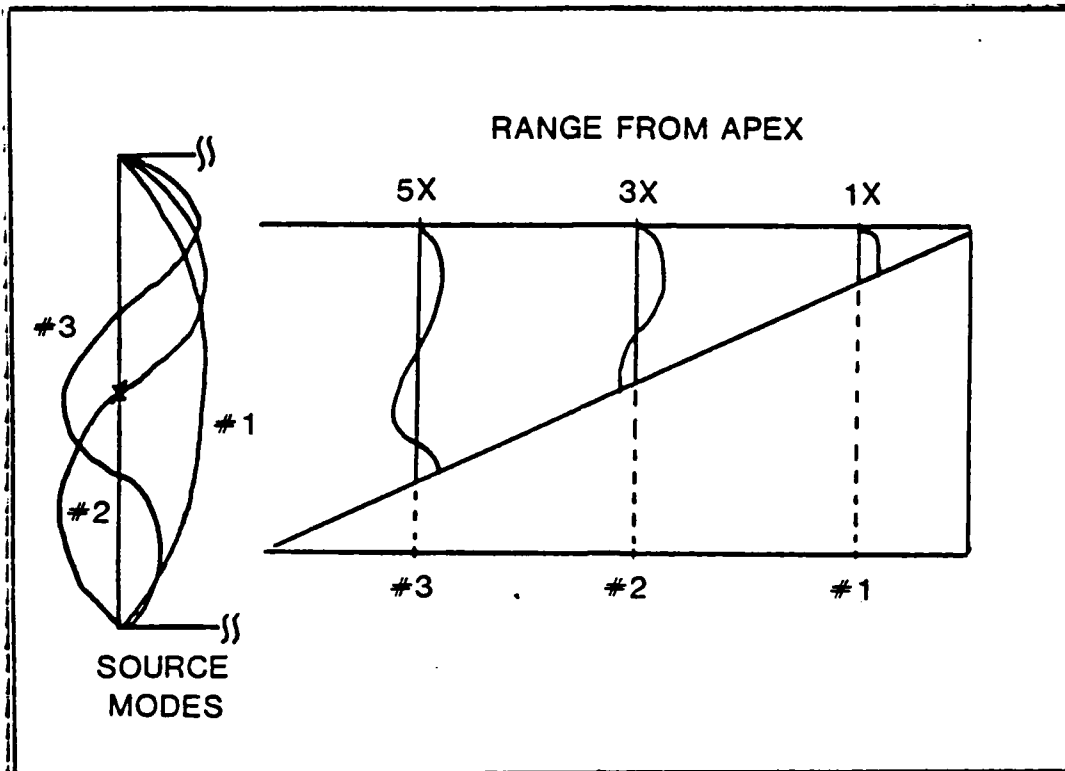


Figure 2.14 Normal Mode Propagation in a Wedge Shaped Ocean.

then they should be seen in the contour plot as reductions of transmission loss in the bottom at ranges of 1952 meters, 1760 meters, 1568 meters, and so on.

From Figure 2.12 it can be seen that there is an obvious decrease in transmission loss at approximately 1950 meters (dump distance #1) and 1760 meters (dump distance #5). There is also a less clearly defined reduction in TL along the bottom at 1565 meters (dump distance #9).

The final contour plot (Figure 2.13) shows transmission loss contours from 1550 meters to 2300 meters. This figure is an extension of Figure 2.12, intended to emphasize how clearly the beam at the first dump distance is defined in the plots. The beam at the fifth dump distance is also

visible but is not nearly as well defined. From this figure, one can also see an indication of a very narrow beam in the sediment at about 1860 meters. This distance corresponds to the third dump distance (second normal mode). Based on adiabatic mode theory the second mode is not expected to be excited. However, adiabatic mode theory is only an approximation of normal mode behavior. This approximation of normal mode behavior becomes less exact as the bottom slope increases and the closer the source is to the apex. The appearance of a narrow beam at the third dump distance indicates that there is a strong possibility that the second mode is present and that the adiabatic approximation is not exact with a ten degree bottom slope.

The basic features of the IFD contour plots are consistent with both physical reasoning and theory. Basic surface reflection and bottom refraction occur where expected and behave as anticipated. In the far field, trapped normal mode propagation is observed and can be verified with simple dump distance calculations. The location of beams dumped into the bottom appear consistent with basic mode theory. In short, the transmission loss contours indicate that the IFD is making reasonable predictions of the acoustic field in a shallow water environment.

5. Verification Summary

It is difficult to say how exact the IFD predictions are for a shallow water environment based on these simple verification techniques. As a minimum it can be said that the model results are at least consistent with other model predictions and expectations based on simple physical reasoning. Model estimates are virtually the same as the Jensen and Kuperman FF model in regions not influenced by a water/sediment boundary. Close to the boundary the IFD results appear to show greater detail and variation than

this IF model. The IFD results also appear consistent with the general trends in pressure amplitude predicted by the Coppens, Hurphries, and Sanders image model. Again differences were noted in the small scale structure. Finally, the IFD II contours verify well with basic expectations based on physical reasoning and theory. Surface reflection and bottom refraction patterns are observed as anticipated. Far field normal mode propagation can be verified in the plots using simple range distance calculations. In short, all verification methods attempted, fail to uncover any inconsistency in IFD performance in a shallow water environment.

III. LABORATORY MEASUREMENTS

A. BACKGROUND

The major attempt at appraising IFD performance involved comparing model results with laboratory measurements. The shallow water environment modeled in the tank is very idealized; a ten degree sloping sand bottom with an isovelocity water column. Although this scenario appears extremely simplistic, it is one that can be reasonably modeled in the laboratory and still approximate conditions in an actual shallow water ocean environment. The methods used to model and measure the acoustic field are relatively untested. Indeed, this attempt at laboratory modeling was performed not only to verify IFD predictions, but also to see if the environment could be successfully modeled in the laboratory.

E. EXPERIMENTAL DESIGN

1. The Tank

A fiberglass coated wooden tank was used. The tank is 304 centimeters in length, 117 centimeters wide and 95 centimeters deep. Sand filling the bottom of the tank was shaped to form the ten degree sloping bottom, and measurements were taken over a range of two meters. Maximum water depth in the tank was 35 centimeters. A 100 kHz source was placed at mid-channel depth (17.5 centimeters). The layout of the tank is depicted in Figure 3.1.

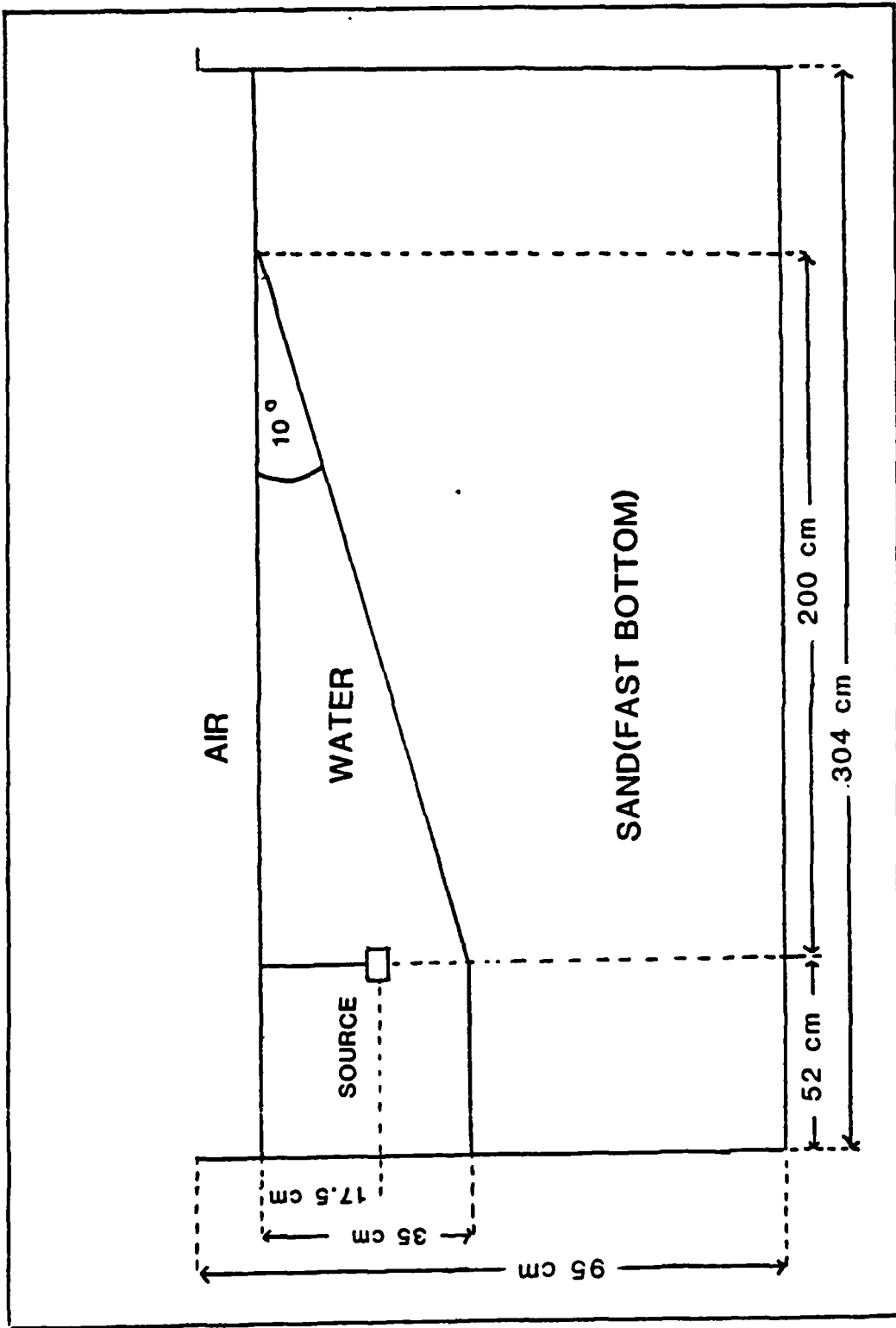


Figure 3.1 Experimental Tank Set Up.

A slope of ten degrees was selected for several reasons. To begin with, even though a ten degree slope is greater than most ocean bottom slopes, it is still small enough to be considered realistic. Perhaps most important, the ten degree slope was selected because given the frequency limitations (discussed later in this chapter) and range limitations, this wedge angle allowed the source to be placed many (41.6) dump distances from the apex. A large number of dump distances was necessary to simulate a distant source.

The bottom material used in the experiment was #30 fine grade sand. The grain size ranged from 0.15 millimeters to 0.70 millimeters. The sand was treated with a technique used by Baek (1984) to remove air from the sediment. This technique used a high speed jet to agitate the sand/water mixture to remove the bubbles and then allowed the sand to settle for several days before the experiment was initiated.

Fresh (tap) water served as the medium in the tank. To remove air bubbles, the water was allowed to settle in a settling tank before being transferred to the experimental tank for use. The water in the tank was periodically treated with chlorine bleach to prevent the growth of biological material.

2. Signal Generating/Receiving Equipment

The acoustic signal used for the measurements was produced by a function generator, sent through an amplifier and then transmitted into the water by a directional transducer resonant at 100 kHz. The dimensions of the active face of the transducer were 7.0 cm in width and 2.0 cm in height. These dimensions resulted in an approximate beamwidth (angle from the acoustic axis to the first theoretical null) of 11.9 degrees in the horizontal and 46.3 degrees in the vertical. The narrow horizontal beam minimized reflections

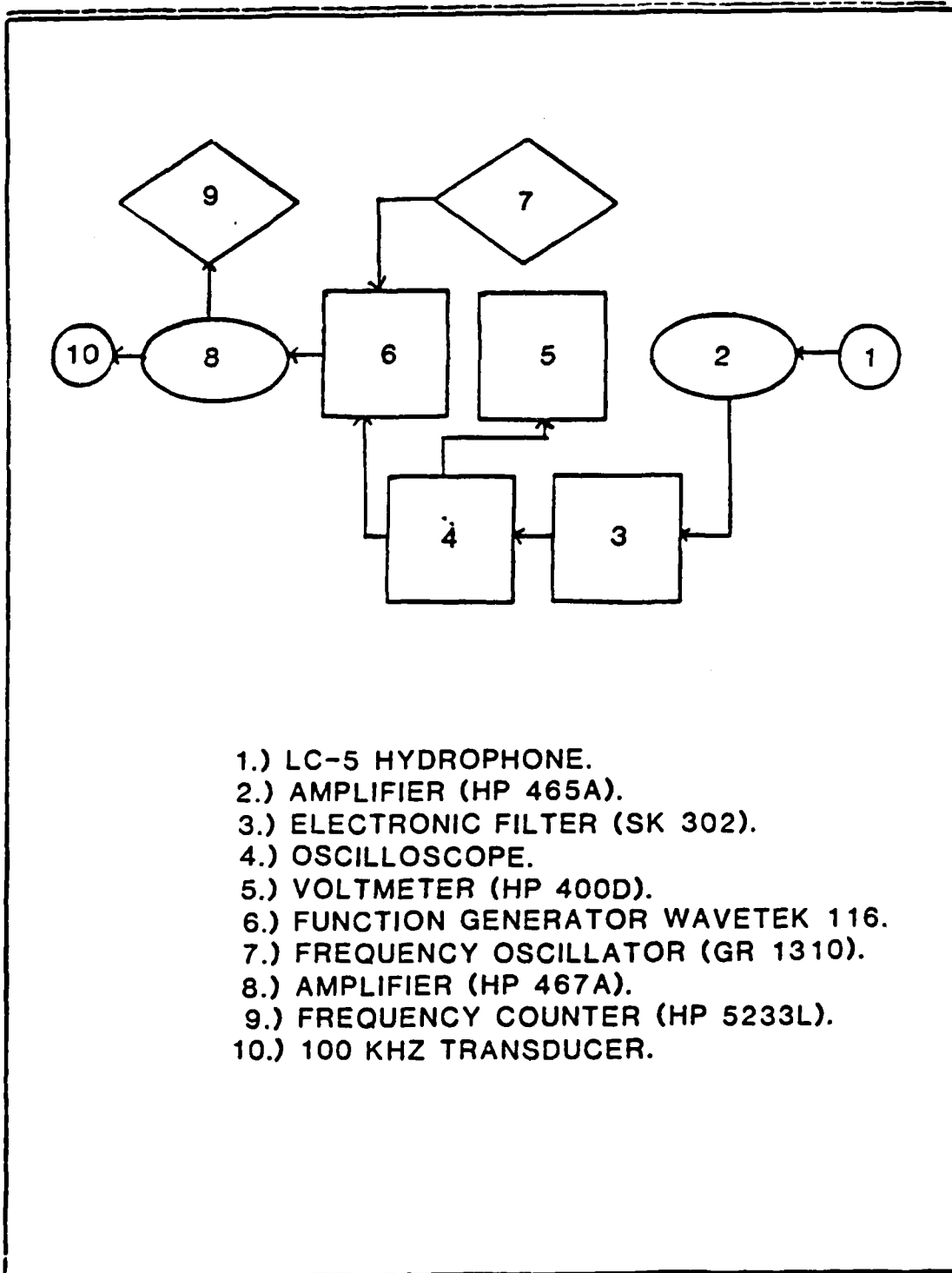
from the sidewalls of the tank, while the wide vertical beam allowed complete ensonification of the channel in the vertical dimension.

The signal was received by an LC-5 omni-directional hydrophone, sent through an amplifier and filter, and then displayed on an oscilloscope and voltmeter. A schematic showing the electronic setup is shown in Figure 3.2.

A frequency of 100 kHz was selected for two practical reasons. First, to avoid particle scattering by the sediment, the acoustic wavelength must be at least three times larger than the grain size of the sediment (Anderson and Liebermann, 1968). The largest grain size in the sand was 0.07 cm, so that a wavelength of 1.45 cm (100 kHz) was sufficiently large enough to be immune to this effect. Second, the 100 kHz frequency and the properties of the sand provide a dump distance that is small enough to allow the source to be positioned many dump distances from the apex.

Shaping the sand bottom into a ten degree wedge with a uniform and smooth interface proved to be a long and tedious process. To facilitate this modeling, wooden supports (two-by-fours) were mounted along the length of both sides of the tank. These supports were elevated at one end of the tank to achieve the required ten degree slope. A scraping device was constructed with wooden supports and a metal scraping blade that extended across the width of the tank. This scraping device consisted of wooden supports along the top that reached across the tank and could be pulled along the elevated wooden supports on both side of the tank. This scraping device was pulled along the supports repeatedly until a smooth slope of ten degrees was sculptured from the sand.

Holes had to be drilled into the metal scraping blade because when a solid blade was used in the shallow portion of the slope, water trapped behind the blade was



- 1.) LC-5 HYDROPHONE.
- 2.) AMPLIFIER (HP 465A).
- 3.) ELECTRONIC FILTER (SK 302).
- 4.) OSCILLOSCOPE.
- 5.) VOLTMETER (HP 400D).
- 6.) FUNCTION GENERATOR WAVETEK 116.
- 7.) FREQUENCY OSCILLATOR (GR 1310).
- 8.) AMPLIFIER (HP 467A).
- 9.) FREQUENCY COUNTER (HP 5233L).
- 10.) 100 KHZ TRANSDUCER.

Figure 3.2 Electronic Equipment Schematic.

forced beneath the scraper gouging the smooth bottom. This bottom modeling technique was slow because, once a pass was made over the bottom, the water became turbid and it was then impossible to see the bottom. When the bottom was not visible, it was impossible to see where further smoothing was necessary until the water settled several hours later. In addition, as this smoothing process continued a silty residue became separated from the sand and settled out on top of the sand. This residue would be easily resuspended and eventually had to be removed using a water siphon.

C. MEASUREMENT PROCEDURES

Measurement of the pressure field within the water was done by lowering the receiver in depth at specific ranges of interest. The receiving hydrophone was attached to a pair of micrometers at right angles to one another, that was in turn bolted to a board which spanned the width of the tank. Once the board was placed close to a range of interest, one micrometer was used to give fine adjustments in range and the other in depth.

The measurements were subject to both an accuracy and a precision error. On a given day, with the water level fixed and the cross-tank support set at a particular place in the tank, it was possible to position the receiving hydrophone with an accuracy in depth and range of plus or minus 0.06 centimeters (one turn of the micrometer). To prevent the sand 'inland' of the apex from drying out when not taking measurements, enough water was added to the tank after each data run to keep the sand completely submerged. The next time measurements were taken, water had to be removed from the tank to reestablish the beach. Because of these small changes in the water level the horizontal position of the beach was subject to a precision error estimated to be within plus or minus one centimeter.

The final decision associated with the measurements centered on whether to use a triggered pulse or a continuous wave (CW) signal. With a triggered pulse it was possible to distinguish the received signal from interference caused by reflections off the side of the tank. On the other hand, by using a triggered pulse there was a possibility that the pulse length was not long enough for the acoustic energy associated with paths reflecting off the top and bottom of the water column to overlap the direct path from the source to receiver. A CW signal would avoid potential pulse length problems, but it would be impossible to distinguish between the actual signal and interference. The use of a source with a narrow horizontal beam reduced the effects of reflections from the side walls, but there was still the possibility of interference from side lobes reflected from the sides.

It was necessary to determine the best means to take measurements. This was done by taking measurements at the same location with different pulse lengths to determine the required pulse length to give consistent results and then comparing these results to those obtained with a CW signal. The third dump distance (14.4 cm from the apex) and just past the tenth dump distance (50.0 cm from the apex) were chosen, and measurements were taken for pulsed signals of 64 and 256 cycles, and a CW signal. These measurements can be seen in Figure 3.3 through Figure 3.5. In the figure depicting results at the third dump distance, the CW measurements are shown as the solid curve, the 64 trigger cycle results are displayed as circular points, and the 256 trigger cycle results are depicted as triangular points. For clarity, the measurements taken just past the tenth dump distance are shown in two figures. Figure 3.4 compares CW results (solid curve) with the 64 trigger cycle signal (circular points). Figure 3.5 compares CW measurements (solid curve) with the 256 cycle results (circular points).

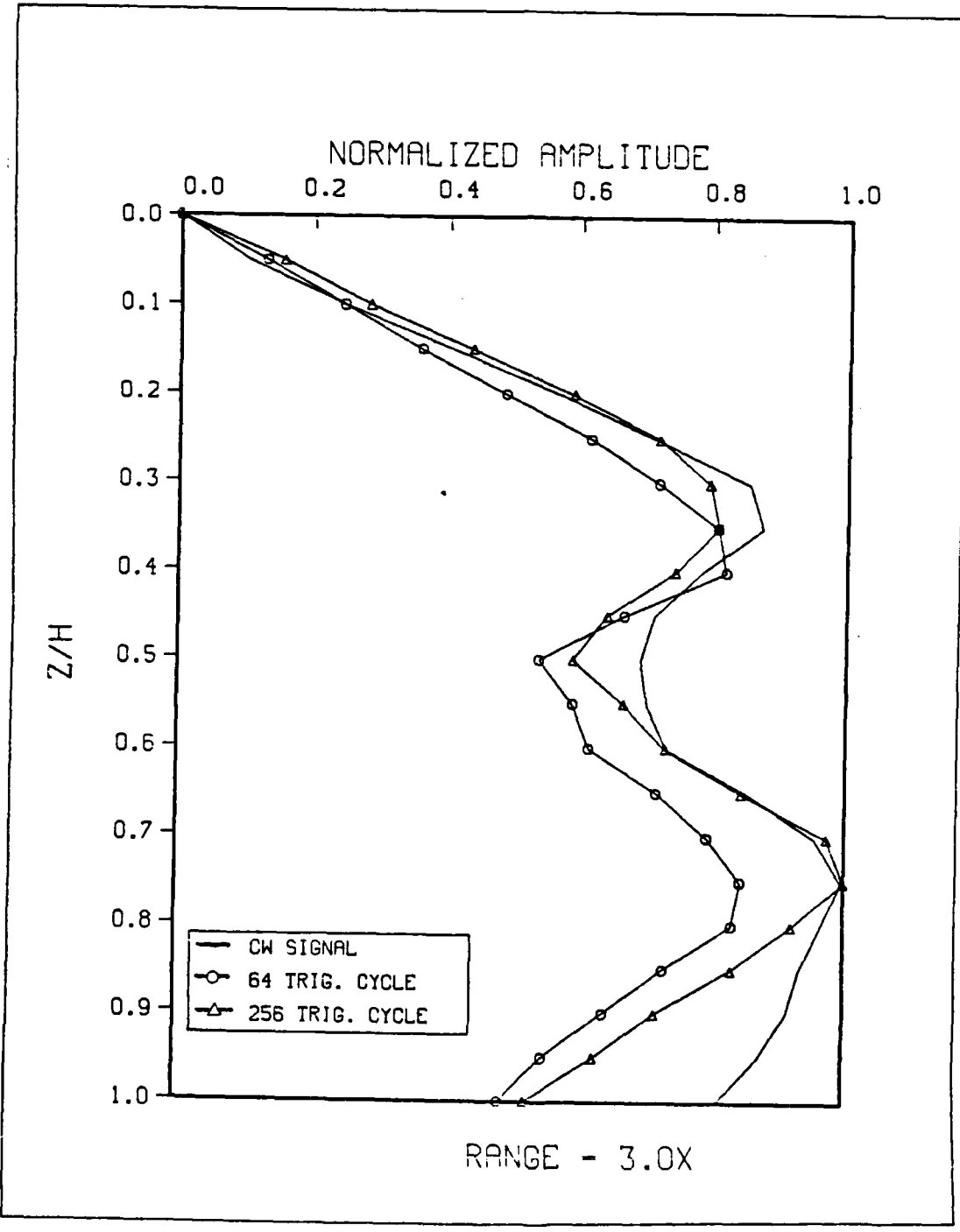


Figure 3.3 Pulse length Analysis at 3.0X.

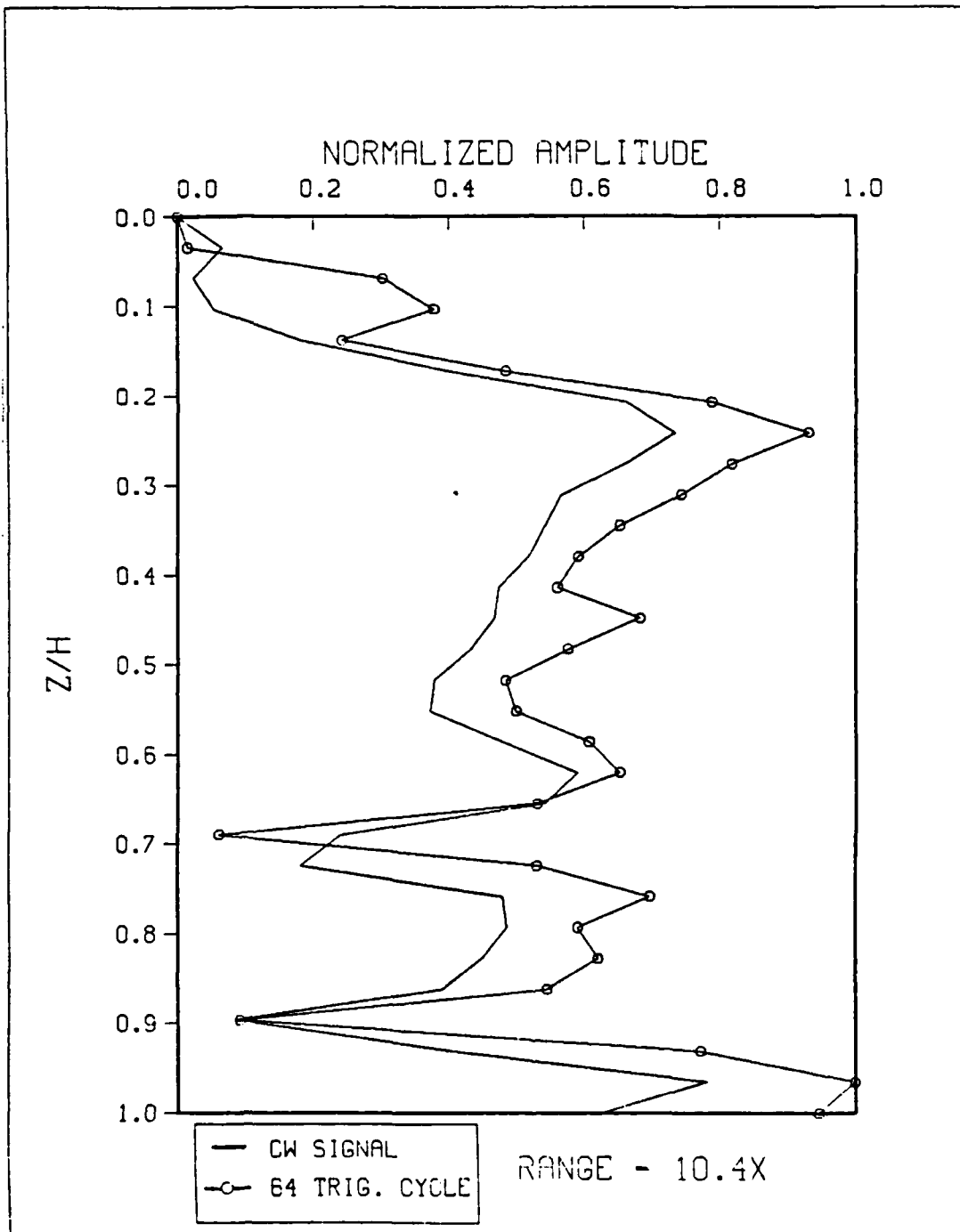


Figure 3.4 Pulse Length Analysis at 10.4X.

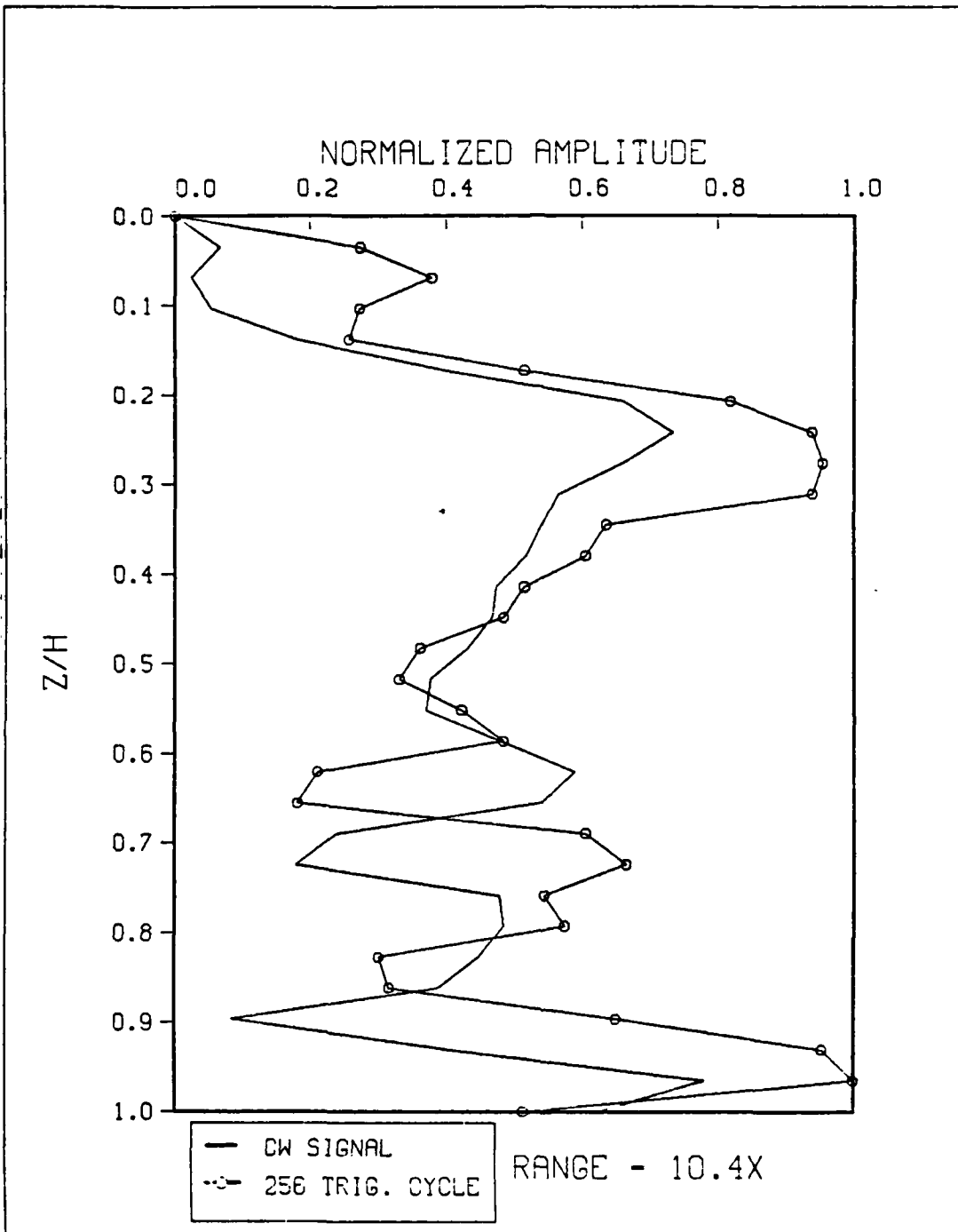


Figure 3.5 Pulse length Analysis at 10.4X.

The pressure amplitude values were normalized by dividing each pressure value by the maximum pressure value in the field. The depth values were also normalized by dividing each depth by the maximum depth.

The results in Figure 3.3 show good agreement between the three curves. In particular, the results for the CW signal and the 256 cycle signal are very similar. The 64 cycle signal shows the same behavior as the CW signal, but differs in magnitude below mid-depth.

The results at 50.0 cm from the apex appear much more complicated than at the third dump distance. Figure 3.4 compares results achieved with the CW signal and the 64 cycle signal. From the figure it can be seen that the two sets of results show good agreement. The measurements depicted in Figure 3.5, which compares the 256 cycle signal and the CW signal show poorer agreement, although the general shapes of both curves remain similar.

These results indicate that interference from the side walls is sufficiently small so that it is possible to make measurements with a CW signal to at least ten dump distances from the apex. Long pulses could also be used, but the difficulty of making voltage measurements with an oscilloscope compared to reading a voltmeter, dictates that measurements should be made with a CW signal.

IV. MODEL RESULT COMPARISONS WITH LABORATORY MEASUREMENTS

A. INTRODUCTION

IFD model predictions and laboratory measurements were obtained for comparison in both a general and detailed analysis. The general analysis compared results every five centimeters from the beach to a range of 50.0 cm from the beach. The measurements were spaced to give results at approximately each of the first ten dump distances. The detailed analysis compared results every centimeter from 3.0 to 11.0 cm from the apex. These measurements were taken to observe the sensitivity of the pressure field to small changes in range.

B. THE GENERAL ANALYSIS

The general analysis compared IFD results and laboratory measurements at approximately each of the first ten dump distances (every five centimeters from the beach). These measurements were obtained by fixing the receiving hydrophone with respect to the cross board and then moving the board out in increments of five centimeters to measure the desired field as a function of depth at each range. The received CW signal was read on the voltmeter.

The comparisons are shown in Figure 4.1 through Figure 4.10. In the figures, the IFD predictions are displayed as a solid line while the experimental measurements are shown as circles connected by a dashed line. Each pressure value was normalized to unity by dividing it by the maximum pressure value for the respective curve. The depth values were also normalized by dividing each depth by the maximum depth in the water column.

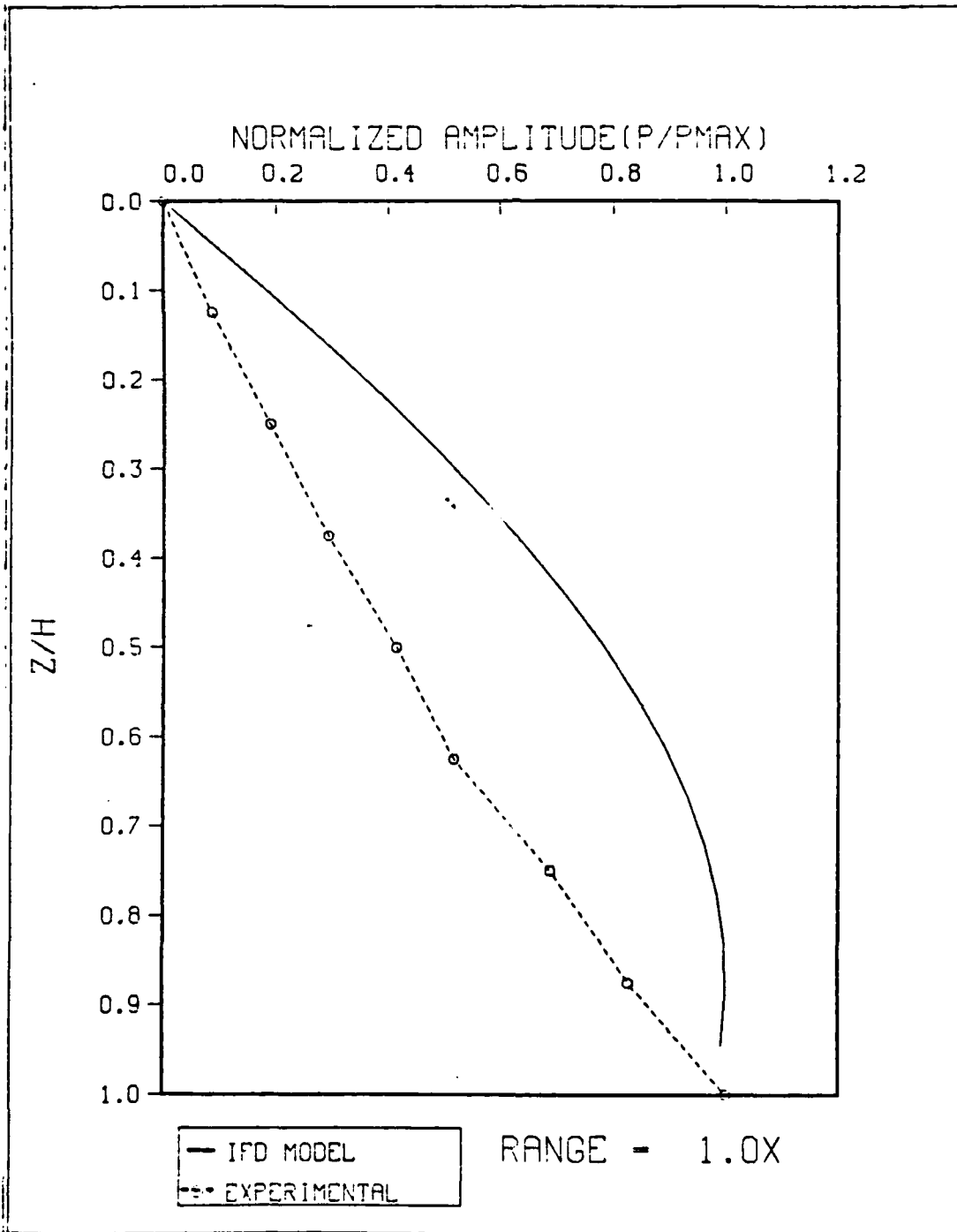


Figure 4.1 Comparison of Results at 1.0X.

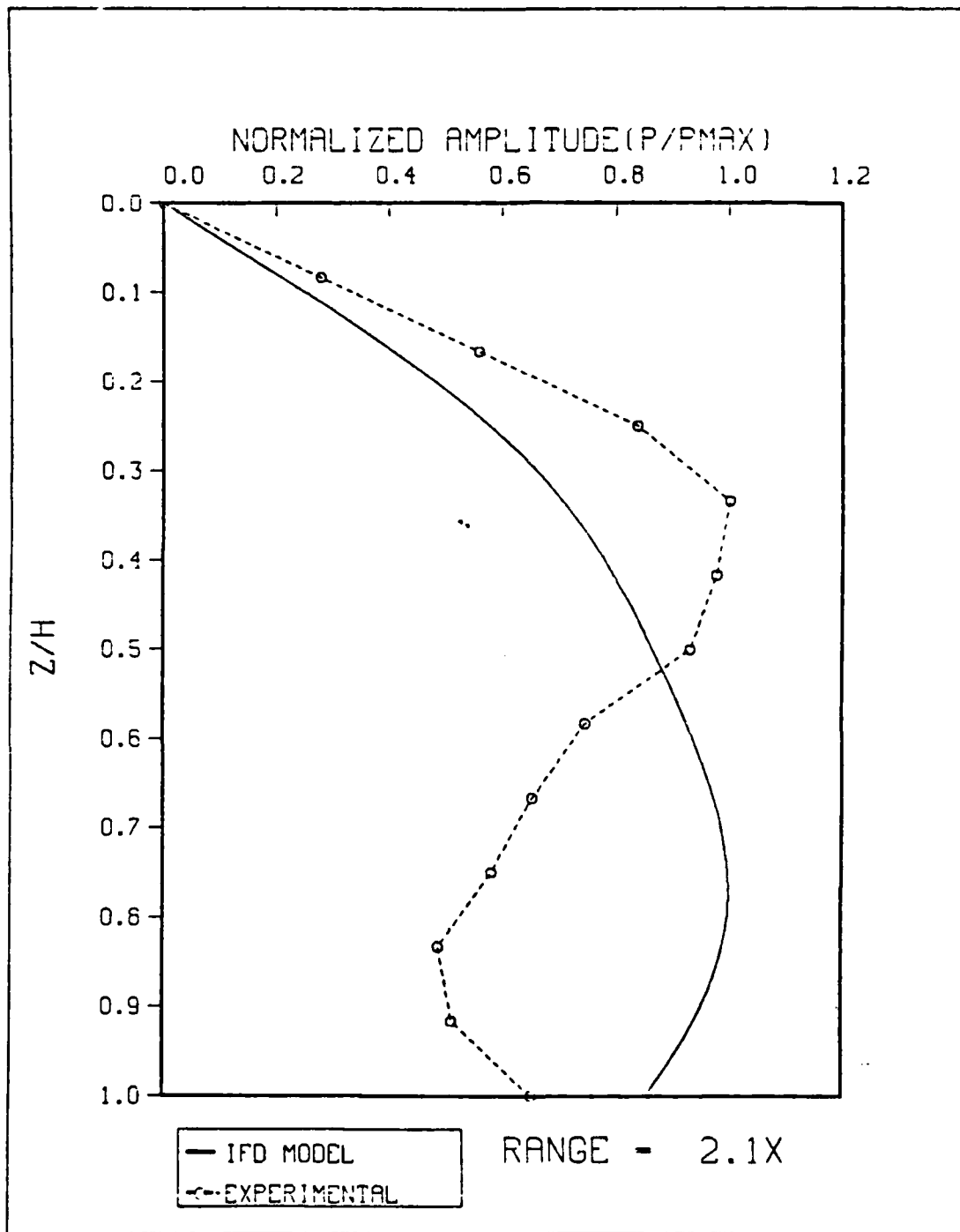


Figure 4.2 Comparison of Results at 2.1X.

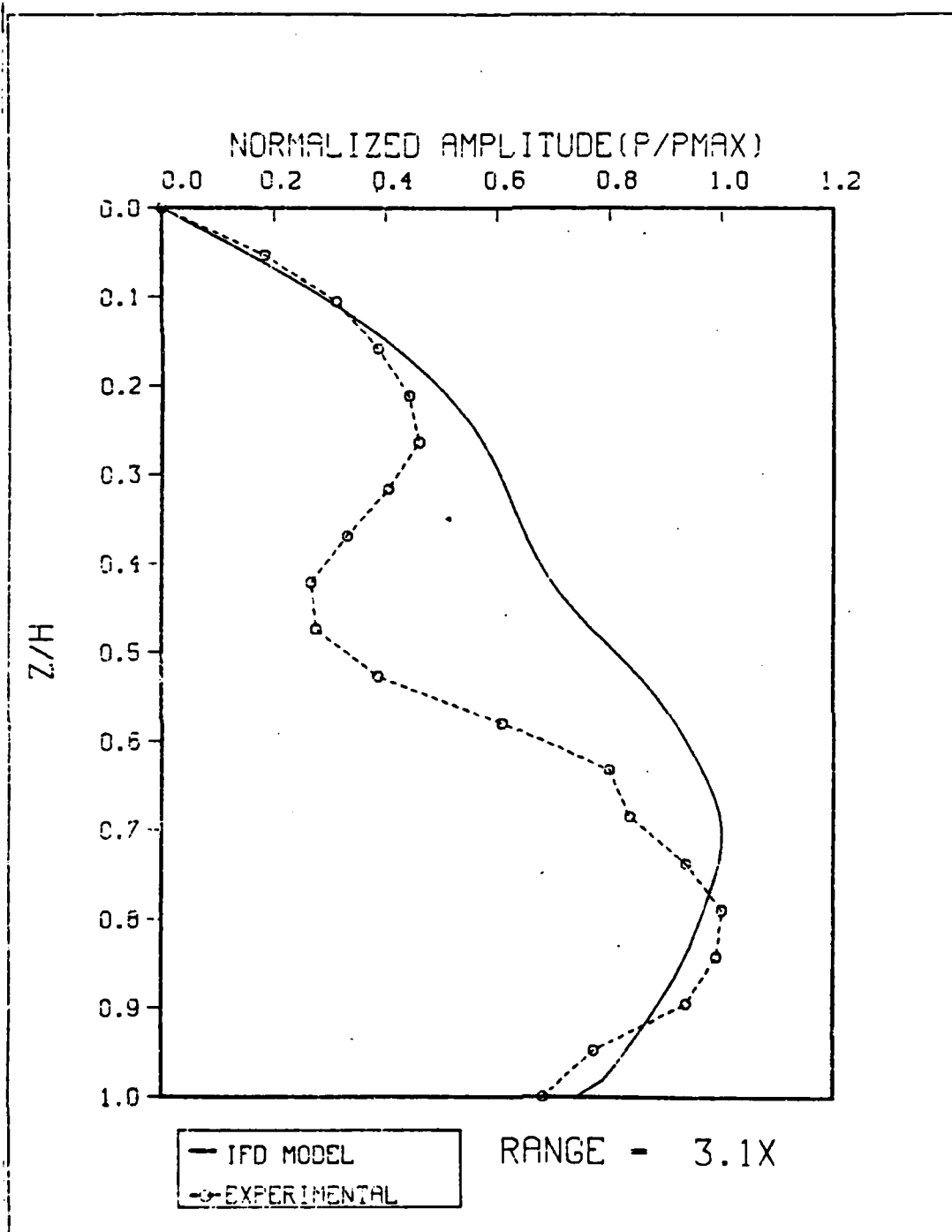


Figure 4.3 Comparison of Results at 3.1X.

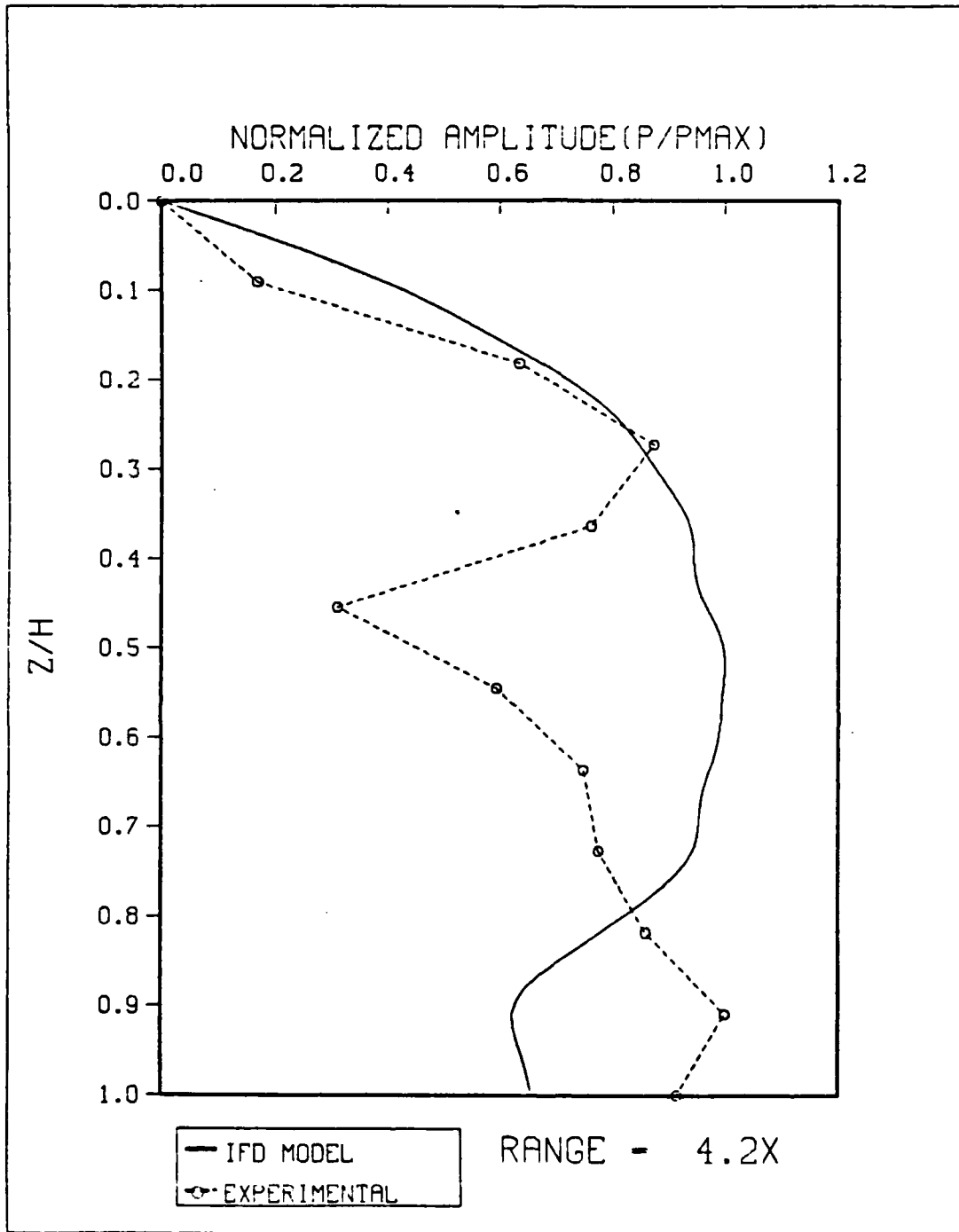


Figure 4.4 Comparison of Results at 4.2X.

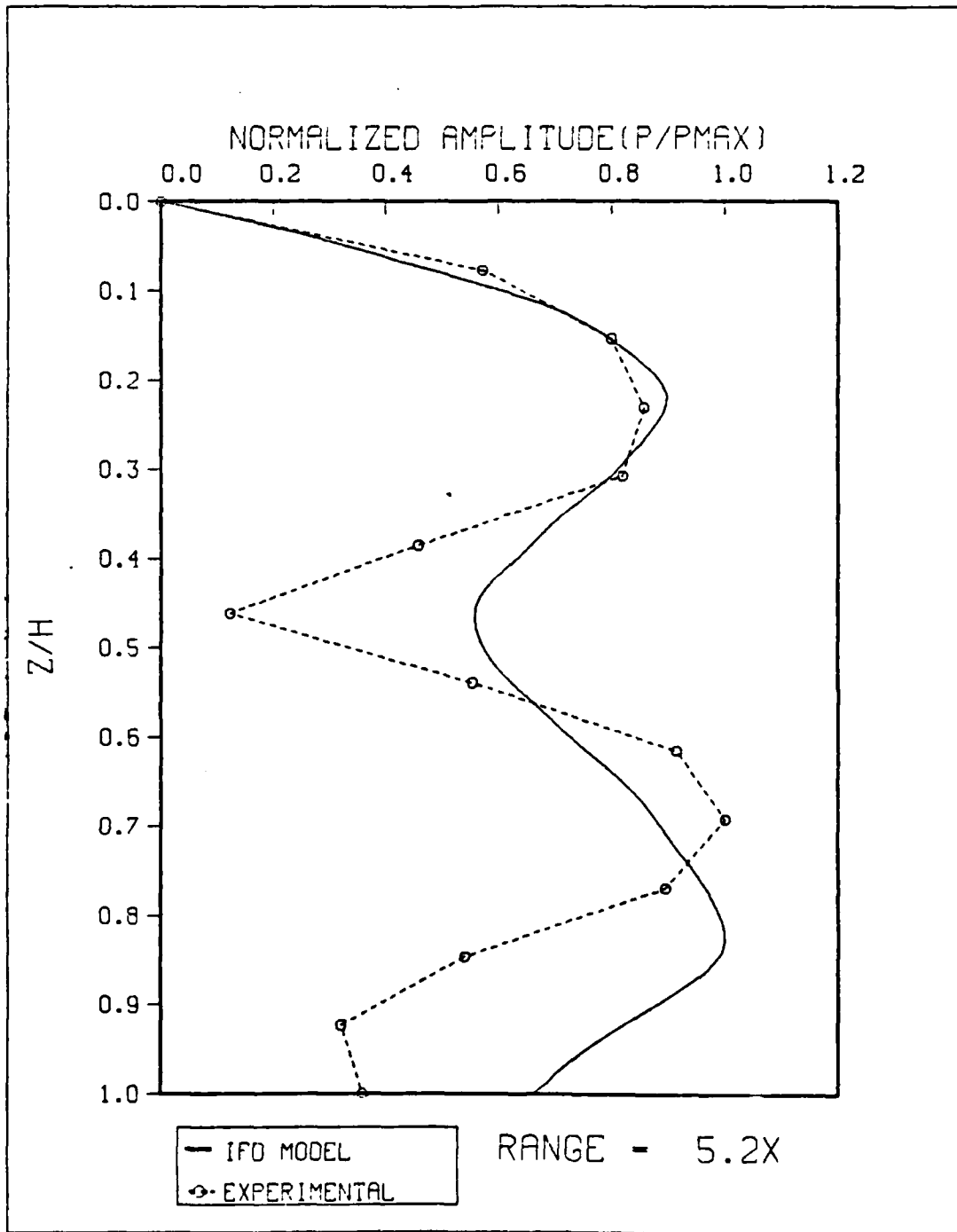


Figure 4.5 Comparison of Results at 5.2X.

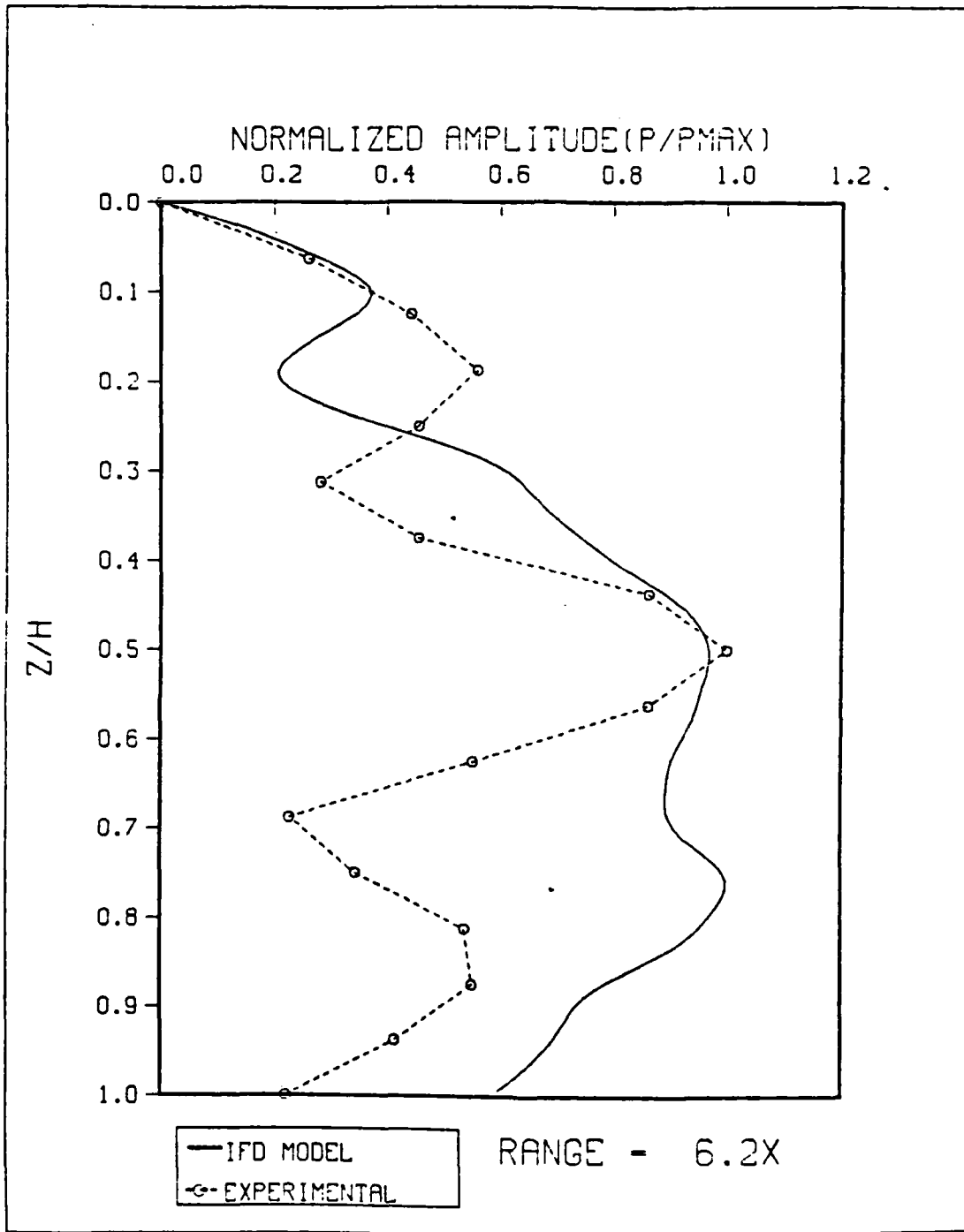


Figure 4.6 Comparison of Results at 6.2X.

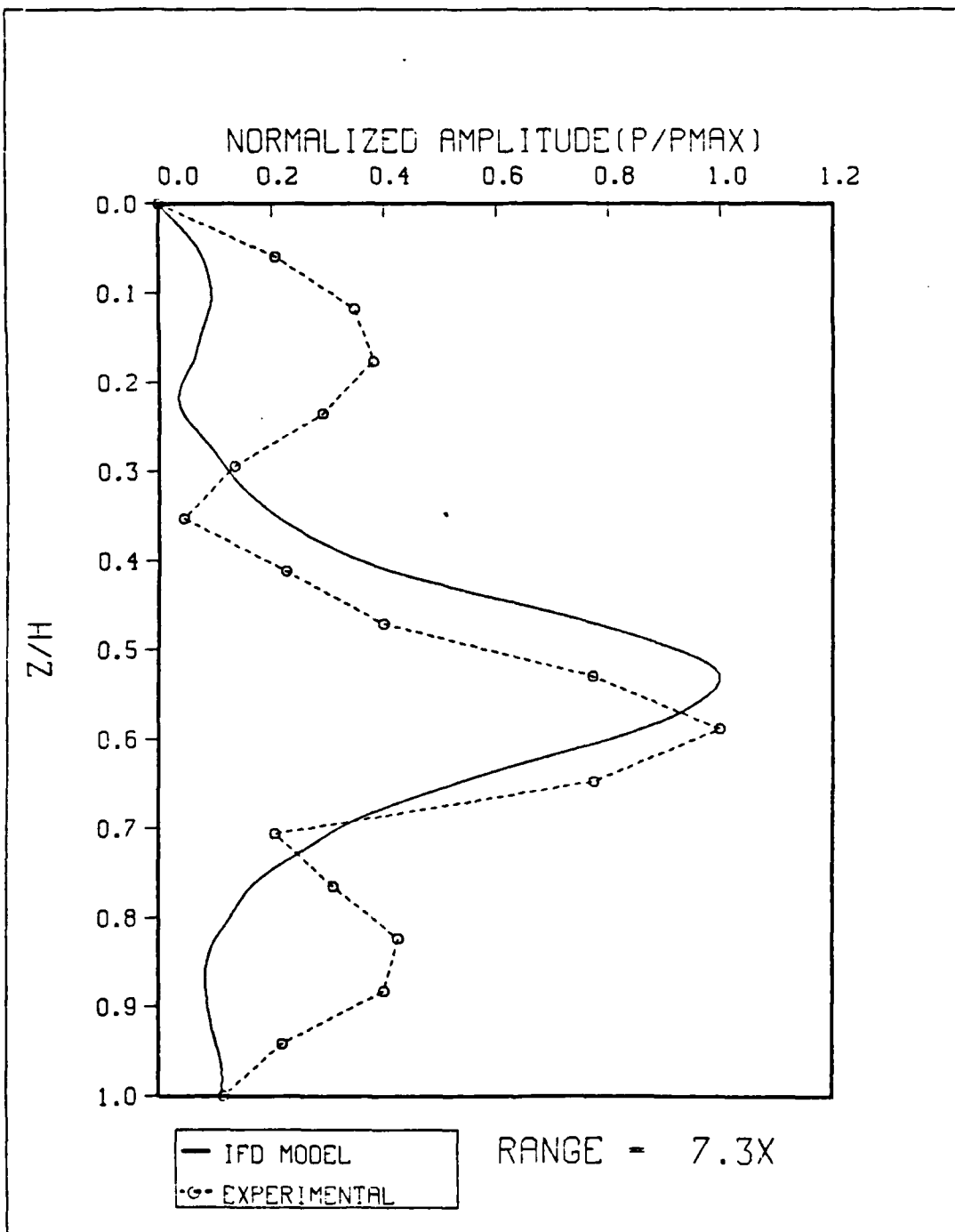


Figure 4.7 Comparison of Results at 7.3X.

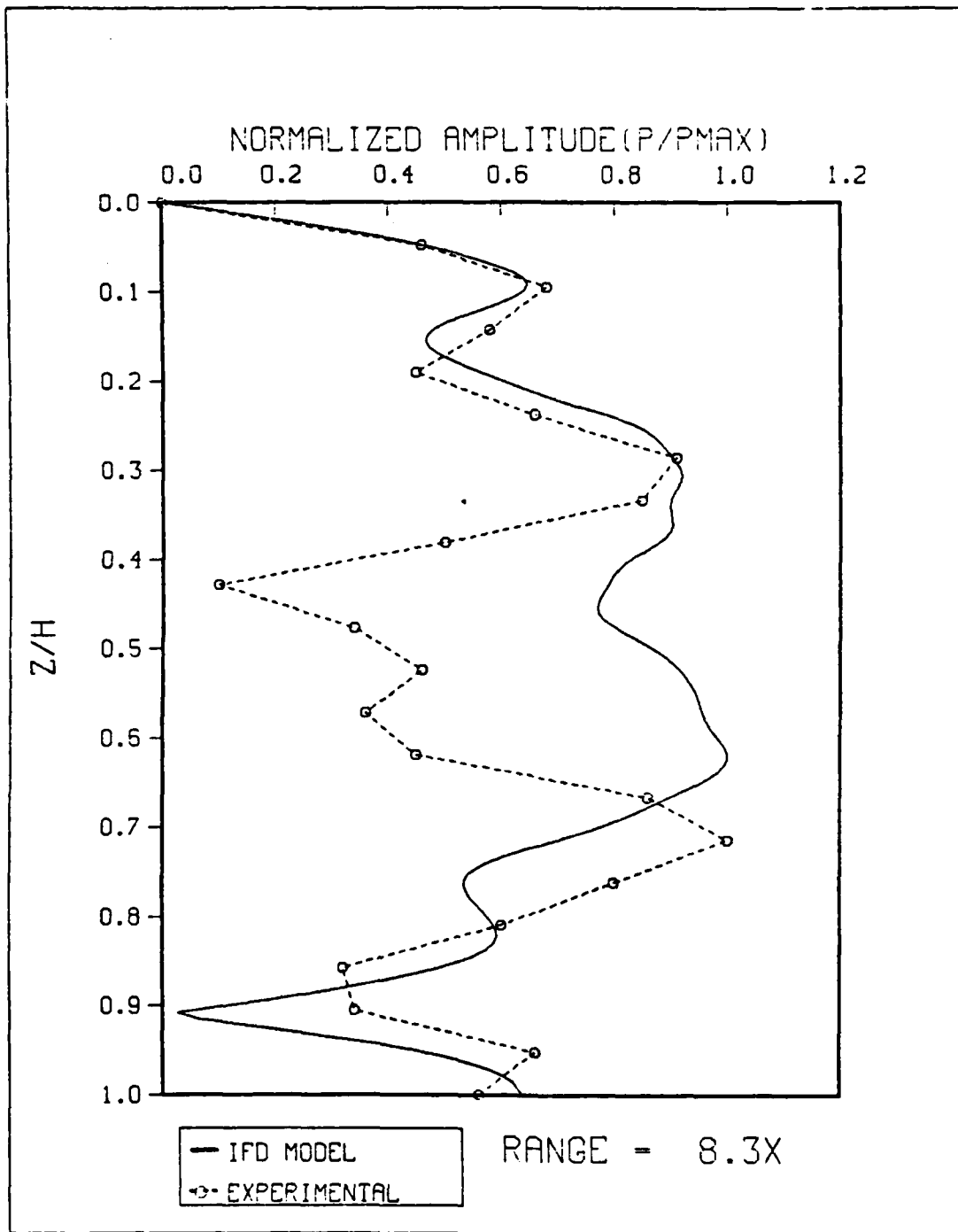


Figure 4.8 Comparison of Results at 8.3X.

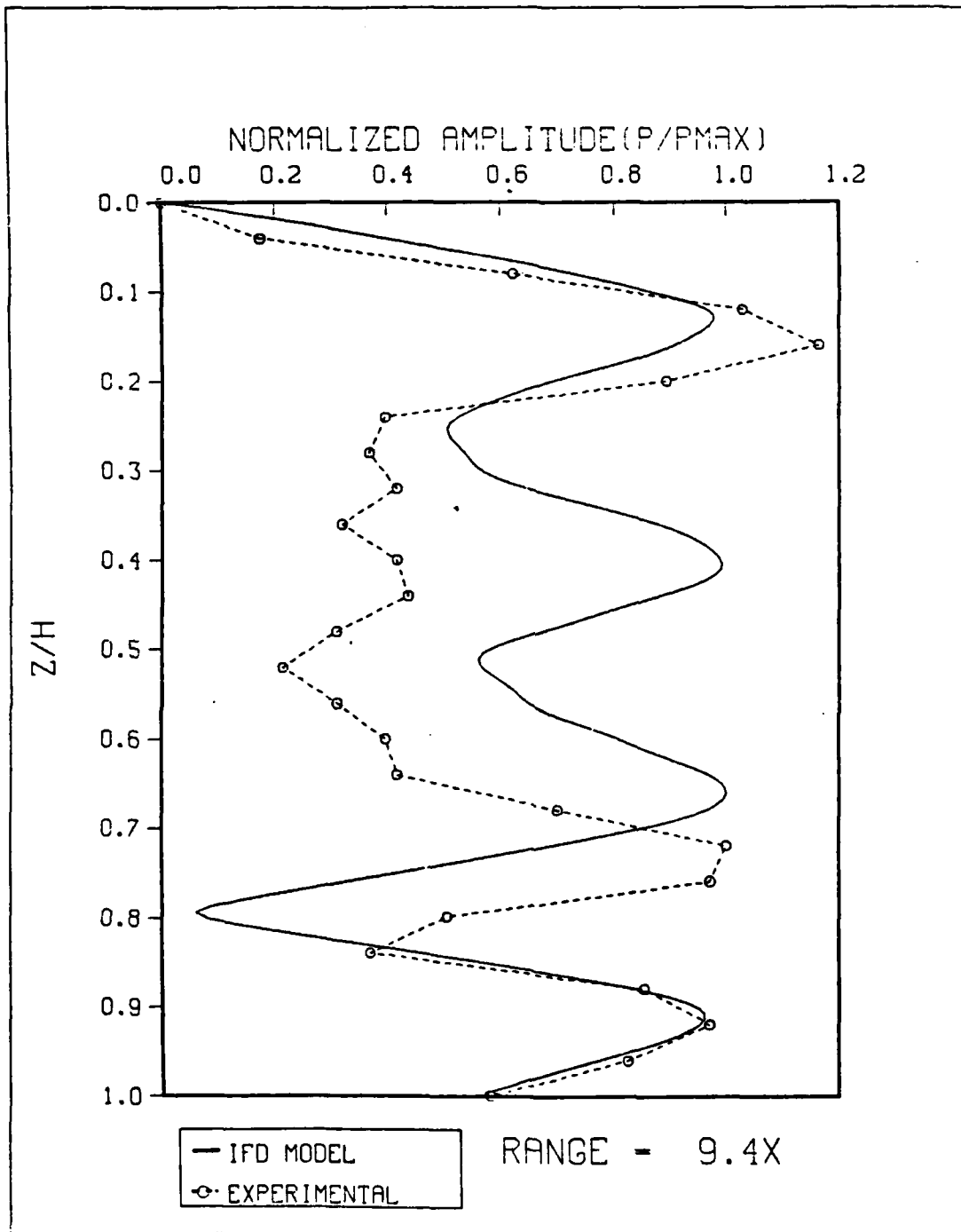


Figure 4.9 Comparison of Results at 9.4X.

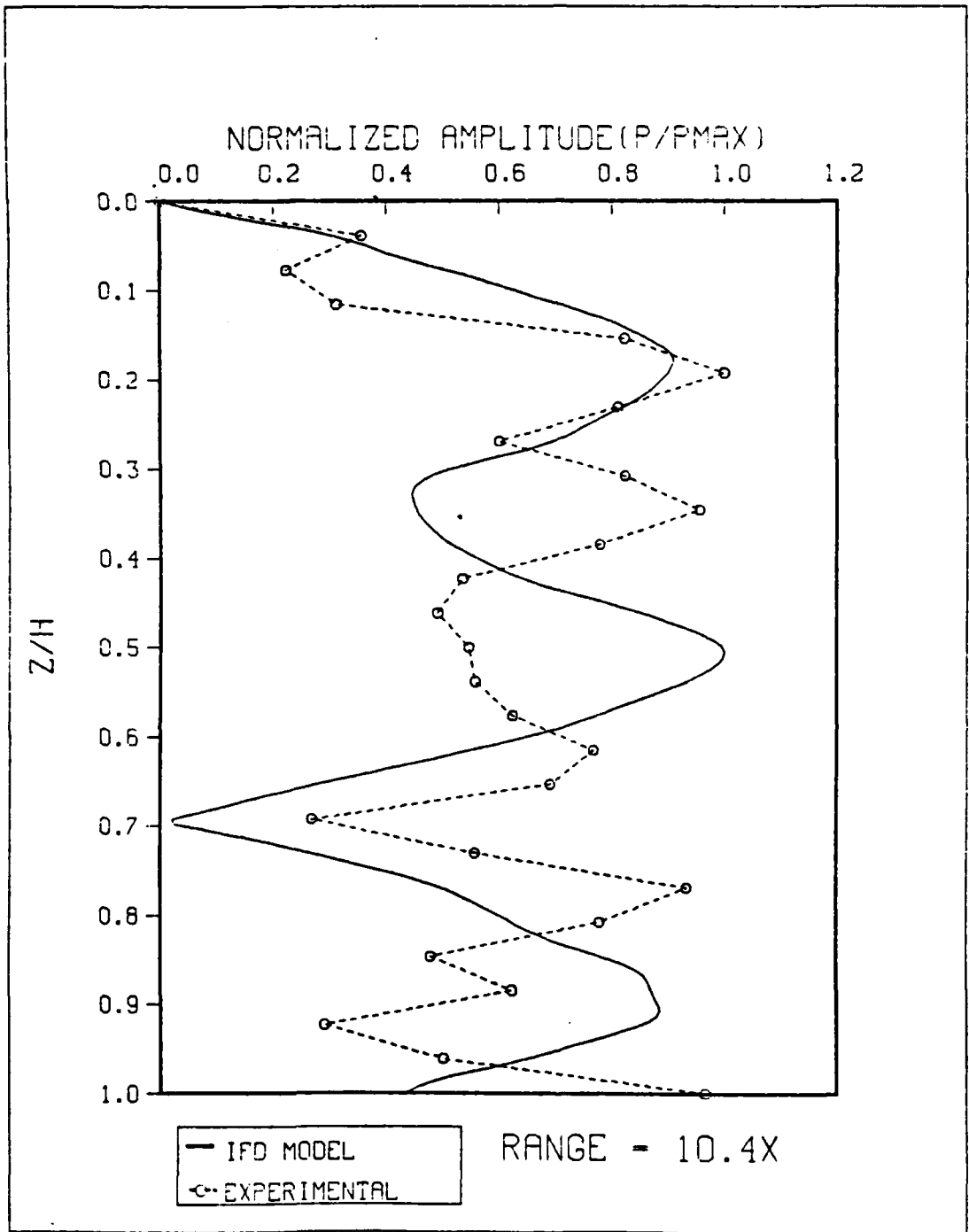


Figure 4.10 Comparison of Results at 10.4X.

In general, the pressure patterns predicted by the IFD and those measured, both become more complicated as the range from the beach increases. At all ranges, there is qualitative agreement in the scale of the predicted features and the scale of the measured features. Quantitative agreement is lacking. This agreement in scale but not detail, suggests that the phases among the normal modes predicted by the model do not accurately reflect the experimental situation.

C. THE DETAILED ANALYSIS

The detailed analysis compared IFD values with experimental measurements every centimeter from 3.0 cm to 11.0 cm from the beach (0.7X to 2.3X). The laboratory measurements were taken by fixing the board at one location and then using the micrometer to adjust the receiver to the desired range. The received CW signal was read from the voltmeter.

These results are depicted in Figures 4.11 through 4.19. In the figures, the IFD predictions are shown as a solid line and the experimental measurements are displayed as circles. Each pressure value was normalized to unity by dividing it by the maximum pressure for the respective curve. The depth values were normalized by dividing each depth by the maximum depth at the particular range.

There is qualitative agreement in the scale of the basic features for all ranges, but quantitative agreement is not observed. The IFD patterns change very little throughout the analysis, while the measured values change more rapidly (especially past 2.0X). The results at 2.1X and 2.3X (Figure 4.18 and Figure 4.19) show that the pressure field can change fairly significantly over a range as short as one centimeter. At those ranges where there is poor agreement between results, there is an indication of phase

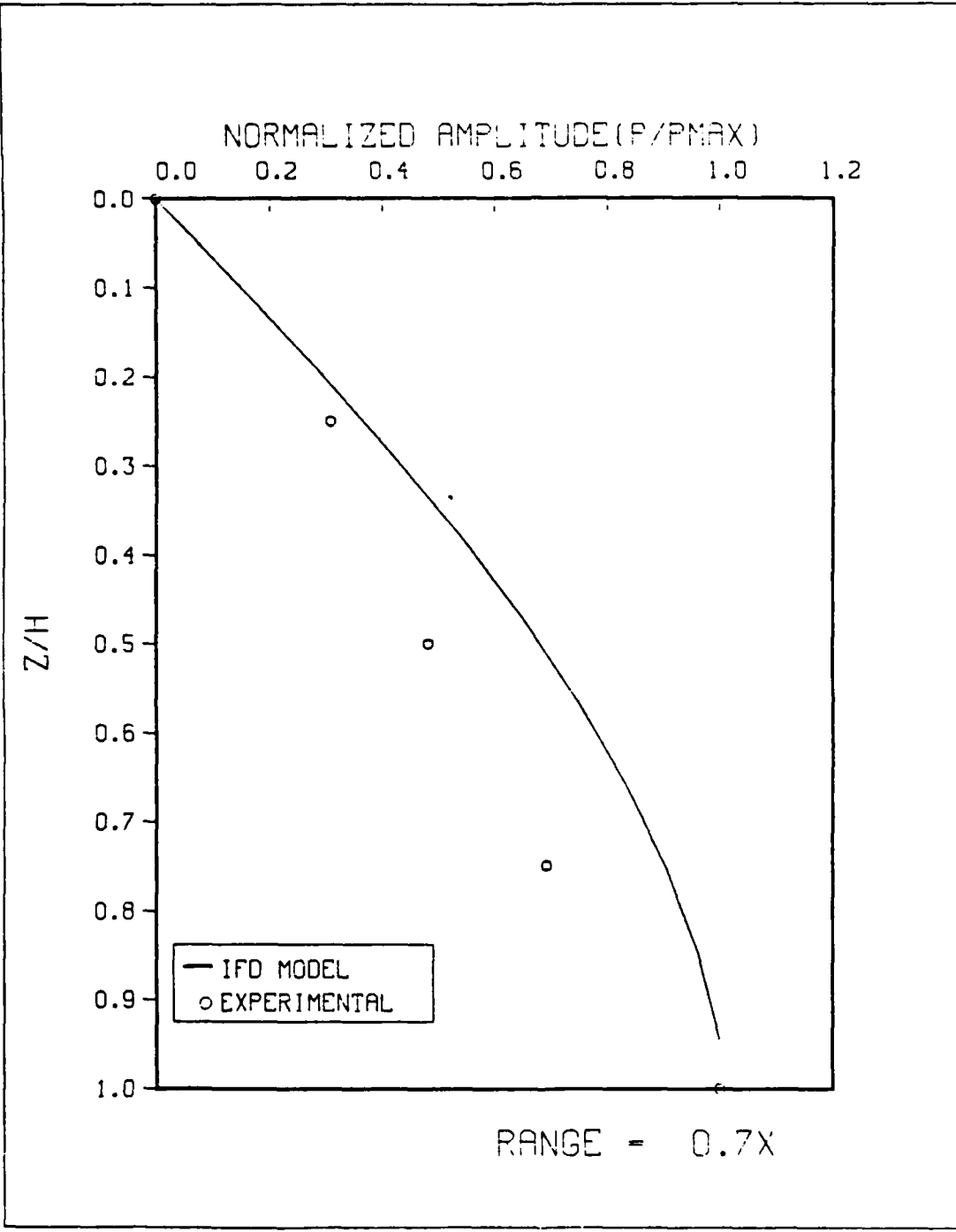


Figure 4.11 Comparison of Results at 0.7X.

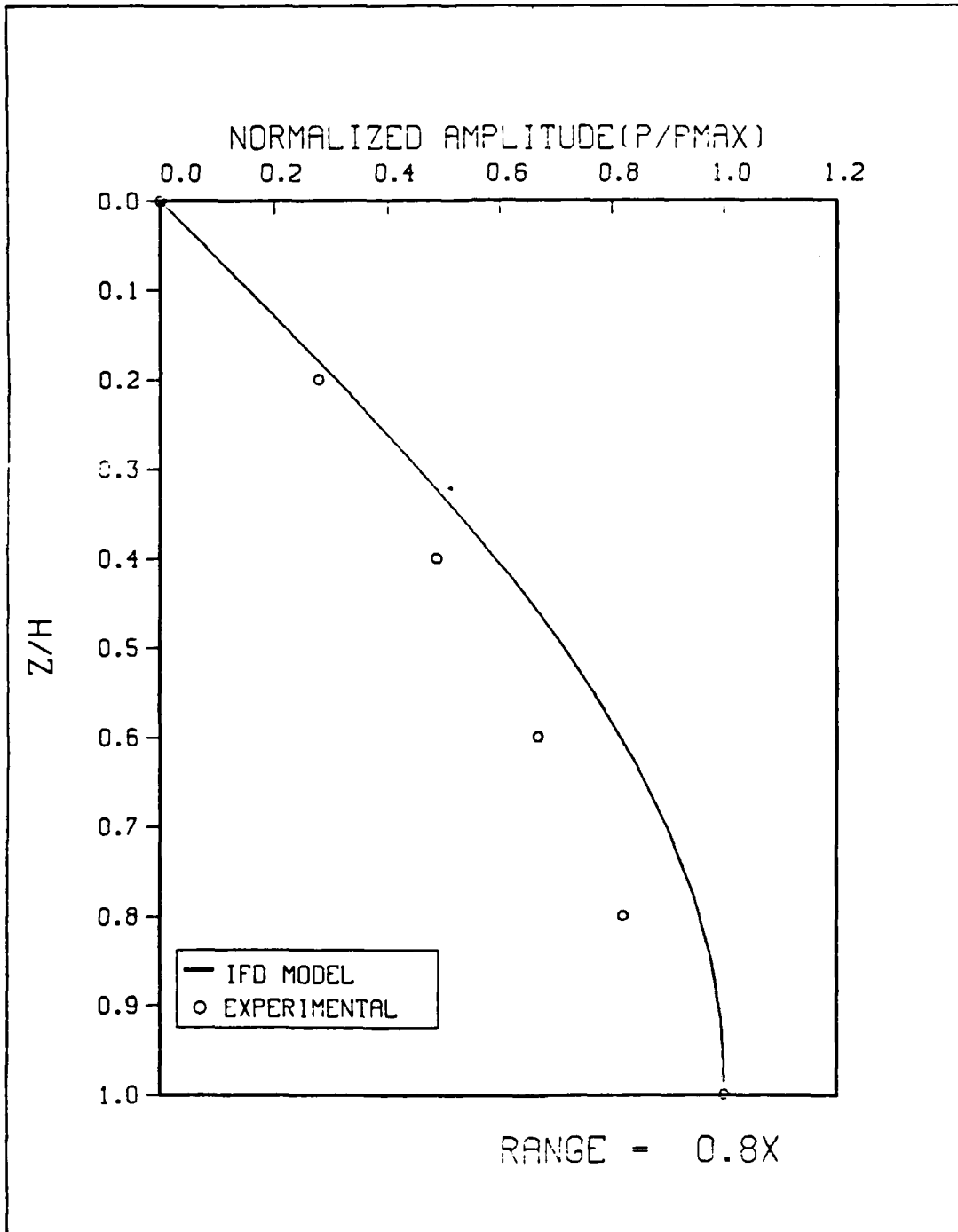


Figure 4.12 Comparison of Results at 0.8X.

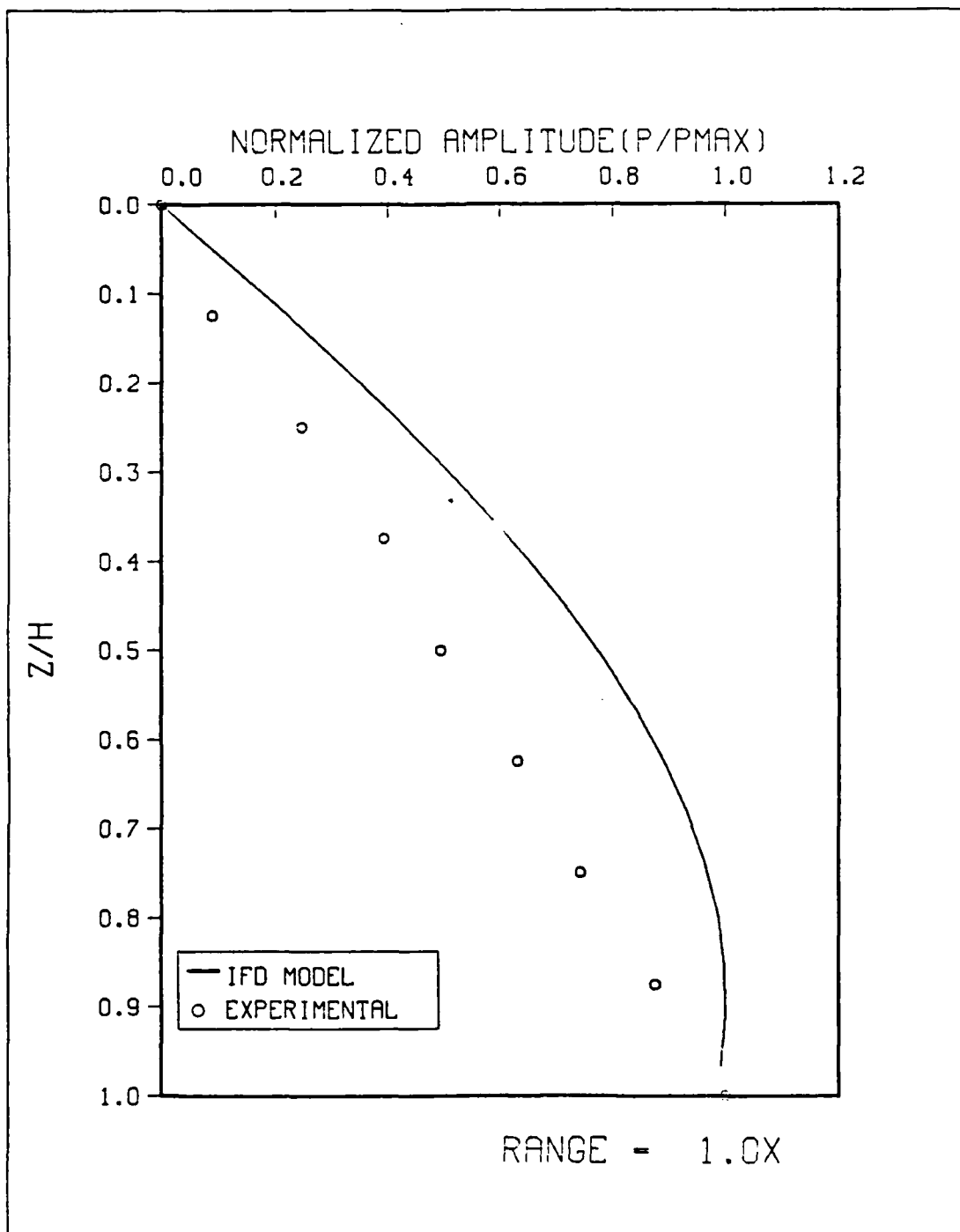


Figure 4.13 Comparison of Results at 1.0X.

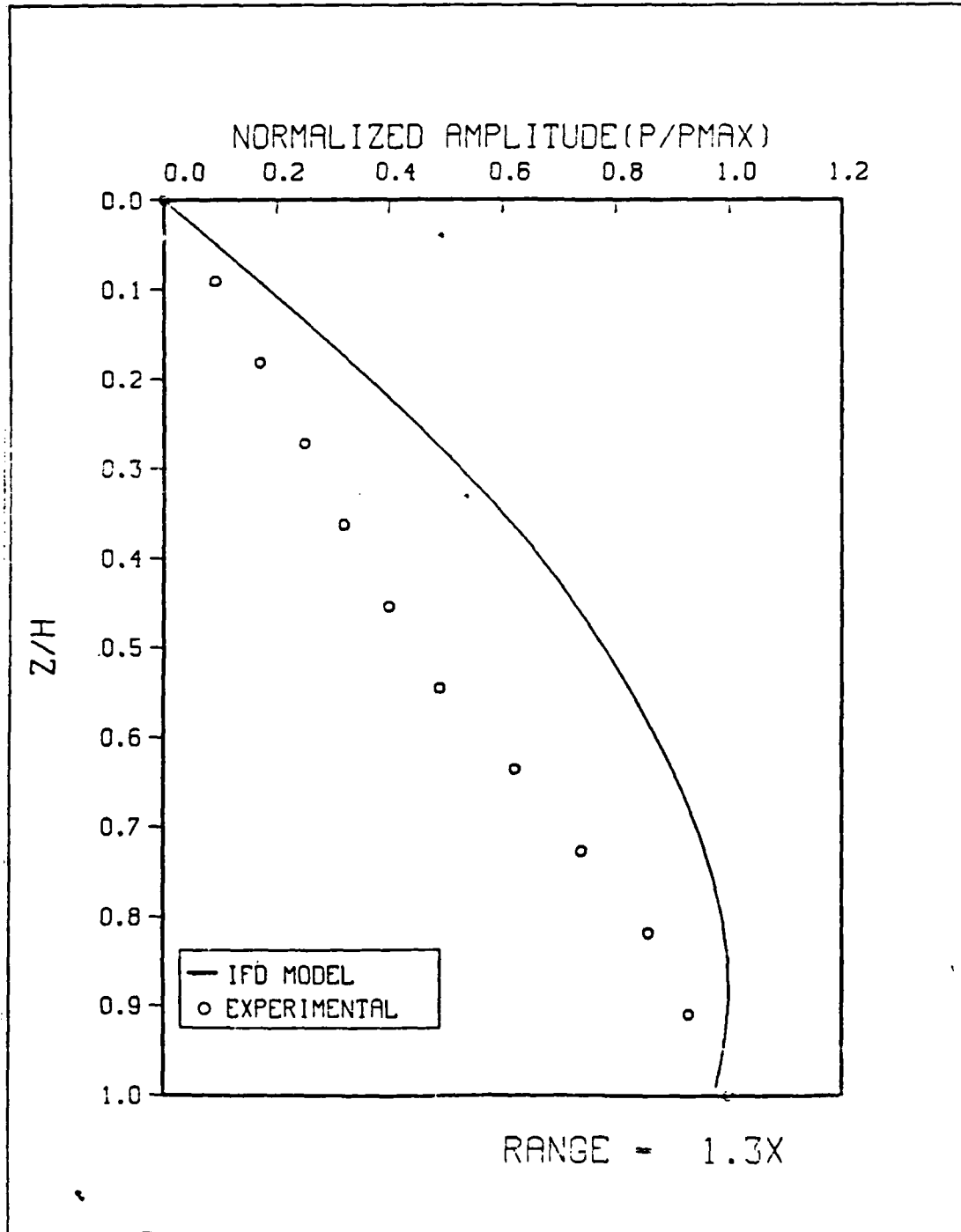


Figure 4.14 Comparison of Results at 1.3X.

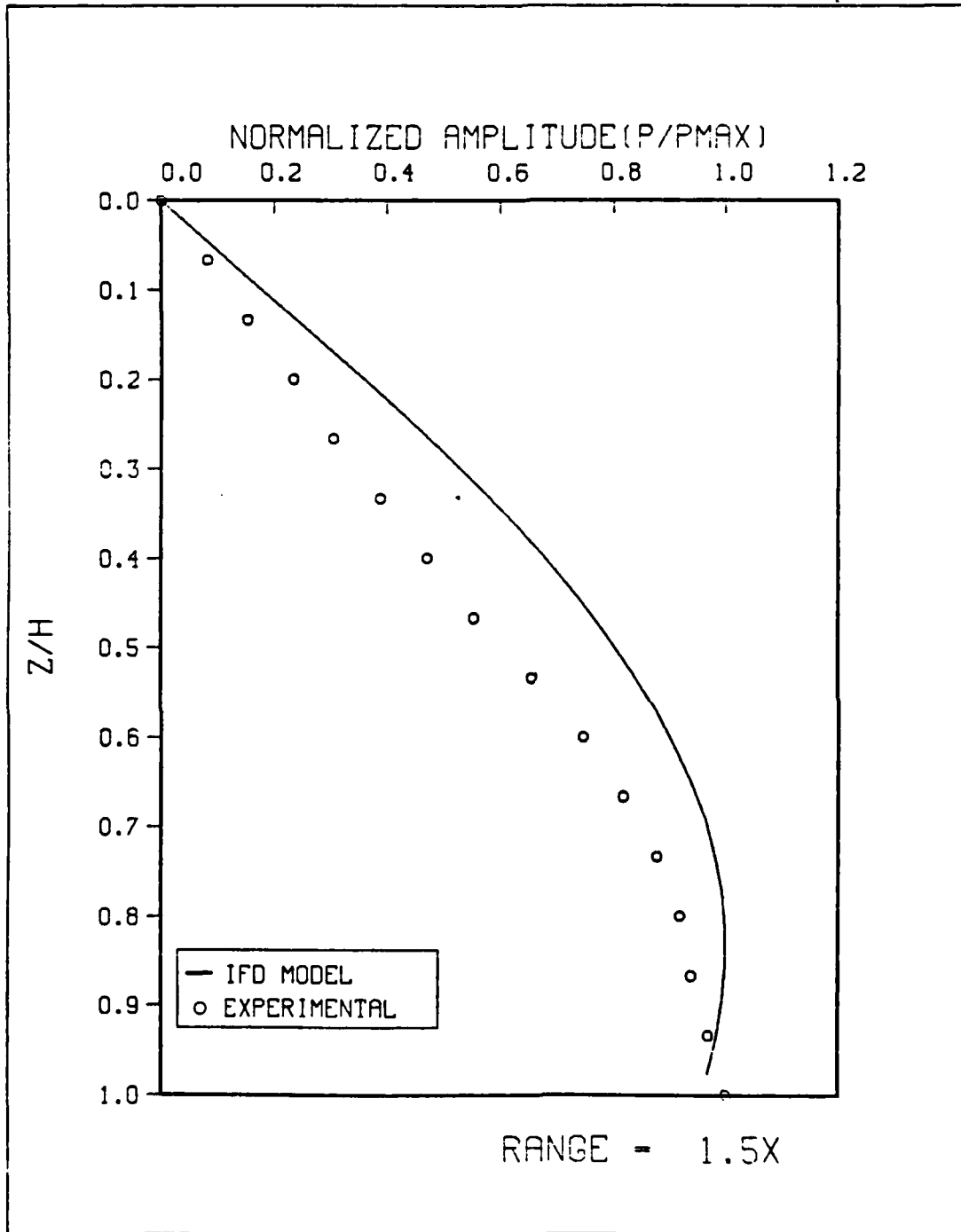


Figure 4.15 Comparison of Results at 1.5X.

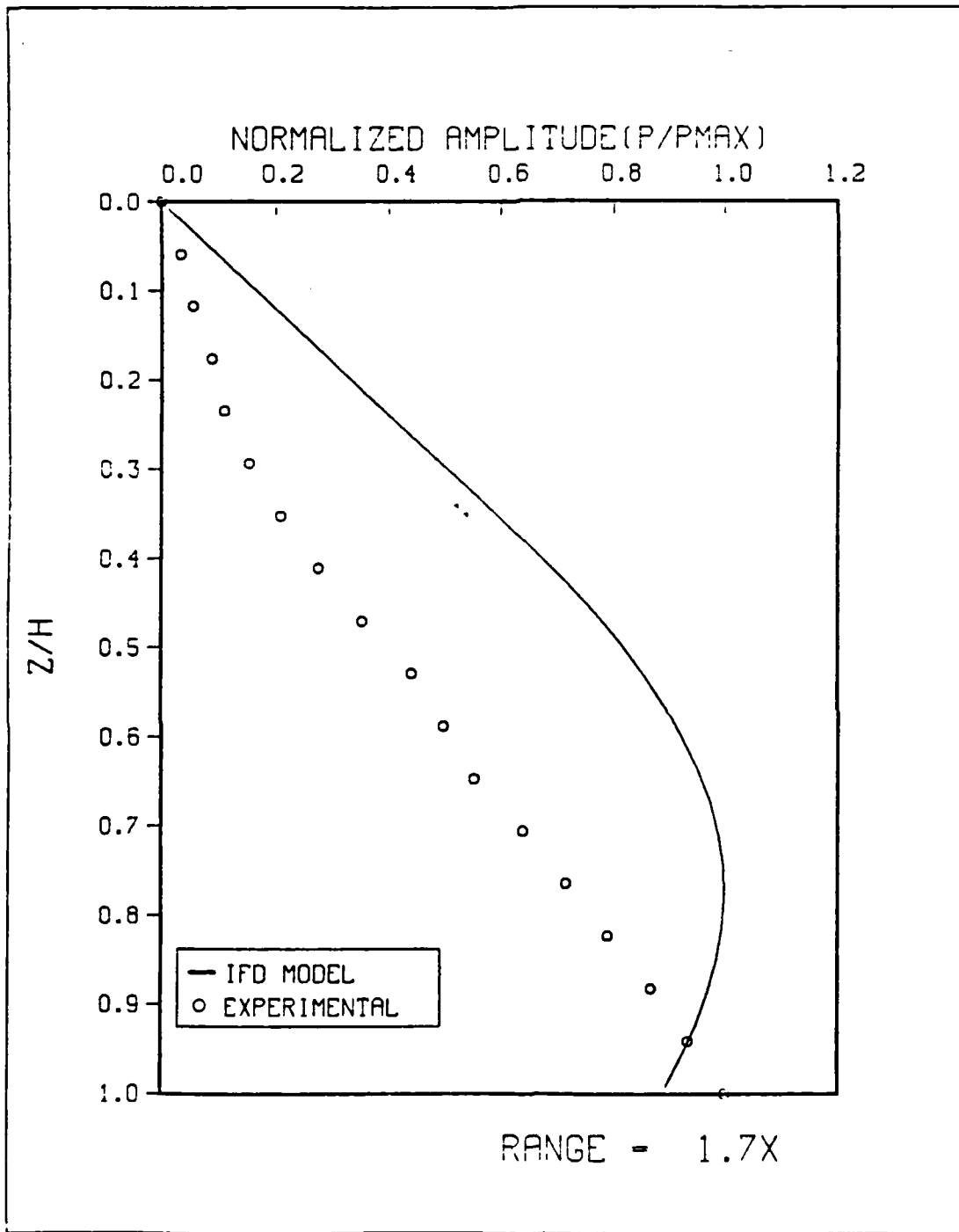


Figure 4.16 Comparison of Results at 1.7X.

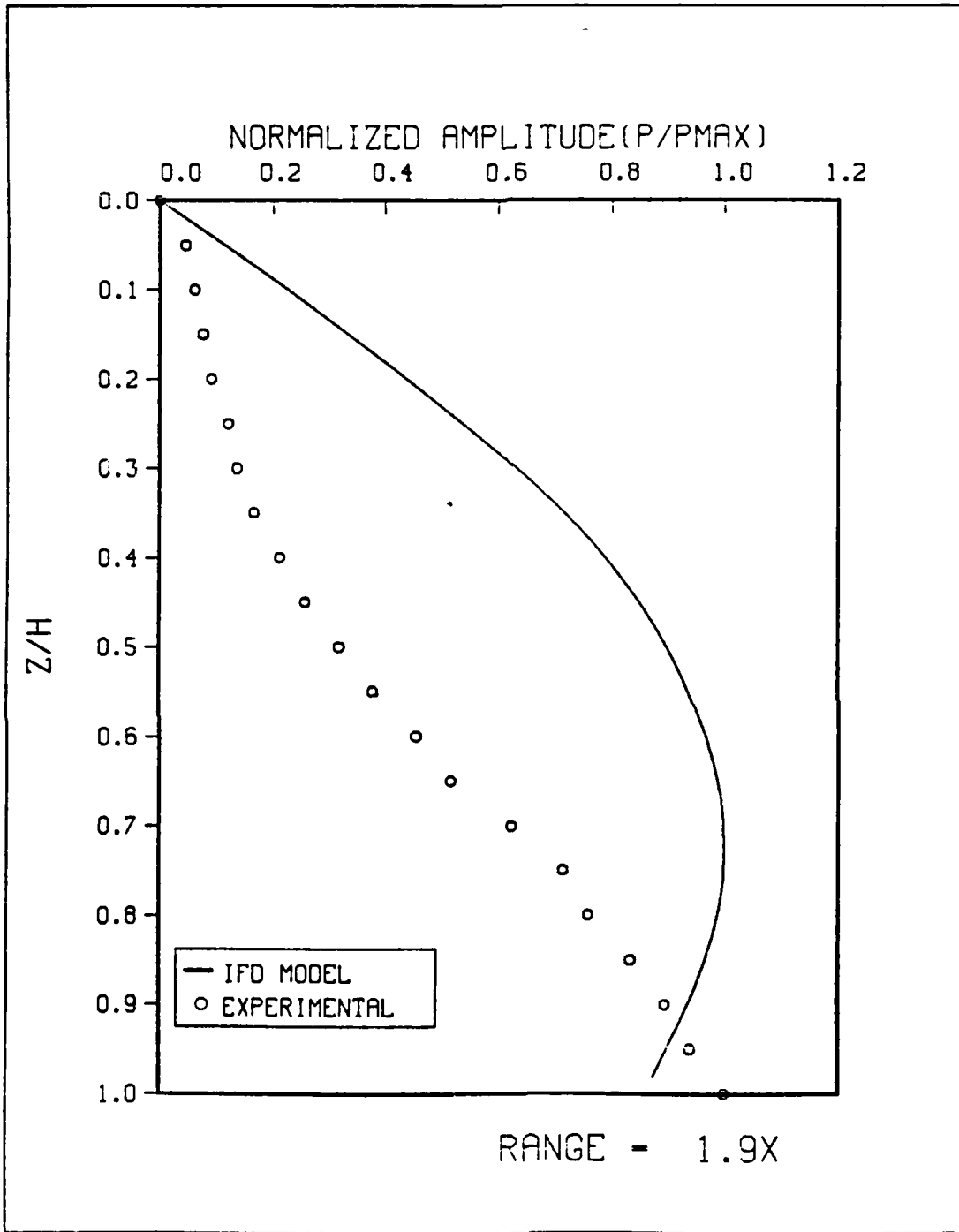


Figure 4.17 Comparison of Results at 1.9X.

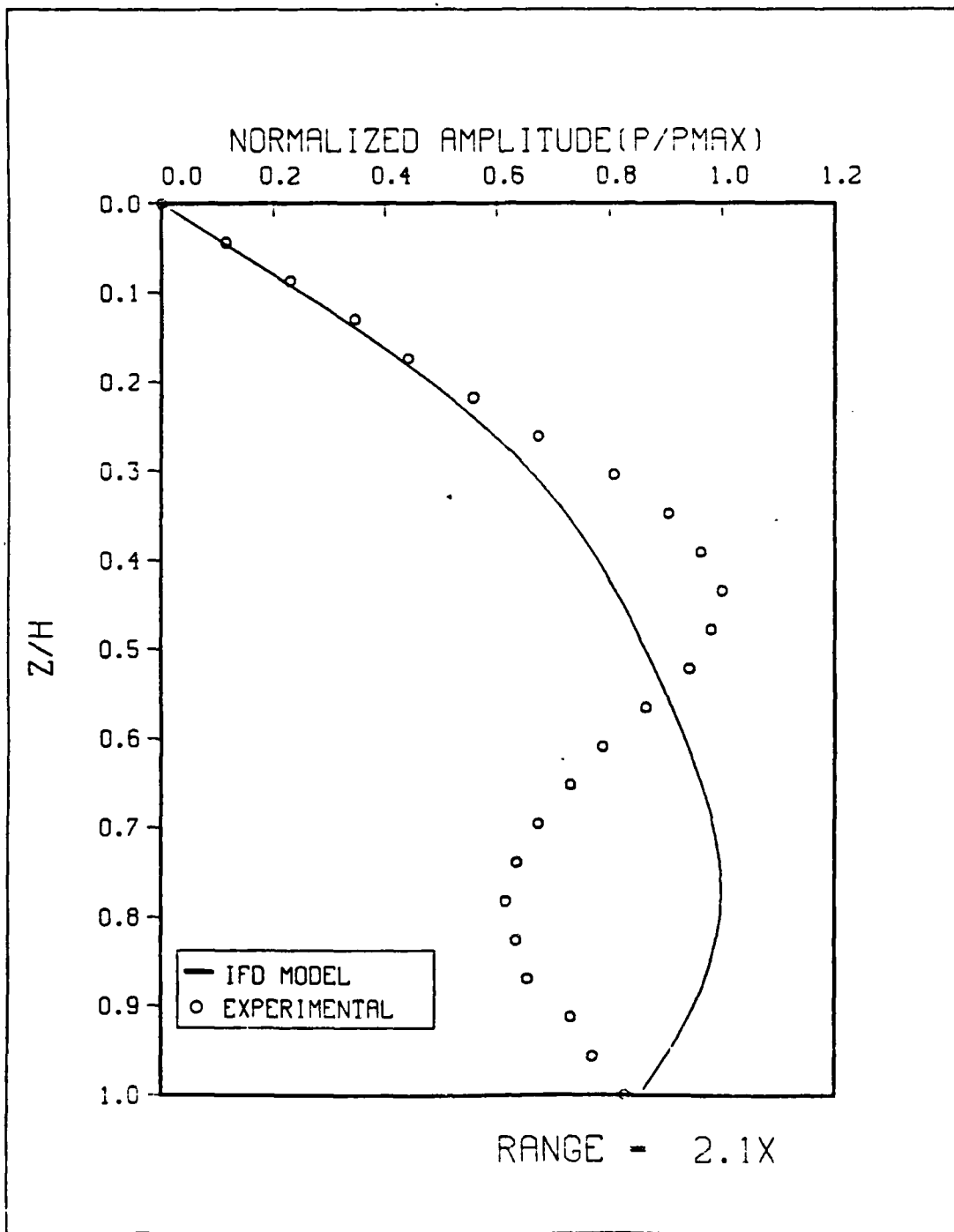


Figure 4.18 Comparison of Results at 2.1X.

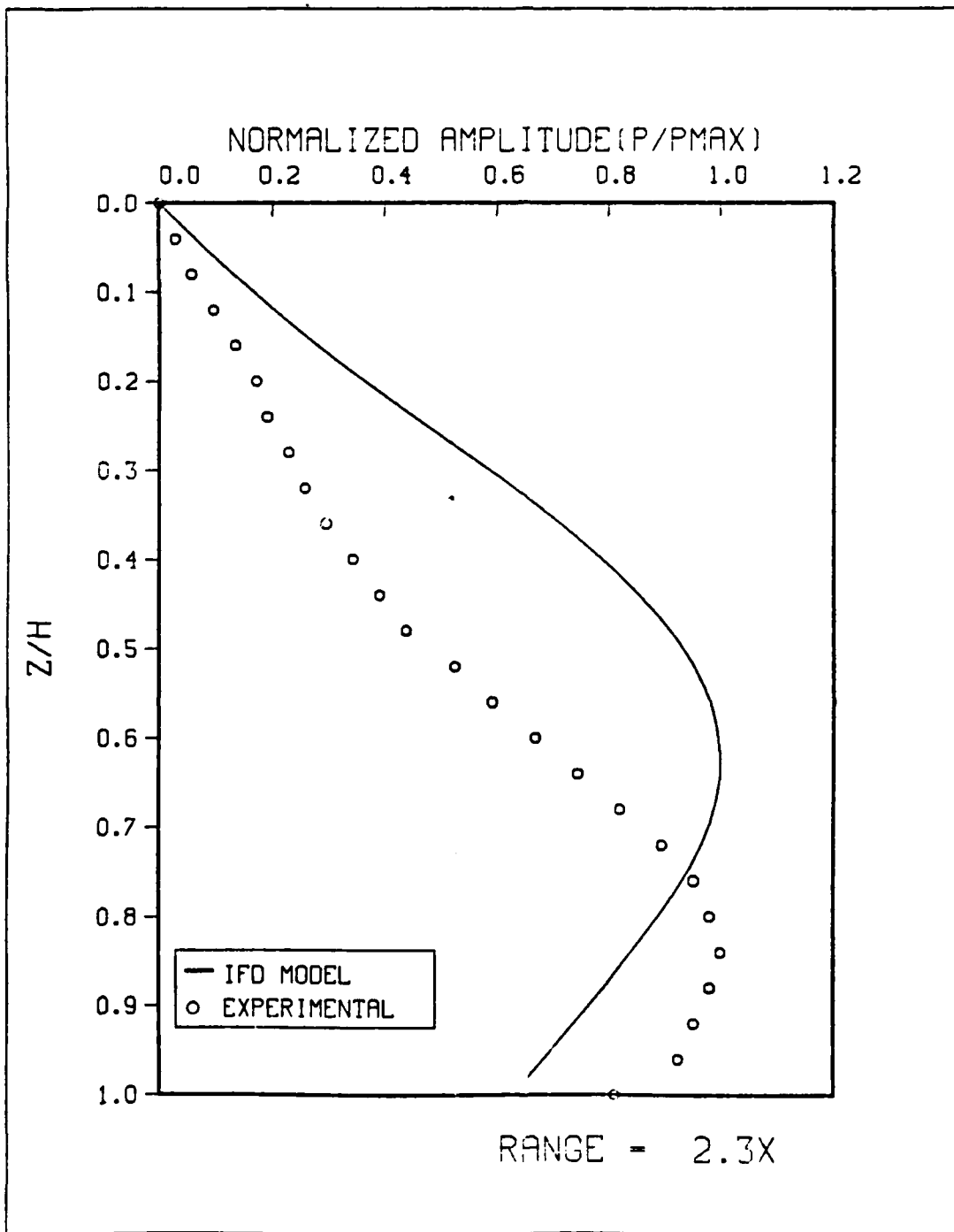


Figure 4.19 Comparison of Results at 2.3X.

interference (Figure 4.18). For distances less than $5X$, theory predicts that for a source at mid-depth, the lowest propagating mode should experience interference from only the evanescent tails of higher modes. Therefore, in the region of the detailed analysis, one expects small interference effects. The experimental results in this region however, show rather significant interference. The interference suggests unsuspected propagating modes are present, or that the evanescent tails are larger than expected. From the trend in the curves it appears as if the phase interference is not a factor from $1.5X$ inward toward the beach (Figures 4.11 through 4.15).

V. CONCLUSIONS/RECOMMENDATIONS

A. CONCLUSIONS

1. Performance of the IFD Model

This analysis of the IFD acoustic model did not uncover any major failures of model performance in a simplified shallow water environment. But this is not to say that the model consistently and accurately performs in such an ocean scenario. Although comparison of IFD predictions with two other models and with simple physical reasoning did not uncover any inconsistencies in performance, the agreement between IFD values and laboratory measurements is insufficient to give complete confidence in the performance of either the model or the experiment.

There is reasonable agreement between the scale of the features predicted by the IFD model and the experiment. Both the model and the measurements show increasing complexity as range is increased from the beach. But despite the similarities, there is poor quantitative agreement in results. One possible cause for the differences may be that the phases of the normal modes predicted by the model are extremely sensitive to minor irregularities in the shape of the interface and the acoustic properties of the bottom. Preliminary work (LeSesne, 1984), suggests that the phase relationships between modes is strongly dependent on the distance of the source from the apex even at great ranges. Consequently, it appears that the collective influence of the normal modes is dependent upon careful geometric control of the experiment.

The detailed analysis around 2X, reveals that large phase interferences occur where only one propagating mode is

expected. This indicates the existence of an extended evanescent tail within cutoff of the higher modes. Kawamura and Iannou (1978), noted that the apparent phases of the evanescent tails are extremely sensitive to the details of the environment. The results indicate that the tail does not decay quickly, and its influence is pervasive (Figures 4.2 and 4.3). From the trend in the curves, it appears this phase interference is not a factor any closer to the beach than 1.5X (Figures 4.11 through 4.15).

2. Modeling/Measurement Procedures

The laboratory measurements represent an initial attempt at modeling an idealized shallow water environment. The experimental techniques are not without problems. All sets of measurements were repeated and showed good agreement. The reproducibility of the measurements suggest that random errors have been minimized. However, systematic errors remain which also contribute to the discrepancies between predicted and measured values. Some of these errors derive from equipment, such as the fact that the size of the hydrophone is of the same order of magnitude as the scale of variations in the pressure field. In addition, the environment in the tank may not be sufficiently close to the ideal environment assumed by the model.

E. RECOMMENDATIONS

Further study and verification of the IFD computer model is recommended. A comparison of IFD predictions with other models not analyzed in this study, may uncover the cause of the inconsistency when compared to measured values. A detailed study of the phase interaction of the normal modes, although extremely complex, may also offer insight into the IFD performance.

It appears that the modeling of an idealized shallow water environment in the laboratory is of value in acoustic model verification. Despite the experimental difficulties, there was qualitative agreement in the basic features between model predictions and laboratory measurements. But the experiment represents only an initial probe into the modeling/measurement techniques of a shallow water environment. Further refinement of these techniques and the experimental equipment may result in better quantitative agreement between model predictions and laboratory measurements.

APPENDIX A

REVISED IPD PROGRAM LISTING

```

*****
** ILLICIT FINITE-DIFFERENCE PROGRAM FOR
** SOLVING THE PARABOLIC EQUATION - REVISED
** VERSION
**
** LT LARRY JAIGER
** U. S. NAVAL ECSTGRADUATE SCHOOL
** MCINTYRE, BY MARK E. KCSNIK (JUNE 1984)
**
** *****
** ALPHABETICAL LIST OF PROGRAM VARIABLES FOLLOWS:
**
** A - ARRAY - COEFFICIENT A IN PARABOLIC EQUATION
**      (IN WATER)
** A2 - COEFFICIENT A IN PARABOLIC EQUATION (IN SEDIMENT)
** ALPHA - COEFFICIENT ATTENUATION - DB/METER
** ATT - VELOCITY ATTENUATION COEFFICIENT FOR ARTIFICIAL
**        ATTENUATION LAYER
** BETA1 - AS DEFINED IN LEE AND MCDANIEL (1983)
** BETA2 - AS DEFINED IN LEE AND MCDANIEL (1983)
** EBITA1 - ATTENUATION IN WATER - LB/WAVELENGTH
** EBITA2 - ATTENUATION IN SEDIMENT - DB/WAVELENGTH
** EBK - RANGE FOR BOTTOM PROFILE - METERS
** EBZ - DEPTH FOR BOTTOM PROFILE - METERS
** EC - ATTAINS TRIANGONAL MATRIX SYSTEM THAT NEEDS
**      TO BE SOLVED (SEE SUBROUTINE TRIDG)
** C0 - REFERENCE SOUND SPEED - METERS/SEC
** C2 - SOUND SPEED IN SEDIMENT
** CC - STORAGE SPACE USED IN SUBROUTINES TRIDG AND
**     TRILL
** CF - STORAGE SPACE USED IN SOUND SPEED PROFILE -
**     METERS/SEC
** CSVP - STORAGE SPACE USED IN SUBROUTINES TRIDG AND
**     TRILL
** CTWO - STORAGE SPACE USED IN SUBROUTINES TRIDG AND
**     TRILL
*****

```

CC

```

*** CWATER - SCUNL SPEED AT GRID POINTS IN WATER COLUMN
*** DELTA AS DEFINED IN LEE AND MCDANIEL (1983)
*** DELIN / DELTA
*** DIFD - STORAGE SPACE FOR TI VALUES USED TO CONTOUR
          PLCT
*** DE - RANGE STEP - METERS
*** DRLVL RANGE STEP ALONG LEVEL INTERFACE - METERS
*** DEMAX MAXIMUM ALLOWABLE RANGE STEP - METERS
*** LZ - DEPTH INCREMENT OF SOLUTION - METERS
*** FVE - COEFFICIENT OF VARIATION
*** FFO - FREQUENCY - HZ
*** GAMMA1 - GAMMA 1 AS DEFINED IN LEE AND MCDANIEL (1983)
*** GAMMA2 - GAMMA 2 AS DEFINED IN LEE AND MCDANIEL (1983)
*** IEOT1 - POINTS TO BOTTOM PROFILE PCINT AT START
*** IEOT2 - POINTS TO BOTTOM PROFILE PCINT AT END
*** ID - AREA - RUN IDENTIFICATION
*** IFACE1 - POINTS TO INTERFACE AT RANGE RA1
*** IFACE2 - POINTS TO INTERFACE AT RANGE RA2
*** IFACEH - IFACE + 1
*** IFACEP - IFACE - 1
*** IIPZ - COUNTER INDEX FOR DEPTH VALUES
*** IFZ - EVERY IPZ TH VALUE IN DEPTH IS PRINTED
*** IK - COUNTER INDEX FOR RANGE VALUES
*** ISLOPE - SLOPE FLAG:
          1 - BOTTOM SLOPES DOWN
          2 - BOTTOM LEVEL
          3 - BOTTOM SLOPES UP
          4 - BOTTOM SLOPES DOWN, BOTTOM MODIFIED
          5 - BOTTOM SLOPES UP, BOTTOM MODIFIED
          - - - - - OTHER VALUES VARIABLE
*** ITEMP - TEMPORARY VARIABLE
*** INZ - GRID POINT CORRESPONDING TO RECEIVER LEFT
*** N - NUMBER OF EQUID-SPACED GRID POINTS IN U
*** NA - INCLUDES POINTS IN ARTIFICIAL ATTENUATION LAYER
*** NIU - NUMBER OF POINTS IN BOTTOM PROFILE (BF AND EZ)
*** NH1 - UNIT NUMBER FOR INPUT DATA
*** NCU - UNIT NUMBER FOR OUTPUT PLOTTER FILE
*** NFOU - UNIT NUMBER FOR RANGE STEPS ALONG A BOTTCM SEGMENT
*** NSTEP - NUMBER OF RANGE STEPS CORRESPONDING TO CNE VERTICAL
*** NSTEP1 - GRID STEP FCN MODIFIED BOTTOM
*** NSVP - NUMBER OF POINTS IN CSVP AND ZS VP
*** NMAX - NUMBER OF GRID POINTS IN WATER AT MAX DEPTH
*** NYLPS - NUMBER OF NEXT LEVEL SECTION FOLLOWING A SLCPING
          SECTION FOR A MODIFIED BOTTOM

```

CC

IFD00390
IFD00400
IFD00410
IFD00420
IFD00430
IFD00440
IFD00450
IFD00460
IFD00470
IFD00480
IFD00490
IFD00500
IFD00510
IFD00520
IFD00530
IFD00540
IFD00550
IFD00560
IFD00570
IFD00580
IFD00590
IFD00600
IFD00610
IFD00620
IFD00630
IFD00640
IFD00650
IFD00660
IFD00670
IFL00680
IFD00690
IFD00700
IFD00710
IFD00720
IFD00730
IFD00740
IFD00750
IFD00760
IFD00770
IFD00780
IFD00790
IFD00800
IFD00810
IFD00820
IFD00830
IFD00840
IFD00850
IFD00860


```

** YIRWS - MATRIX ELEMENT, Y MATRIX, OFF-DIAGONAL, IN WATER AND
** YMI - MATRIX ELEMENT, Y MATRIX, MAIN DIAGONAL, ON INTERFACE
** YPS - MATRIX ELEMENT, Y MATRIX, MAIN DIAGONAL, IN SEDIMENT
** YPW - MATRIX ELEMENTS, Y MATRIX, MAIN DIAGONAL, IN
** YFI - MATRIX ELEMENT, Y MATRIX, UPPER DIAGONAL, ON INTERFACE
** YFIV - MATRIX FOR LEVELING INTERFACE
** YFIZ - MATRIX FOR SLOPING INTERFACE
** Z1 - DEPTH OF WATER AT RANGE R1 - METERS
** Z2 - DEPTH OF WATER AT RANGE R2 - METERS
** ZABLYR - DEPTH OF WATER EDGE OF ARTIFICIAL ATTENUATION
** Z1YR1 - DEPTH OF GRILL POINT - METERS
** Z1YR2 - MAXIMUM WATER DEPTH - METERS
** Z1 - DEPTH OF WATER SURFACE - METERS
** Z2 - RECEIVED DEPTH - METERS
** ZSVP - SOURCE DEPTH - METERS
** ZZ... - ARRAY VARIABLES THAT BEGIN WITH ZZ HAVE NO SPECIAL PHYSICAL
SIGNIFICANCE BUT THEY CONTRIBUTE TO COMPUTATIONAL EFFICIENCY. ALL ZZ VARIABLES ARE CALCULATED IN SEQUENTIAL ORDER AND ALL ARE USED TO CALCULATE MATRIX ELEMENTS.
** INPUT *****
** UNIT NUMBER = NUNIT *****
** FILENAME AND FILES IN FREE DATA *****
** COMMENTS: CARL FREQ, CO, N *****
CARL 1 : : : ZDR, WDR, PDR, PLZ *****
CARL 2 : : : ZDR, WDR, PDR, PLZ *****
CARL 3 : : : ZDR, WDR, PDR, PLZ *****
CARL 4 : : : ZDR, WDR, PDR, PLZ *****
CARL N+1 : : : -1, -1 *****
CARL N+2 : : : Z1YR1, RHC1, BETA1 *****
CARL N+3 : : : ZSVP(1), CSVP(1) *****
CARL N+4 : : : ZSVP(2), CSVP(2) *****
CARL N+M : : : ZSVP(J), CSVP(J) *****
CARL N+M+1 : : : Z1YR2, RHC2, BETA2, C2 *****
CARL N+M+2 : : : ZABLYR *****

```

CC

```

WHERE:
PRC  = FREQUENCY (HZ)
ZS   = SOURCE DEPTH (M)
ZR   = RECEIVER DEPTH (M)
CO   = REFERENCE SOUND SPEED (M/S) IN WATER COLUMN. IF CO = 0.0, CO IS
N    = SET TO AVERAGE SOUND SPEED IN WATER COLUMN.
      = NUMBER OF GRID POINTS
RMAX = MAXIMUM RANGE (M) OF SCATTERION INTERFACE. IF
DRVL  = RANGE STEP (M) ALONG LEVEL TO 1/2 WAVELENGTH. IF
      = DRVL IS GREATER THAN DRMAX, DRVL SET TO DRMAX. IF
DRMAX = MAXIMUM ALLOWABLE RANGE STEP (M). IF DRMAX = 0.0,
WDR   = DRMAX IS SET TO ONE WAVELENGTH.
      = RANGE STEP (M) AT WHICH SOLUTION IS WRITTEN TO
      = FILE USED BY PLOTTING ROUTINE.
PDR   = ROUNDED TO NEAREST DR.
      = RANGE STEP (M) AT WHICH SOLUTION IS PRINTED.
PDZ   = ROUNDED TO NEAREST DR.
      = DEPTH INCREMENT AT WHICH SOLUTION IS PRINTED.
      = ROUNDED TO NEAREST DZ.
BR    = RANGE (M) OF BOTTOM PROFILE
BZ    = DEPTH (M) OF BOTTOM PROFILE
ZLYR1 = MAXIMUM WATER DEPTH (M)
RHO1  = DENSITY IN WATER (GM/CM**3)
BETA1 = ATTENUATION (DB/WAVELENGTH) IN WATER. IF BETA1
      = NEGATIVE THEN ATTENUATION COMPUTED.
ZSVP  = DEPTH (M) ARRAY FOR SOUND SPEED PROFILE
CSVP  = SOUND SPEED (M/S) ARRAY FOR SOUND SPEED PROFILE
ZLYR2 = DEPTH (M) OF PRESSURE RELEASE SURFACE
RHC2  = DENSITY (GM/CM**3) IN SEDIMENT
BETA2 = ATTENUATION (DB/WAVELENGTH) IN SEDIMENT
C2    = SOUND SPEED (M/S) IN SEDIMENT
ZALYR = DEPTH (M) OF UPPER SURFACE OF ARTIFICIAL
      = ATTENUATION LAYER
*****
***  C U T P U T
***  *****
***  OUTPUT UNIT NUMBER FOR FILE USED BY PLOTTING ROUTINE = NOU
***  FILENAME AND FILETYPE FOR OUTPUT PLOTTER FILE = IFECUT ELCITER
*****
CUTPUT UNIT NUMBER FOR PRINT FILE = NPOUT
*****

```

```

IFD01830
IFD01840
IFD01850
IFD01860
IFD01870
IFD01880
IFD01890
IFD01900
IFD01910
IFD01920
IFD01930
IFD01940
IFD01950
IFD01960
IFD01970
IFD01980
IFD01990
IFD02000
IFD02010
IFD02020
IFD02030
IFD02040
IFD02050
IFD02060
IFD02070
IFD02080
IFD02090
IFD02100
IFD02110
IFD02120
IFD02130
IFD02140
IFD02150
IFD02160
IFD02170
IFD02180
IFD02190
IFD02200
IFD02210
IFD02220
IFD02230
IFD02240
IFD02250
IFD02260
IFD02270
IFD02280
IFD02290
IFD02300

```

```

CCCCCCCCCCCCCCCCCCCCCCCCCCCCCCCCCCCCCCCCCCCCCCCCCCCCCCCCCCCC

```



```

20      CALL DCHN
C      GO TO 70
30      *** EOTTON IS LEVEL
C      CALL LEVEL
C      GO TO 70
40      *** ECTTON SLCPES UP
C      CALL UP
C      GO TO 70
50      *** EOTTON SLCPES DOWN SLOWLY, 3 CTICH MOLIFIED
C      CALL S SLCEE
60      *** ECTTON SLCPES UP SLOWLY, BOTICH MCLIFIED
C      CALL S SIOEE

CONTINUE
CALL ATTINU(U, ATT, IA, NA)
RA2E = RA2+0.5
*** TIME TO WRITE?
** IF (RA2P.GE.XWR) CALL WRITE2
** TIME TO PRINT?
** IF (RA2P.GE.XER) CALL PRINT2
** TIME TO TERMINATE?
** IF (RA2.GE.RHAX) GO TO 90

80      CCCONTINUE
C      *** GC BACK ANI CONTINUE WITH NEXT LINEAR BOTTOH SEGMENT
C      GC TO 10

C      *** TIME TC TERMINATE
C      CCXTINDE
C      WRITE(21,100) ((LIED(I,J),J=1,151),I=1,151)
C      FCENAY(16F7.2)
C      WRITE(27,101) ((LIED(I,J),J=1,121),I=1,121)
C      FCENAY(16F7.2)
C      CALL END (RA2)
C      STCF
C      INI

SUECUTINE REAL
(1) THIS SUBROUTINE HEADS ALL INPUT DATA.
(2) THE DATA IS READ FROM INPUT UNIT NUMBER: NIU = 51
(3) INPUT FILENAME AND FILETYPE ARE: IFCIN LATAIN
(4) DATA IS READ IN FREE FORMAT.
(5) DATA IS TRANSFERRED BACK TO MAIN PROGRAM VIA COMMON BLOCK

```

```

IFD02790
IFD02800
IFD02810
IFD02820
IFD02830
IFD02840
IFD02850
IFD02860
IFD02870
IFD02880
IFD02890
IFD02900
IFD02910
IFD02920
IFD02930
IFD02940
IFD02950
IFD02960
IFD02970
IFD02980
IFD02990
IFD03000
IFD03010
IFD03020
IFD03030
IFD03040
IFD03050
IFD03060
IFD03070
IFD03080
IFD03090
IFD03100
IFD03110
IFD03120
IFD03130
IFD03140
IFD03150
IFD03160
IFD03170
IFD03180
IFD03190
IFD03200
IFD03210
IFD03220
IFD03230
IFD03240
IFD03250
IFD03260

```

```

C      CCMCN / IN, IA, IBOT1, IFACE, IPZ, ISLOPE, ISTEP, IW2, N, NA, NBCT, NM1,
*      NSSTEP, NSTEP1, NSVP, NMAX, NYLFS
C      CCMCN / REAL, ALPHA, AT(5000), BETA1, BETA2, BK(101), BZ(101), CO
*      CSVP(101), C2, CHAFTER(500), DK, DRIVER, DMAX, FZ, FRC, FDR, FLZ,
*      R1, RA1, FA2, RHCI, RH02, RHAX, THETA, XK0, XLAMLA, XPR, XX4, XX10,
*      YX11, YEF, HBR, ZLYR1, ZLYR2, ZR, ZS, ZSVP(101), ZAEIYR
C      LAIA NIU/51, NFOU/55/
C      *** READ INPUT PARAMETERS
C      READ (NIU, *, END=100) FRC, ZS, ZR, CO, N
C      READ (NIU, *, END=100) RHAX, DRLVL, DRMAX, WDE, FDE, FLZ
C      *** HEAD BCTTCZ PROFILE - RANGE, DEPTH
C      LC 10 I=1, 101
C      READ (NIU, *, END=100) BR(I), BZ(I)
C      NBOI=I
C      *** END OF PROFILE?
C      IF (ER(I) - LT .0) GO TO 20
C      *** NO
C      CCNTINDE
C      CCNTINDE
C      *** EXTEND LAST DEPTH BEYOND MAX RANGE
C      EF(NBOT) = 1.0E+10
C      E2(NBOT) = E2(NBOT-1)
C      *** FIRST LAYER IS WATER. SECOND IS SEDIMENT.
C      *** READ MAX DEPTH, DENSITY AND ATTENUATION OF FIRST LAYER
C      READ (NIU, *, END=100) ZIYR1, RHO1, BETA1
C      *** READ SCUND SPEED PROFILE IN FIRST LAYER
C      LC 25 I=1, 101
C      NSVP=I
C      READ (NIU, *, END=100) ZSVP(I), CSVF(I)
C      *** REAL ANOTHER PROFILE PCINT?
C      IF (ZSVP(I) - LT .ZLYR1) GO TO 25
C      *** NO
C      *** WAS THAT THE LAST PROFILE POINT?
C      IF (ZSVP(I) - EC .ZLYR1) GO TO 30
C      *** NO, THERE IS ERROR.
C      GO TO 101
C      CCNTINDE
C      25
C      *** DOES THE SCUND SPEED PROFILE START AT THE SURFACE?
C      IF ( ZSVP(1) - NE .0) GO TO 102
C      *** YES
C      30

```

```

IFD03270
IFD03280
IFD03290
IFD03300
IFD03310
IFD03320
IFD03330
IFD03340
IFD03350
IFD03360
IFD03370
IFD03380
IFD03390
IFD03400
IFD03410
IFD03420
IFD03430
IFD03440
IFD03450
IFD03460
IFD03470
IFD03480
IFD03490
IFD03500
IFD03510
IFD03520
IFD03530
IFD03540
IFD03550
IFD03560
IFD03570
IFD03580
IFD03590
IFD03600
IFD03610
IFD03620
IFD03630
IFD03640
IFD03650
IFD03660
IFD03670
IFD03680
IFD03690
IFD03700
IFD03710
IFD03720
IFD03730
IFD03740

```



```

C C ***CALCULATE VERTICAL STEP SIZE
C C DZ = ZLYR2 / FLOAT (N)
C C ***CALCULATE NUMBER OF GRID POINTS IN WATER COLUMN
C C NMAX = INT((ZLYR1/DZ)+0.5)
C C ***CALCULATE SCONE SPEED AT ALL GRID POINTS IN WATER COLUMN
C C I = 1
C C DO 20 I=1, NMAX
C C ZI = I * DZ
C C LP1 = I + 1
C C ***NEED IC UPDATE PROFILE ENDPOINTS?
C C IF (ZI.LE.ZSVP(IP1)) GO TO 10
C C ***YES
C C I = I + 1
C C LP1 = I + 1
C C WATER(I) = CSVP(LP1) + (CSVP(LP1)-CSVP(L)) * (ZI-ZSVP(L)) /
C C (ZSVP(LP1)-ZSVP(L))
C C CCNTINUE
C C
C C RETURN
C C END
C C
C C SUBROUTINE INITIAL
C C (1) THIS SUBROUTINE INITIALIZES CONSTANTS AND VARIABLES
C C (2) VALUES ARE TRANSFERRED TO/FROM MAIN PROGRAM VIA COMMON
C C BLOCK.
C C
C C CMCMCN / IN, IA, IBOT1, IFACE, IPZ, ISLOPE, ISTEP, IWZ, N, NA, NBCT, NH1,
C C NSTEP, NSTEP1, NSVE, NMAX, NXLFS
C C CMCMCN / REAL, ALPHA, AT(5000), BETA1, BETA2, BR(101), BZ(101), CO, EDZ,
C C CSVP(10), C2, CWATER(5000), DR, DR1VL, DRMAX, LZ, PRC, PDR, PDZ,
C C R1, RA1, FA2, EHC1, EHC2, RMAX, THETA, XKO, XLAMFA, XPR,
C C XX11, XWB, WDR, ZLYR1, ZLYR2, ZR, ZS, ZSVP(101), ZAEIYR
C C DATA EL/3.141592654/
C C
C C *** IF CO NOT SPECIFIED, SET CO TO AVERAGE SPEED IN WATER COLUMN
C C *** (USING MAX LEFTH PROFILE)
C C IF (CO.NE.0.0) GO TO 11
C C EC 10 I=2, NSVP
C C CO=CO + (ZSVP(I)-ZSVP(I-1)) * (CSVP(I-1) +
C C ZSVP(I)-CSVP(I-1))
C C CCNTINUE
C C
C C 10
C C

```

```

IPD04230
IFD04240
IFD04250
IFD04260
IFD04270
IFD04280
IFD04290
IFD04300
IFD04310
IFD04320
IFD04330
IFD04340
IFD04350
IFD04360
IFD04370
IFD04380
IFD04390
IFD04400
IFD04410
IFD04420
IFD04430
IFD04440
IFD04450
IFD04460
IFD04470
IFD04480
IFD04490
IFD04500
IFD04510
IFD04520
IFD04530
IFD04540
IFD04550
IFD04560
IFD04570
IFD04580
IFD04590
IFD04600
IFD04610
IFD04620
IFD04630
IFD04640
IFD04650
IFD04660
IFD04670
IFD04680
IFD04690
IFD04700

```

```

IFD04710
IFD04720
IFD04730
IFD04740
IFD04750
IFD04760
IFD04770
IFD04780
IFD04790
IFD04800
IFD04810
IFD04820
IFD04830
IFD04840
IFD04850
IFD04860
IFD04870
IFD04880
IFD04890
IFD04900
IFD04910
IFD04920
IFD04930
IFD04940
IFD04950
IFD04960
IFD04970
IFD04980
IFD04990
IFD05000
IFD05010
IFD05020
IFD05030
IFD05040
IFD05050
IFD05060
IFD05070
IFD05080
IFD05090
IFD05100
IFD05110
IFD05120
IFD05130
IFD05140
IFD05150
IFD05160
IFD05170
IFD05180

```

```

11
C      CO = CO/ZSVE(NSVP)
C      CCNTINUE
C
C      *** INITIALIZE RANGE
C      RA1 = 0.0
C
C      *** INITIALIZE POINTER THAT POINTS TO BCCTM FCFFILE PCINT
C      IEOT1 = 0
C
C      *** COMPUTE REFERENCE WAVE NUMBER
C      YK0 = 2.0*FI*FRQ/CO
C
C      *** COMPUTE REFERENCE WAVELENGTH
C      XLAMDA = CC/FRQ
C
C      *** IF DRLVL=0 SET DRLVL EQUAL TO 1/2 REFERENCE WAVELENGTH
C      IF ( DRLVL.EQ.0.0 ) DRLVL = 0.5 * XLAMDA
C
C      *** IF DRMAX=0 SET DRMAX EQUAL TO REFERENCE WAVELENGTH
C      IF ( DRMAX.EQ.0.0 ) DRMAX = XLAMDA
C
C      *** IF DRLVL GREATER THAN DRMAX SET DRLVL EQUAL TO DRMAX
C      IF ( DRLVL.GT.DRMAX ) DRLVL = DRMAX
C
C      *** COMPUTE ATTENUATION - SACLANT MEMO SM-121 (JENSEN + FERLA)
C      *** MODIFIED AS FOLLOWS:
C      *** IF INPUT EL BETA IS IT 0.0, ALPHA IS COMPUTED IN DB/METER
C      *** AND USED FOR BETA
C      ALPHA=FRQ*FFQ*(.007+ (.155*1.7)/(1.7*1.7+FRQ*FRQ*.000001))
C      *
C
C      *** INITIALIZE POINTER THAT POINTS TO INTERFACE GFIL PCINT
C      IFACE = INT ( BZ(1)/DZ + 0.5 )
C
C      RETURN
C      END
C
C      SUBROUTINE MATCCN
C
C      THIS SUBROUTINE CALCULATES VARIOUS VARIABLES NEEDED TO COMPUTE
C      THERMODYNAMIC MATRIX ELEMENTS. VARIABLES BEGINNING WITH YX HAVE
C      NO SPECIAL PHYSICAL SIGNIFICANCE BUT THEY CONTRIBUTE TO
C      COMPUTATIONAL EFFICIENCY.
C
C      CCMEX XN1

```

IFD05190
 IFD05200
 IFD05210
 IFD05220
 IFD05230
 IFD05240
 IFD05250
 IFD05260
 IFD05270
 IFD05280
 IFD05290
 IFD05300
 IFD05310
 IFD05320
 IFD05330
 IFD05340
 IFD05350
 IFD05360
 IFD05370
 IFD05380
 IFD05390
 IFD05400
 IFD05410
 IFD05420
 IFD05430
 IFD05440
 IFD05450
 IFD05460
 IFD05470
 IFD05480
 IFD05490
 IFD05500
 IFD05510
 IFD05520
 IFD05530
 IFD05540
 IFD05550
 IFD05560
 IFD05570
 IFD05580
 IFD05590
 IFD05600
 IFD05610
 IFD05620
 IFD05630
 IFD05640
 IFD05650
 IFD05660

```

C CREFLEX A A2 C CR CTWC EYE XMS XRI XRIZ XX12 XX11M
* YL1 XL1 XLRHS XMI XX6 XX7 XX8 XX9 XX10 XX11
* YL1 XL1 XLRHS XMI XX6 XX7 XX8 XX9 XX10 XX11
* U Z25 Z26 Z27 Z28 Z29 Z30
C CCMCN / IN / IA / IBOPI / KSTEP / IFACE / NHMAX / BETA1 BETA2 B R (101) BZ (101) CR EDZ
* / NSIEP / ALPHA / A CT / CHATER (5000) DR DELV1 DMAX FZ FRC FDR EDZ
C CCHMCN / REAL / ALPHA / A CT / CHATER (5000) DR DELV1 DMAX FZ FRC FDR EDZ
* / CSVP (101) / C2 / RHCI / RH2 / RH3 / RH4 / RH5 / RH6 / RH7 / RH8 / RH9 / RH10
* R1 R2 R3 R4 R5 R6 R7 R8 R9 R10 R11 R12 R13 R14 R15 R16 R17 R18 R19 R20
C CCEHCN / CPLX / A (5000) / XRES XMI XMS XRI XRIZ
* EYE XL1 XL2 XL3 XL4 XL5 XL6 XL7 XL8 XL9 XL10 XL11 XL12 XL13 XL14 XL15 XL16 XL17 XL18 XL19 XL20
* YL1 YL2 YL3 YL4 YL5 YL6 YL7 YL8 YL9 YL10 YL11 YL12 YL13 YL14 YL15 YL16 YL17 YL18 YL19 YL20
* U (5000) Z25 Z26 Z27 Z28 Z29 Z30
C EYE = CMPLX(0.0,1.0)
C
C XN1 = CMPLX ( XN1 , +0.25/(DZ*DZ*XK0) )
*** COMPUTE COEFFICIENT A IN SEDIMENT LAYER
*** FIRST CALCULATE REAL INDEX OF REFRACTION
XN = CO/CC2
*** THEN CALCULATE COMPLEX INDEX OF REFRACTION SQUARED
(XN1 = CMPLX ( XN*XN , XN*XN*BETA2/27.287527 )
*** CALCULATE A2
A2 = 0.5 * EYE * XK0 * (XN1-1.0)
XN3 = 0.5*A2 - XN2
XN4 = 1.0 + RHC1/RHO2
XN5 = XN2*(1.0/XN4 - 1.0) + A2/(2.0*(RHC2/RHO1 + 1.0))
XN6 = XN2/XN4
XN7 = RHO1/RHO2 * XN6
XN8 = CMPLX ( XN8 , -DZ*XK0 )
XN9 = 1.0 / XN8
XN10 = RHO1 + EHO2
XN11 = RHO1 - REC2
XN12 = 4.0 * XN1
*** THIS SECTION PERTAINS TO PCINTS IN WATER COLUMN
DO 10 I=1,NHMAX
  I=1,NHMAX
  REAL INDEX OF REFRACTION IN WATER
  XN = CO/CHATER(I)
  *** CALCULATE ATTENUATION AS PER COMMENTS IN SUBROUTINE INITIAL
  IF (BETA1-11.0.0) BETA1 = ALPHA*CHATER(I)/FRQ
  *** CALCULATE COMPLEX INDEX OF REFRACTION SQUARED

```

```

C    *** (SEE PAGE 2-11 IN TR 6659)
C    *** XN1 = CMFLX ( XN*XN  XN*XN*BE TA1/27.2E7527 )
C    *** CALCULATE COEFFICIENT A (I)
C    *** A (J) = 0.5 * EYE * XK0 * (XN1-1.0)
C    *** CALCULATE XN1M
C    *** XN1H(I) = 0.5 * A(I) - XX2
10  CONTINUE
RETURN
END

SBEROUTINE SFIELD(FRQ,CO,ZS,N,DZ,U)
*** THIS SUBROUTINE IS IDENTICAL TO SUBROUTINE SFIELD AS PER
*** NUSC TECHNICAL REPORT 6659.
*** *****
*** GAUSSIAN STARTING FIELD - SEE NORDA TECH NCTE 12 BY H.K.BROCK
*** *****
*** CALLING ROUTINE SUPPLIES:
FRQ - FREQUENCY IN HZ
CO   - REFERENCE SOUND SPEED - METERS/SEC
ZS   - DEPTH OF SOURCE IN METERS
NZ   - NUMBER OF POINTS IN ARRAY
LZ   - DEPTH INCREMENT - METERS
SFIELD SUBROUTINE SUPPLIES:
U    - COMPILEX STARTING FIELD
*****
CCFLX U(1)
DATA FL/3.1415926535/

THE FIELD IS DEFINED AS A GAUSSIAN BEAM AT RANGE = C.
ICCAL VARIABLES - GA GAUSSIAN AMPLITUDE
YKC=2.0*PI*PRQ/CO
GW=2.0*CM(XK0)/GW
DC TO I=1,N
ZM=I*IZ
EB=GAUSS(GA,ZM,ZS,GW) --GAUSS (GA, -ZM,ZS,GW)
U(I)=CMPLX(PR,0.0)
CCM INUE
RETURN
END
FUNCTION GAUSS(GA,Z,GI,GW)

```

```

IFD05670
IFD05680
IFD05690
IFD05700
IFD05710
IFD05720
IFD05730
IFD05740
IFD05750
IFD05760
IFD05770
IFD05780
IFD05790
IFD05800
IFD05810
IFD05820
IFD05830
IFD05840
IFD05850
IFD05860
IFD05870
IFD05880
IFD05890
IFD05900
IFD05910
IFD05920
IFD05930
IFD05940
IFD05950
IFD05960
IFD05970
IFD05980
IFD05990
IFD06000
IFD06010
IFD06020
IFD06030
IFD06040
IFD06050
IFD06060
IFD06070
IFD06080
IFD06090
IFD06100
IFD06110
IFD06120
IFD06130
IFD06140

```


IFD06630
IFD06640
IFD06650
IFD06660
IFD06670
IFD06680
IFD06690
IFD06700
IFD06710
IFD06720
IFD06730
IFD06740
IFD06750
IFD06760
IFD06770
IFD06780
IFD06790
IFD06800
IFD06810
IFD06820
IFD06830
IFD06840
IFD06850
IFD06860
IFD06870
IFD06880
IFD06890
IFD06900
IFD06910
IFD06920
IFD06930
IFD06940
IFD06950
IFD06960
IFD06970
IFD06980
IFD06990
IFD07000
IFD07010
IFD07020
IFD07030
IFD07040
IFD07050
IFD07060
IFD07070
IFD07080
IFD07090
IFD07100

*** WRITE STARTING VALUE
WRITE(NOU,*) RA1, ZB, U(IWZ)

RETURN
END

SCURCUTINE PRINT1

(1) THIS SUBROUTINE OUTPUTS FORMATTED DATA TO A FILE
WHICH IS READY TO BE SENT TO THE PRINTER.
(2) THE FILE CORRESPONDS TO UNIT FILE NUMBER: NPOUT = 55
(3) THE FILENAME AND FILETYPE FOR THIS FILE ARE:
IPDCUT EPRINTER

DIMENSION ID(17)
COMMON /IN/, IABOT1, IFAZ, IPZ, ISLOPE, ISTEP, IWZ, N, NA, NECT, NM1,
* NSIEP, NSTEP1, NSVF, NNM, NKX1FS
COMMON /REAL/, ALPHA, AT(5000), BETA1, BETA2, B, B(101), C0, C01, C02,
* CSVP(101), C2, CWAITER(5000), DR, DRIVL, DRMAX, LZ, FRQ, FDR, LDZ,
* R1, RA1, FAZ, RHCI, RHOC2, RMAX, THETA, XK0, XLAMDA, XPR, XY4, XY10,
* XY11, XME, HDR, ZLYR1, ZLYR2, ZR, ZS, ZSVP(101), ZAELYR
LATA NPOUT/55/

*** EFOHPT USER FOR RUN IDENTIFICATION

WRITE(6,890)

*** READ USER RESPONSE

READ(5,891) (ID(I), I=1,16)

*** PRINT SELECTED PARAMETERS OF INTEREST

WRITE(NPOUT,900) (ID(I), I=1,16), DRIVL, DRMAX, ZS, ZF, DZ, C0, XK0,
* XLAMDA, RMAX, EMAX, DRVLR, DRHAX, WDR, ZABLYR, N

*** PRINT SOUND SPEED PROFILE IN WATER

WRITE(NPOUT,904)

DC 5 I=1, NSVF

*** WRITE(NFCUT,905) ZSVP(I), CSVP(I)

CCONTINUE

*** PRINT MORE SELECTED PARAMETERS OF INTEREST

WRITE(NPOUT,901) ZLYR1, RHO1, BETA1, ZLYR2, RHO2, BETA2, C2

*** PRINT EOTICM PROFILE

WRITE(NPOUT,902)

NEOTH = NECT - 1

IFD07110
IFD07120
IFD07130
IFD07140
IFD07150
IFD07160
IFD07170
IFD07180
IFD07190
IFD07200
IFD07210
IFD07220
IFD07230
IFD07240
IFD07250
IFD07260
IFD07270
IFD07280
IFD07290
IFD07300
IFD07310
IFD07320
IFD07330
IFD07340
IFD07350
IFD07360
IFD07370
IFD07380
IFD07390
IFD07400
IFD07410
IFD07420
IFD07430
IFD07440
IFD07450
IFD07460
IFD07470
IFD07480
IFD07490
IFD07500
IFD07510
IFD07520
IFD07530
IFD07540
IFD07550
IFD07560
IFD07570
IFD07580

```
DC 10 I=1, XIOTM1  
WRITE (NECUT,903) ER(I), BZ(I)  
CCONTINUE  
  
*** COMPUTE DEPTH PRINT INCREMENT TO NEAREST DZ  
IFZ = INT ( PDZ/DZ+0.5 )  
IF ( IFZ.EC.0 ) IFZ = 1  
  
*** INITIALIZE RANGE VARIABLE AT WHICH SOLUTION IS TO BE PRINTED  
YER = HA1+PIR  
  
FCFMAI (16A4) 1X, ' ENTER RUN IDENTIFICATION: '  
FCFMAI (16A4) 1X, ' IFD PRINTED OUTPUT: '//, 1X, ' & UN I.L. : ',  
FCFMAI (16A4) 1X, ' GAUSSIAN STARTING '//, 1X, ' (FCF FURTHER INFORMATION ON VARIABLES',  
* ' F I E E H A I N ' I F D P R O G R A M L I S T I N G ) ' , //  
* ' F R Q = ' , F9.2, ' H Z', //  
* ' Z S = ' , F9.3, ' M', //  
* ' Z R = ' , F9.3, ' M', //  
* ' D Z = ' , F9.3, ' M', //  
* ' C O = ' , F9.3, ' M / S', //  
* ' X K L A M D A = ' , F9.3, ' M', //  
* ' R M A X = ' , F9.3, ' M', //  
* ' D R L V I = ' , F9.3, ' M', //  
* ' D R M A X = ' , F9.3, ' M', //  
* ' W D R = ' , F9.3, ' M', //  
* ' Z A B L Y R = ' , F9.3, ' M', //  
* ' Z N = ' , I6, ' I 6', //  
* ' L E N S I T Y ( G / C M * 3 ) = ' , //  
  
FOEMAI (20X, F10.3) ' SCUND SPEED', //, 20X, ' DEPTH',  
FCFMAI (10X, F10.3, M, 6X, F10.2, M/S, /)  
FCFMAI (14X, F10.3, M, 6X, F10.2, M/S, /)  
  
RETURN  
END  
  
SLERCUTINE NEWSIG  
C
```

IFDD07590
 IFDD07600
 IFDD07610
 IFDD07620
 IFDD07630
 IFDD07640
 IFDD07650
 IFDD07660
 IFDD07670
 IFDD07680
 IFDD07690
 IFDD07700
 IFDD07710
 IFDD07720
 IFDD07730
 IFDD07740
 IFDD07750
 IFDD07760
 IFDD07770
 IFDD07780
 IFDD07790
 IFDD07800
 IFDD07810
 IFDD07820
 IFDD07830
 IFDD07840
 IFDD07850
 IFDD07860
 IFDD07870
 IFDD07880
 IFDD07890
 IFDD07900
 IFDD07910
 IFDD07920
 IFDD07930
 IFDD07940
 IFDD07950
 IFDD07960
 IFDD07970
 IFDD07980
 IFDD07990
 IFDD08000
 IFDD08010
 IFDD08020
 IFDD08030
 IFDD08040
 IFDD08050
 IFDD08060

```

THIS SUBROUTINE IS CALLED AT THE START OF EACH NEW EOTICM
SEGMENT. THE SUBROUTINE DOES THE FOLLOWING TASKS FOR EACH
SECTION SEGMENT:
(1) UPDATE BOTTOM PROFILE POINTERS: IBC1 & IBC2
(2) COMPUTES SLOPE: THETA
(3) COMPUTES NUMBER OF RANGE STEPS IN SEGMENT: NSTEP
(4) COMPUTES RANGE STEP: DR
(5) SETS SICPE FLAG: ISLOPE
    (A) ISLOPE = 1
    (B) ISLOPE = 2
    (C) ISLOPE = 3
    (D) ISLOPE = 4
    (E) ISLOPE = 5
(6) INITIALIZES RANGES: RA1 & RA2
(7) CHECKS THAT RANGE STEP IS LESS THAN DRMAX
(8) ISSUES ERROR OR WARNING MESSAGES AS APPROPRIATE

COMMON /IN/ IA, IBOT1, IFACE, IPZ, ISLOPE, ISTEP, INZ, N, NA, NBCT, NM1,
NSTEP, NSTEP1, NSV, NWMAX, NXLFS
CCHMCN /REAL/ ALPHA, AT(5000), BETA1, BETA2, BR(101), EZ(101), CO
* CSVP(101), C2, CWATER(5000), DK, DRLV, DRMAX, LZ, PRQ, RDR, PDZ,
* R1, RA1, FA2, RH, C1, RH02, RMAX, THETA, XA, XKB, XLAMFA, XPR,
* XX11, YAF, WDR, Z1YR1, Z1YR2, ZR, ZS, ZSVP(101), ZAEIYA
LATA NPOUT/55/

** UPDATE BOTIICM PROFILE FCINTER
IFOT1 = IBC11 + 1
IFOT2 = IBC11 + 1
** GET STARTING AND ENDING RANGES AND DEPTHS FOR THIS SEGMENT
R1 = EK(IBC11)
R2 = BZ(IBC11)
K2 = EK(IBC12)
**
** ERROR CHECK
IF (R2 - IE, R1) GC TO 100
PUT Z1 = INT Z2 CN NEAREST GRID PCINTS
Z1 = DZ * FLOAT(ITEMP)
Z2 = DZ * FLOAT(ITEMP)
Z2 = DZ * FLOAT(ITEMP)
** COMPUTE SICPE
THETA = ATAN2 (Z2 - Z1, R2 - R1)
DCES BCTON SLOPE DCWN, LEVEL OR UP?
IF (THETA .GT. 0.0) GC TO 10
IF (THETA .LT. 0.0) GC TO 20
** BOTTOM IS LEVEL
** DETERMINE NUMBER OF RANGE STEPS FOR SEGMENT
  
```

```

IFD08070
IFD08080
IFD08090
IFD08100
IFD08110
IFD08120
IFD08130
IFD08140
IFD08150
IFD08160
IFD08170
IFD08180
IFD08190
IFD08200
IFD08210
IFD08220
IFD08230
IFD08240
IFD08250
IFD08260
IFD08270
IFD08280
IFD08290
IFD08300
IFD08310
IFD08320
IFD08330
IFD08340
IFD08350
IFD08360
IFD08370
IFD08380
IFD08390
IFD08400
IFD08410
IFD08420
IFD08430
IFD08440
IFD08450
IFD08460
IFD08470
IFD08480
IFD08490
IFD08500
IFD08510
IFD08520
IFD08530
IFD08540

```

```

C      *** NSTEEL = INT ( (R2-R1)/DRLVL + 0.99999 )
C      *** DETERMINE RANGE STEP
C      *** DR = (R2-R1) / FLOAT (NSTEP)
C      *** SET ISLOPE
C      *** ISLOPE = 2
C      GO TO 80
C
C      *** BOTTOM SLOPES DCHN
C      *** DETERMINE NUMBER OF RANGE STEPS
C      *** NSTEEL = INT ( (Z2-Z1+0.05)/DZ )
C      *** DETERMINE RANGE STEP
C      *** DR = (R2-R1)/FLOAT(NSTEP)
C      *** SET ISLOPE
C      *** ISLOPE = 1
C      GO TC 30
C
C      *** BOTTOM SLOPES UP
C      *** DETERMINE NUMBER OF RANGE STEPS
C      *** NSTEEL = INT ( (Z1-Z2+0.05)/DZ )
C      *** DETERMINE RANGE STEP
C      *** DR = (R2-R1)/FLOAT(NSTEP)
C      *** SET ISLOPE
C      *** ISLOPE = 3
C
C      *** IS RANGE STEP TOO LARGE?
C      *** IF ( DR.LE. DRMAX ) GC TO 80
C      *** IF ( BCTTON MUST BE MODIFIED
C      *** SET ISLOPE
C      *** ISLOPE = 4
C      *** IF ( TETA.LT. 0.0 ) ISLOPE = 5
C      *** DETERMINE NUMBER OF RANGE STEPS REQUIRED TO MOVE UP
C      *** DR DCN = INT FCINT
C      *** NSTEEL1 = INT ( DR/DRMAX + 0.99999 )
C      *** DETERMINE RANGE STEP
C      *** DR = DR / FLOAT (NSTEEL1)
C      *** REDETERMINE NUMBER OF RANGE STEPS
C      *** NSTEEL = NSTEEL * NSTEEL1
C      *** COMPUTE SLOPE OF SLOPING SECTION
C      *** TETA = ATAN2 (DZ, DR)
C      *** COMPUTE LOCATION OF NEXT LEVEL SECTION FCILCWING A
C      *** SLOPES SECTION
C      *** NXCICAT = NSTEEL1/2 + 2
C      *** INDCICAT = 5 * LZ
C      *** TEMP = (6.903) R1 R2 TEMP
C      *** WRITE (6,903) R1, R2, TEMP
C      WRITE (NFOUT,903) R1, R2, TEMP
C

```

AD-A150 784

THE IMPLICIT FINITE-DIFFERENCE (IFD) ACOUSTIC MODEL IN
A SHALLOW WATER ENVIRONMENT(U) NAVAL POSTGRADUATE
SCHOOL MONTEREY CA M E KOSNIK JUN 84

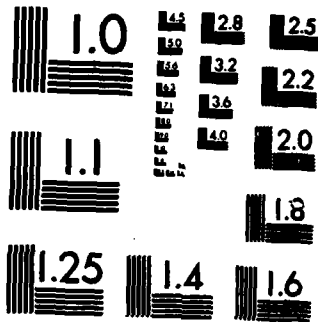
2/2

UNCLASSIFIED

F/G 20/1

NL

							END						
							FILMED						
							DTIC						



MICROCOPY RESOLUTION TEST CHART
 NATIONAL BUREAU OF STANDARDS-1963-A

```

80 C CONTINUE
C *** INITIALIZE RA1 & RA2
RA1 = R1
RA2 = RA1+IF
C *** INDICATE TC USER HOW FAR SOLUTION FIELD HAS PROGRESSED
WRITE(6,902) R1
C *** IF RANGE STEP GREATER THAN 1 (?) WAVELENGTH WRITE WARNING
IF (DR-LE XLAMDA) GO TO 90
WRITE(6,901) R1, F2, DR, XLAMDA
WRITE(NCUT,901) R1, R2, DR, XLAMDA
C 90 RETURN
C *** ERROR EXIT
WRITE(6,900) IBOT1
WRITE(NPOT,900) IBOT2, IBOT1
C STOP
C 900 FCMAT(1,1) IS ERROR: THE RANGE AT BOTTOM PROFILE PCINT NUMBER
12, NUMBER 12, //, 1X, EXECUTION TERMINATED. //
C 901 FCMAT(1,1) WARNING: THE HORIZONTAL RANGE STEP BETWEEN RANGE R = F8.1
(METERS) IS F5.1 METERS.
THE REFERENCE WAVELENGTH IS F5.1 METERS.
FCMAT(1,1) THE PROGRAM HAS REACHED RANGE R = F8.1, AND RANGE
FCMAT(1,1) NOTICE: THE BOTTOM BEING MODIFIED BECAUSE OF ITS VERY SHAL
1/CP1.8X, THE DIFFERENCE BETWEEN THE HORIZONTAL
BOTTOM AND YOUR //8X, INPUT BOTTOM IS NEVER GREATER
'THAN' F5.2, METERS. //
C ENL
C C C C C
C SUECUTINE NEWMAT
THIS SUBROUTINE IS CALLED AT THE START OF EACH NEW EOTTCM
SEGMENT. THE SUBROUTINE DOES THE FOLLOWING TASKS:
(1) COMPUTE TRIDIAGONAL MATRIX ELEMENTS FOR MATRIX Y
(A) MATRIX Y IS AT RANGE WHERE FIELD IS KNOWN: RANGE=RA 1
(B) Y MATRIX CN EHS OF EQUATION

```

```

IFD08550
IFD08560
IFD08570
IFD08580
IFD08590
IFD08600
IFD08610
IFD08620
IFD08630
IFD08640
IFD08650
IFD08660
IFD08670
IFD08680
IFD08690
IFD08700
IFD08710
IFD08720
IFD08730
IFD08740
IFD08750
IFD08760
IFD08770
IFD08780
IFD08790
IFD08800
IFD08810
IFD08820
IFD08830
IFD08840
IFD08850
IFD08860
IFD08870
IFD08880
IFD08890
IFD08900
IFD08910
IFD08920
IFD08930
IFD08940
IFD08950
IFD08960
IFD08970
IFD08980
IFD08990
IFD09000
IFD09010
IFD09020

```



```

IFD09510
IFD09520
IFD09530
IFD09540
IFD09550
IFD09560
IFD09570
IFD09580
IFD09590
IFD09600
IFD09610
IFD09620
IFD09630
IFD09640
IFD09650
IFD09660
IFD09670
IFD09680
IFD09690
IFD09700
IFD09710
IFD09720
IFD09730
IFD09740
IFD09750
IFD09760
IFD09770
IFD09780
IFD09790
IFD09800
IFD09810
IFD09820
IFD09830
IFD09840
IFD09850
IFD09860
IFD09870
IFD09880
IFD09890
IFD09900
IFD09910
IFD09920
IFD09930
IFD09940
IFD09950
IFD09960
IFD09970
IFD09980
IFD09990

***
C      YIRWS = -YIRWS
C      CCMPUTE = 1.0 + DR*XX1M(1)
C      YMW(1) = U(1)*YMW(1) + U(2)*YLRWS
C      CCMPUTE = U(1)*YMW(1) + U(2)*YLRWS
C      CCMPUTE = 2.0 - YMW(1)
C      C(1,2) = XIRWS
C      CCMPUTE = XIRWS
C      IFACEP = IIFACEP - 1
DC 10 I=2,IFACEP
C      ***
C      YMW(I) = 1.0 + DR*XX1M(I)
C      C(I,4) = U(I)*YMW(I) + (U(I-1)+U(I+1))*YIRWS
C      ***
C      WORK WITH IHS
C      C(I,1) = XIRWS
C      C(I,2) = 2.0 - YMW(I)
C      C(I,3) = XIRWS
C      CCNTINUE
C      CCMPUTE LHS & RHS ELEMENTS IN SEDIMENT
C      IFACEP = IIFACEP + 1
DC 20 I=IFACEP,NN1
C      ***
C      RHS
C      C(I,4) = U(I)*YMS + (U(I-1)+U(I+1))*YLRWS
C      ***
C      LHS
C      C(I,1) = XIRWS
C      C(I,2) = XIRWS
C      C(I,3) = XIRWS
C      CCNTINUE

***
C      IF ENTIRE SEGMENT LEVEL GO TO 50
C      IF ( ISLOPE.EQ.2 ) GC TO 50

***
C      INTERFACE SIGRES FITTER UP OR DOWN
C      ***
C      CALCULATE CCNSTANTIS FOR COMPUTING MATRIX ELEMENTS
C      SINE = SIN (THETA)
C      CCSE = COS (THETA)
C      DELTA = XY10 + XY11*(XY8+XY9)*SINE*CCSE
C      BEPA1 = DELTA / DELTA
C      GAMMA1 = DELTA * XY12 * RHO1
C      EIDA2 = DELTA * XY11 * SINE*CCSE + RHO1*SINE*SINE +
C      GAMMA2 = DELTA * XY12 * RHO1 * COSI*CCSE + RHO2*SINE*SINE +
C      ZZ1 = DELTA * (RHO1*SINE*SINE + RHO2*CCSE*CCSE +
C      XY8*SINE*CCSE*XY11)

```

```

222 = DELIM * (RHC1*A2 - (COSE-XX8*SINE) *XX9*XX11*EYE*YK0*
      SINE)
223 = DELIM * RHO2
224 = DELIM * ( A2 * ( RHO1*COSE*CCSE + RHO2*SINE*SINE
      + XX8*SINE*CCSE*XX11 )
      - CCSE + XX8*SINE ) *XX9*XX11*EYE*YK0*SINE )
225 = C.5*IS*ZZ1
226 = 1.0 + 0.5*DB*(ZZ2-BEDA1-GAMMA1)
227 = -0.5*IR*ZZ3
228 = 1.0 - 0.5*DR*ZZ4
229 = 2.0 - 228
230 = 2.0 - 226

*** IF BOTTM SLOPES UP GO TO 40
*** IF ( ISLOPE.EQ.3.CM. ISLOPE.EQ.5 ) GC IC 40
*** BOTTM SLOPES DOWN
IFACE2 = IFACEP
*** COMPUTE OFF-DIAGONAL, Y MATRIX ELEMENTS ON INTERFACE
YLI = 0.5 * LR * GAMMA1
YRI = 0.5 * DR * BEDA1
*** COMPUTE MAIN DIAGONAL, Y MATRIX ELEMENT ON INTERFACE
YHI = A(IFACE) * ZZ5 + ZZ6
*** COMPUTE INTERFACE ELEMENT *YLI + U(IFACE)*YHI +
C(IFACE,4) = U(IFACEP)*YRI
*** COMPUTE Y MATRIX ELEMENTS ON INTERFACE
XLI = -0.5*DR * GAMMA2
XRI = A(IFACE2) * ZZ7 + ZZ8
*** IF MODIFIED BOTTOM THEN NO NEED TO ADJUST LHS
IF ( ISLOPE.EQ.4 ) GO TO 45
C(IFACE,1) = XLI
C(IFACE,2) = YLI
C(IFACE,3) = XRI
*** COMPUTE Y MATRIX ELEMENTS ONE ROW ABOVE INTERFACE
C(IFACE,1) = XLRWS
C(IFACE,2) = YLRWS
C(IFACE,3) = XLRWS
GO TO 60

*** BOTTM SLOPES UP
IFACE2 = IFACEM
*** COMPUTE OFF-DIAGONAL, Y MATRIX ELEMENTS ON INTERFACE
YLI = 0.5 * LR * GAMMA2
YRI = 0.5 * DR * BEDA2
*** COMPUTE MAIN DIAGONAL, Y MATRIX ELEMENT ON INTERFACE
YHI = A(IFACE) * ZZ7 + ZZ9
*** COMPUTE INTERFACE ELEMENT IN RHS C COLUMN VECTOR
C(IFACE,4) = U(IFACEP)*YRI

```

```

IFD09990
IFD10000
IFD10010
IFD10020
IFD10030
IFD10040
IFD10050
IFD10060
IFD10070
IFD10080
IFD10090
IFD10100
IFD10110
IFD10120
IFD10130
IFD10140
IFD10150
IFD10160
IFD10170
IFD10180
IFD10190
IFD10200
IFD10210
IFD10220
IFD10230
IFD10240
IFD10250
IFD10260
IFD10270
IFD10280
IFD10290
IFD10300
IFD10310
IFD10320
IFD10330
IFD10340
IFD10350
IFD10360
IFD10370
IFD10380
IFD10390
IFD10400
IFD10410
IFD10420
IFD10430
IFD10440
IFD10450
IFD10460

```

```

C (IFACE,4) = U(IFACE)*YLI + U(IFACE)*YRI +
*** COMPUTE X MATRIX ELEMENTS ON INTERFACE
XLI = -0.5*DR*GAMMA1 + ZZ5
XMI = -A(IFACE2)*ZZ5 + ZZ10
XRI = -0.5*DR*BEDA1
*** IF MOLIFIED BOTTOM THEN NO NEED TO ADJUST LHS
*** IF (ISLCEE.EQ.5) GO TO 45
C (IFACE,1) = YLI
C (IFACE,2) = XMI
C (IFACE,3) = XLENS
*** COMPUTE MATRIX ELEMENTS ONE ROW EACH INTERFACE
C (IFACE,1) = XMS
C (IFACE,2) = XLENS
C (IFACE,3)
GO TO 60
*** SAVE INTERFACE VALUES ON SLOPING SECTION
YLI2 = YLI
YRI2 = YRI
XLI2 = XLI
XRI2 = XRI
*** SEGMENT LEVEL 4
IFACE2 = IFACE
YLI = LF + DR
YRI = LF*XX7
C (IFACE,1) = U(IFACE)*YLI + U(IFACE)*YRI
C (IFACE,2) = -YLI
C (IFACE,3) = -YRI
*** SAVE INTERFACE VALUES ON LEVEL SECTION
YLI4 = YLI
YRI4 = YRI
CCOMPUTE MATRIX ELEMENTS CN INTERFACE
C (IFACE,1) = U(IFACE)/XX4 + XX5
C (IFACE,2) = U(IFACE)*YLI + U(IFACE)*YRI
C (IFACE,3) = U(IFACE)*YRI
C (IFACE,4) = U(IFACE)*YLI + U(IFACE)*YRI
C (IFACE,5) = U(IFACE)*YLI + U(IFACE)*YRI
C (IFACE,6) = U(IFACE)*YLI + U(IFACE)*YRI
C (IFACE,7) = U(IFACE)*YLI + U(IFACE)*YRI
C (IFACE,8) = U(IFACE)*YLI + U(IFACE)*YRI
C (IFACE,9) = U(IFACE)*YLI + U(IFACE)*YRI
C (IFACE,10) = U(IFACE)*YLI + U(IFACE)*YRI
C (IFACE,11) = U(IFACE)*YLI + U(IFACE)*YRI
C (IFACE,12) = U(IFACE)*YLI + U(IFACE)*YRI
C (IFACE,13) = U(IFACE)*YLI + U(IFACE)*YRI
C (IFACE,14) = U(IFACE)*YLI + U(IFACE)*YRI
C (IFACE,15) = U(IFACE)*YLI + U(IFACE)*YRI
C (IFACE,16) = U(IFACE)*YLI + U(IFACE)*YRI
C (IFACE,17) = U(IFACE)*YLI + U(IFACE)*YRI
C (IFACE,18) = U(IFACE)*YLI + U(IFACE)*YRI
C (IFACE,19) = U(IFACE)*YLI + U(IFACE)*YRI
C (IFACE,20) = U(IFACE)*YLI + U(IFACE)*YRI
C (IFACE,21) = U(IFACE)*YLI + U(IFACE)*YRI
C (IFACE,22) = U(IFACE)*YLI + U(IFACE)*YRI
C (IFACE,23) = U(IFACE)*YLI + U(IFACE)*YRI
C (IFACE,24) = U(IFACE)*YLI + U(IFACE)*YRI
C (IFACE,25) = U(IFACE)*YLI + U(IFACE)*YRI
C (IFACE,26) = U(IFACE)*YLI + U(IFACE)*YRI
C (IFACE,27) = U(IFACE)*YLI + U(IFACE)*YRI
C (IFACE,28) = U(IFACE)*YLI + U(IFACE)*YRI
C (IFACE,29) = U(IFACE)*YLI + U(IFACE)*YRI
C (IFACE,30) = U(IFACE)*YLI + U(IFACE)*YRI
C (IFACE,31) = U(IFACE)*YLI + U(IFACE)*YRI
C (IFACE,32) = U(IFACE)*YLI + U(IFACE)*YRI
C (IFACE,33) = U(IFACE)*YLI + U(IFACE)*YRI
C (IFACE,34) = U(IFACE)*YLI + U(IFACE)*YRI
C (IFACE,35) = U(IFACE)*YLI + U(IFACE)*YRI
C (IFACE,36) = U(IFACE)*YLI + U(IFACE)*YRI
C (IFACE,37) = U(IFACE)*YLI + U(IFACE)*YRI
C (IFACE,38) = U(IFACE)*YLI + U(IFACE)*YRI
C (IFACE,39) = U(IFACE)*YLI + U(IFACE)*YRI
C (IFACE,40) = U(IFACE)*YLI + U(IFACE)*YRI
C (IFACE,41) = U(IFACE)*YLI + U(IFACE)*YRI
C (IFACE,42) = U(IFACE)*YLI + U(IFACE)*YRI
C (IFACE,43) = U(IFACE)*YLI + U(IFACE)*YRI
C (IFACE,44) = U(IFACE)*YLI + U(IFACE)*YRI
C (IFACE,45) = U(IFACE)*YLI + U(IFACE)*YRI
C (IFACE,46) = U(IFACE)*YLI + U(IFACE)*YRI
C (IFACE,47) = U(IFACE)*YLI + U(IFACE)*YRI
C (IFACE,48) = U(IFACE)*YLI + U(IFACE)*YRI
C (IFACE,49) = U(IFACE)*YLI + U(IFACE)*YRI
C (IFACE,50) = U(IFACE)*YLI + U(IFACE)*YRI
C (IFACE,51) = U(IFACE)*YLI + U(IFACE)*YRI
C (IFACE,52) = U(IFACE)*YLI + U(IFACE)*YRI
C (IFACE,53) = U(IFACE)*YLI + U(IFACE)*YRI
C (IFACE,54) = U(IFACE)*YLI + U(IFACE)*YRI
C (IFACE,55) = U(IFACE)*YLI + U(IFACE)*YRI
C (IFACE,56) = U(IFACE)*YLI + U(IFACE)*YRI
C (IFACE,57) = U(IFACE)*YLI + U(IFACE)*YRI
C (IFACE,58) = U(IFACE)*YLI + U(IFACE)*YRI
C (IFACE,59) = U(IFACE)*YLI + U(IFACE)*YRI
C (IFACE,60) = U(IFACE)*YLI + U(IFACE)*YRI
C (IFACE,61) = U(IFACE)*YLI + U(IFACE)*YRI
C (IFACE,62) = U(IFACE)*YLI + U(IFACE)*YRI
C (IFACE,63) = U(IFACE)*YLI + U(IFACE)*YRI
C (IFACE,64) = U(IFACE)*YLI + U(IFACE)*YRI
C (IFACE,65) = U(IFACE)*YLI + U(IFACE)*YRI
C (IFACE,66) = U(IFACE)*YLI + U(IFACE)*YRI
C (IFACE,67) = U(IFACE)*YLI + U(IFACE)*YRI
C (IFACE,68) = U(IFACE)*YLI + U(IFACE)*YRI
C (IFACE,69) = U(IFACE)*YLI + U(IFACE)*YRI
C (IFACE,70) = U(IFACE)*YLI + U(IFACE)*YRI
C (IFACE,71) = U(IFACE)*YLI + U(IFACE)*YRI
C (IFACE,72) = U(IFACE)*YLI + U(IFACE)*YRI
C (IFACE,73) = U(IFACE)*YLI + U(IFACE)*YRI
C (IFACE,74) = U(IFACE)*YLI + U(IFACE)*YRI
C (IFACE,75) = U(IFACE)*YLI + U(IFACE)*YRI
C (IFACE,76) = U(IFACE)*YLI + U(IFACE)*YRI
C (IFACE,77) = U(IFACE)*YLI + U(IFACE)*YRI
C (IFACE,78) = U(IFACE)*YLI + U(IFACE)*YRI
C (IFACE,79) = U(IFACE)*YLI + U(IFACE)*YRI
C (IFACE,80) = U(IFACE)*YLI + U(IFACE)*YRI
C (IFACE,81) = U(IFACE)*YLI + U(IFACE)*YRI
C (IFACE,82) = U(IFACE)*YLI + U(IFACE)*YRI
C (IFACE,83) = U(IFACE)*YLI + U(IFACE)*YRI
C (IFACE,84) = U(IFACE)*YLI + U(IFACE)*YRI
C (IFACE,85) = U(IFACE)*YLI + U(IFACE)*YRI
C (IFACE,86) = U(IFACE)*YLI + U(IFACE)*YRI
C (IFACE,87) = U(IFACE)*YLI + U(IFACE)*YRI
C (IFACE,88) = U(IFACE)*YLI + U(IFACE)*YRI
C (IFACE,89) = U(IFACE)*YLI + U(IFACE)*YRI
C (IFACE,90) = U(IFACE)*YLI + U(IFACE)*YRI
C (IFACE,91) = U(IFACE)*YLI + U(IFACE)*YRI
C (IFACE,92) = U(IFACE)*YLI + U(IFACE)*YRI
C (IFACE,93) = U(IFACE)*YLI + U(IFACE)*YRI
C (IFACE,94) = U(IFACE)*YLI + U(IFACE)*YRI

```

IPD10950
 IPD10960
 IPD10970
 IPD10980
 IPD10990
 IPD11000
 IPD11010
 IPD11020
 IPD11030
 IPD11040
 IPD11050
 IPD11060
 IPD11070
 IPD11080
 IPD11090
 IPD11100
 IPD11110
 IPD11120
 IPD11130
 IPD11140
 IPD11150
 IPD11160
 IPD11170
 IPD11180
 IPD11190
 IPD11200
 IPD11210
 IPD11220
 IPD11230
 IPD11240
 IPD11250
 IPD11260
 IPD11270
 IPD11280
 IPD11290
 IPD11300
 IPD11310
 IPD11320
 IPD11330
 IPD11340
 IPD11350
 IPD11360
 IPD11370
 IPD11380
 IPD11390
 IPD11400
 IPD11410
 IPD11420

```

CONTINUE
*** SOLVE FOR SOLUTION FIELD AT RANGE RA2
CALL TRIDG (C,U,N,CR,CTWO)

*** APPLY ARTIFICIAL ATTENUATION
CALL ATTEND (U,ATT,IA,NA)

RA2P = RA2 + 0.5
*** TIME TO WRITE?
IF ( RA2P-GE.XWR ) CALL WRITE2
*** TIME TO PRINT?
IF ( RA2P-GE.XPR ) CALL PRINT2

*** UPDATE INTERFACE FCINTER
IFACE = IFACE2

RETURN
END

SUBROUTINE TRIDG (C,U,N,CR,CTWO)
*** THIS SUBROUTINE SOLVES A SET OF N - 1 (NH1) LINEAR
*** SIMULTANEOUS EQUATIONS HAVING A TRIANGONAL COEFFICIENT
*** MATRIX. MATRIX ELEMENTS IN THE LOWER DIAGONAL, MAIN DIAGONAL
*** AND UPPER TRIANGONAL ARE STORED IN C(I,1), C(I,2), AND C(I,3)
*** RESPECTIVELY. THE RHS COLUMN VECTOR IS STORED IN C(I,4).
*** THE SOLUTION FIELD IS STORED IN U(I).
*** WE NEED ONLY SOLVE AN NH1 X NH1 SYSTEM (RATHER THAN
*** AN N X N SYSTEM) BECAUSE U(N) IS KNOWN: U(N)=0.0
*** THE SUBROUTINE IS A MODIFIED VERSION OF SUBROUTINE
*** TRIDG FROM:
*** "APPLIED NUMERICAL ANALYSIS" (SECOND EDITION)
*** BY: CURTIS F. GERALD
*** PUBLISHED BY ADDISON-WESLEY PUBLISHING CO. 1980
*** THE MAIN MODIFICATIONS TO THE ROUTINE IN THE TEXT
*** INVOLVED:
(4) INTRODUCING ARRAYS CTWO AND CR TO PRESERVE THE
*** ORIGINAL VALUES IN C(I,2) AND TO MAKE THE ROUTINE
*** MORE EFFICIENT. THIS RESULTS IN A CONSIDERABLE
*** SAVINGS IN EXECUTION TIME FOR THE CASE OF A
*** HORIZONTAL BOTTOM. (SEE SUBROUTINE TRIDI)
*** MODIFYING THE ROUTINE TO SOLVE AN NH1 X NH1
*** SYSTEM.
  
```

IFD11430
 IFD11440
 IFD11450
 IFD11460
 IFD11470
 IFD11480
 IFD11490
 IFD11500
 IFD11510
 IFD11520
 IFD11530
 IFD11540
 IFD11550
 IFD11560
 IFD11570
 IFD11580
 IFD11590
 IFD11600
 IFD11610
 IFD11620
 IFD11630
 IFD11640
 IFD11650
 IFD11660
 IFD11670
 IFD11680
 IFD11690
 IFD11700
 IFD11710
 IFD11720
 IFD11730
 IFD11740
 IFD11750
 IFD11760
 IFD11770
 IFD11780
 IFD11790
 IFD11800
 IFD11810
 IFD11820
 IFD11830
 IFD11840
 IFD11850
 IFD11860
 IFD11870
 IFD11880
 IFD11890
 IFD11900

*** (5) SEE PAGES 129 AND 133 IN THE TEXT FOR FURTHER INFO.

CCMEX C(5000,4), U(5000), CR(5000), CTWO(5000)

NM1 = N - 1
 NM2 = N - 2
 CINC(1) = C(1,2)
 DO 10 I=2, NM1
 C(I,1) = C(I,1) * C(I-1,3)
 C(I,2) = CR(I) * C(I-1,4)
 C(I,4) = C(I,4) * C(I-1,3)
 CCNTINUE

U(N) = 0.0

*** NOW PERFORM BACK SUBSTITUTION

U(NM1) = C(NM1,4) / CINC(NM1)

DO 20 I=1, NM2
 H = NM1 - I
 U(H) = (C(H,4) - C(H,3)*U(H+1)) / CTWO(H)
 CCNTINUE

RETURN
 END

SUBROUTINE TRILI (C,U,N,CR,CTWO)

*** THIS SUBROUTINE IS A MODIFIED VERSION OF SUBROUTINE TRILG
 FROM THE ILL PROGRAM. SUBROUTINE TRILG IS IN TURN A MODIFIED
 VERSION OF TRIDG AS PER THE REFERENCE BELOW.
 *** THE SUBROUTINE SOLVES A SET OF N - 1 (NM1) LINEAR
 SIMULTANEOUS EQUATIONS HAVING A TRIANGULAR COEFFICIENT
 MATRIX. THE MATRIX ELEMENTS IN THE LOWER TRIANGULAR
 AND UPPER TRIANGULAR ARE STORED IN C(I,1) AND C(I,3)
 RESPECTIVELY. THE RIGHT HAND SIDE STORED IN C(I,4).
 THE SOLUTION VECTOR IS STORED IN U(I).
 *** THE INDEX I REFERS TO ROW NUMBER.
 WE NEED ONLY SOLVE AN NM1 X NM1 SYSTEM (RATHER THAN
 AN N X N SYSTEM) BECAUSE U(N) IS KNOWN: U(N) = 0.0
 THE SUBROUTINE IS A MODIFIED VERSION OF ILL SUB-
 ROUTINE TRIDG WHICH IN TURN IS A MODIFIED VERSION
 OF SUBROUTINE TRIDG AS PER:
 "APPLIED NUMERICAL ANALYSIS" (SECOND EDITION)
 BY: CURTIS P. GERRAL


```

CCMCMCN / REAL, ALPHA, AIT(5000), BETA1, BETA2, BR(101), BZ(101), C0, EDZ,
* CSVP(101), C2, CWATER(5000), DR, DRIVL, DRHAX, CZ, FRC, EDR, FX10,
* R1, RA1, RA2, RHCI, RHO2, RMAY, THETA, XK0, XLAM, LA, IPR, XI4, XI10,
* XX11, XWA, WDR6, Z1, YR1, ZL, YR2, ZR, ZS, ZSUP, (101), ZAEIYA
CCMCMCN / CPLEX, A(5000), A2, C(5000,4), CR(5000), CTMC(5000),
* EYI, YLI, YLIZ, YLHS, YMI, XHS, XRI9, XRIZ,
* XX1, XX2, XX3, XX5, XX6, XX7, XX8, XX9, XX12, XX1H(5000)
* YLI, YLI4, YLIZ, YLHS, YMI, YMS, YMH(5000), YRI, YRIV, YRIZ,
* U(5000), Z25, Z26, Z27, Z28, Z29, Z210
C *** UPDATE IPAC12
C IFACE2 = IFACE + 1
C *** UPDATE Y MATRIX, MAIN DIAGONAL, INTERFACE ELEMENT
C YEI = A( IFACE) * Z25 + Z26
C *** UPDATE Y MATRIX, MAIN DIAGONAL, WATER ELEMENT, CNE ROW
C AECVE INTERFACE
C YMH( IFACE-1) = 1.0 + DR * XX1H( IFACE-1)
C *** UPDATE RHS
C CALL RHS
C *** UPDATE LHS
C *** UPDATE X MATRIX ELEMENTS ONE ROW ABOVE INTERFACE
C( IFACE, 1) = XLRMS
C( IFACE, 2) = 1.0 - DR * XX1H( IFACE)
C( IFACE, 3) = XI, RNS
C *** UPDATE X MATRIX ELEMENTS ON INTERFACE
C( IFACE, 1) = XLI
C( IFACE, 2) = A( IFACE2) * Z27 + Z28
C( IFACE, 3) = YRI
C *** SOLVE THE TRIDIAGONAL SYSTEM
C CALL TRIDG (C, U, N, CR, CTWO)
C *** UPDATE IFACE
C IFACE = IFACE2
C RETURN
C ENI
CCCCC
SUBROUTINE UP
THIS SUBROUTINE UPDATES THE RHS & LHS OF THE EQUATION AND
SOLVES FOR THE SOLUTION VECTOR VALUES ARE STORED IN C(I,4)
{1} THE INTERFACE AT RANGE RA1 IS AT GRIDPOINT IFACE
{2} THE INTERFACE AT RANGE RA2 IS AT GRIDPOINT IFACE2
{3} ( WHERE IFACE2 = IFACE - 1 )
CCCCC

```

```

IFD12390
IFD12400
IFD12410
IFD12420
IFD12430
IFD12440
IFD12450
IFD12460
IFD12470
IFD12480
IFD12490
IFD12500
IFD12510
IFD12520
IFD12530
IFD12540
IFD12550
IFD12560
IFD12570
IFD12580
IFD12590
IFD12600
IFD12610
IFD12620
IFD12630
IFD12640
IFD12650
IFD12660
IFD12670
IFD12680
IFD12690
IFD12700
IFD12710
IFD12720
IFD12730
IFD12740
IFD12750
IFD12760
IFD12770
IFD12780
IFD12790
IFD12800
IFD12810
IFD12820
IFD12830
IFD12840
IFD12850
IFD12860

```


IFD13830
 IFD13840
 IFD13850
 IFD13860
 IFD13870
 IFD13880
 IFD13890
 IFD13900
 IFD13910
 IFD13920
 IFD13930
 IFD13940
 IFD13950
 IFD13960
 IFD13970
 IFD13980
 IFD13990
 IFD14000
 IFD14010
 IFD14020
 IFD14030
 IFD14040
 IFD14050
 IFD14060
 IFD14070
 IFD14080
 IFD14090
 IFD14100
 IFD14110
 IFD14120
 IFD14130
 IFD14140
 IFD14150
 IFD14160
 IFD14170
 IFD14180
 IFD14190
 IFD14200
 IFD14210
 IFD14220
 IFD14230
 IFD14240
 IFD14250
 IFD14260
 IFD14270
 IFD14280
 IFD14290
 IFD14300

```

*** MAIN DIAGONAL IN WATER, ONE ROW ABOVE INTERFACE
  IF ( ISLOPE.EQ.5 ) GO TO 25
  YMW ( IFACE-1 ) = 1.0 + DR * XX1M ( IFACE-1 )
  UPDATE RHS INTERFACE ELEMENTS
  YLI = YLIV
  YMI = 1.0 + DR * ( XX1M ( IFACE ) / XX4 + XX5 )
  YRI = YRIV
  YPATE IHS
  C ( IFACE, 1 ) = -YLI
  C ( IFACE, 2 ) = 2.0 - YMI
  C ( IFACE, 3 ) = -YRI
  SOLVE SYSTEM
  CALL RHS
  CALL FBIDG ( C, U, N, CR, CTWO )
  GC TO 50

```

```

*** SLOPING SECTION INTERFACE ELEMENTS
  UPDATE YLI = YLIZ
  YRI = YRIZ
  XLI = XLIZ
  YRI = YRIZ
  SOLVE SYSTEM AS APPROPRIATE
  IF ( ISICPE.EQ.4 ) CALL DOWN
  IF ( ISICPE.EQ.5 ) CALL UP

```

```

CONTINUE
RETURN
END

```

SUBROUTINE RHS

THIS SUBROUTINE MULTIPLIES TRIDIAGONAL MATRIX Y TIMES SCITUION
 FIELD U TO OBTAIN AN UPDATED RHS.
 (1) THE RHS COLUMN VECTOR VALUES ARE STORED IN C(I,4).

```

CCHMEX A A2 C CR CTWC EYE, XMS, XRI, XRIZ, XX1 2, XX1M, XRIZ,
XLI, YLI, YLIZ, YLIV, YLIZ, YLIV, YLIV, YLIV, YLIV, YLIV, YLIV,
XX1, XX2, XX3, XX4, XX5, XX6, XX7, XX8, XX9, XX10, XX11, XX12,
YLI, YLIV, YLIZ, YLIV, YLIV, YLIV, YLIV, YLIV, YLIV, YLIV,
YLI, YLIV, YLIZ, YLIV, YLIV, YLIV, YLIV, YLIV, YLIV, YLIV,
CCHMCHN / IN / A, IBOT1, NSVP, NUNHA, NXLFS
CCHMCHN / REAL, ALPHA, AT ( 5000 ), BETA1, BETA2, BR ( 101 ), C0,
CCHMCHN / CSVP ( 101 ), C2, CHATER ( 5000 ), DR, DRIVL, DMMAX, FZ, FRQ, LDR, FLZ,

```

IFD14310
IFD14320
IFD14330
IFD14340
IFD14350
IFD14360
IFD14370
IFD14380
IFD14390
IFD14400
IFD14410
IFD14420
IFD14430
IFD14440
IFD14450
IFD14460
IFD14470
IFD14480
IFD14490
IFD14500
IFD14510
IFD14520
IFD14530
IFD14540
IFD14550
IFD14560
IFD14570
IFD14580
IFD14590
IFD14600
IFD14610
IFD14620
IFD14630
IFD14640
IFD14650
IFD14660
IFD14670
IFD14680
IFD14690
IFD14700
IFD14710
IFD14720
IFD14730
IFD14740
IFD14750
IFD14760
IFD14770
IFD14780

```
* R1 RA1 RA2 RHC1 RHO2 RMAX THETA XKO XLAMLA XPR XX4, XX10,  
* XX11, XX6F, HDR6 ZL1R1 ZL1R2, ZR, ZS, ZSVP, (101), ZAEIYA  
* CCNHCN / CPIX/ A (5000) A2 C (5000, 4) CR (5000), CTW6 (5000),  
* RY1, XLI, XLIZ, YLRWS, XMI, XMS, XRI, XRI2,  
* XX1, XX2, XX3, XX5, XX6, XX7, XX8, XX9, XX12, XX1H (5000)  
* YL1, YL14, YL1Z, YLRWS, XMI, XMS, YMH (5000), YRI, YRIV, YRIZ,  
* U (5000), Z25, Z26, Z27, Z28, Z29, Z310
```

```
C *** UPDATE IFACEN & IFACEP  
C IFACEN = IFACE - 1  
C IFACEP = IFACE + 1  
C *** UPDATE RHS  
C (1, 4) = U (1) * YMH (1) + U (2) * YLRS  
C (1, 10) I=2, IFACEN = U (I) * YMH (I) + (U (I-1) + U (I+1)) * YLRS  
C CONTINUE 4  
C (IFACE, 4) = U (IFACEN) * YLI + U (IFACE) * YMI + U (IFACEP) * YFI  
C (20) I=IFACEN, NM1  
C (I, 4) = U (I) * YMS + (U (I-1) + U (I+1)) * YLRS  
C CONTINUE
```

FEJGEN
END

108

SUERCUTINE LEVEL

THIS SUBROUTINE UPDATES THE RHS OF THE EQUATION AND SOLVES FOR THE SOLUTION FIELD AT RANGE RA2.
{1} THE SOLUTION COLUMN VECTOR VALUES ARE STORED IN C (I, 4).
{2} FOR THE LEVEL INTERFACE THE LHS TRIDIAGONAL MATRIX ELEMENTS NEED NOT BE UPDATED.

```
CCRFLX A A2 C CR CTWC EYE, XMS, XRI, XRI2, XMS, XRI, XRI2, XX8, XX9, XX12, XX1H, YRIZ,  
* XLI, XLIZ, YLRWS, XMI, XMS, XRI, XRI2, XX7, XX8, XX9, XX12, XX1H, YRIZ,  
* XLI, XLIZ, YL1, YL1Z, YLRWS, XMI, XMS, XRI, YRIV, YRIZ,  
* U (5000), Z26, Z27, Z28, Z29, Z310  
CCNHCN / IN/ IA NSTEP1, NSTEP2, ISLOPE, ISTEP, INZ, N, NA, NBCT, NF1,  
* NREAL, ALPHA, AT (5000), BETA1, BETA2, BR (101), BZ (101), CO, EDZ,  
* CSVP (101), C2, CHA TER, D (5000), DR, DRIV, DDMAX, FZ, FRQ, LBR, EDZ,  
* R1, RA1, RA2, RHC1, RHO2, RMAX, THETA, XKO, XLAMLA, XPR, XX4, XX10,  
* XX11, XX6F, HDR6 ZL1R1, ZL1R2, ZR, ZS, ZSVP, (101), ZAEIYA  
* CCNHCN / CPIX/ A (5000) A2 C (5000, 4) CR (5000), CTW6 (5000),  
* RY1, XLI, XLIZ, YLRWS, XMI, XMS, XRI, XRI2, XX8, XX9, XX12, XX1H, YRIV, YRIZ,
```

IFD14790
 IFD14800
 IFD14810
 IFD14820
 IFD14830
 IFD14840
 IFD14850
 IFD14860
 IFD14870
 IFD14880
 IFD14890
 IFD14900
 IFD14910
 IFD14920
 IFD14930
 IFD14940
 IFD14950
 IFD14960
 IFD14970
 IFD14980
 IFD14990
 IFD15000
 IFD15010
 IFD15020
 IFD15030
 IFD15040
 IFD15050
 IFD15060
 IFD15070
 IFD15080
 IFD15090
 IFD15100
 IFD15110
 IFD15120
 IFD15130
 IFD15140
 IFD15150
 IFD15160
 IFD15170
 IFD15180
 IFD15190
 IFD15200
 IFD15210
 IFD15220
 IFD15230
 IFD15240
 IFD15250
 IFD15260

* * * XX1, XX2, XX3, XX5, XX6, XX7, XX8, XX9, XX12, XX1M (5000), YH1, YHIV, YRIZ,
 YL1, YL12, YL1Z, YL1S, YMI, YMS, YMH (5000), YHI, YHIV, YRIZ,
 U (5000), Z25, Z26, Z27, Z28, Z29, Z310
 * * *

C C *** UPDATE RHS
 C C CALL RHS
 C C *** SOLVE THE TRIDIAGONAL SYSTEM
 C C CALL TELDL (C, U, N, CR, CTWO)

IFJOBK
 ENL

SOEXECUTE PRINT2
 (1) THIS SUBROUTINE IS EFFECTIVELY THE CONTINUATION OF
 SUBROUTINE PRINT1.
 (2) THE FILE CREATED CORRESPONDS TO UNIT FILE NUMBER:
 NPCT = 55.
 (3) THE FILENAME AND FILETYPE FOR THIS FILE ARE:
 IFPCUT

DIMENSION FRMAG (5000), FIVE (121, 121)
 CCRFLX A(2, C, CTWO), EYE, XMS, XRI, XRIZ, XX9, XX12, XX1M
 XLI, XLI2, XLI3, XLI6, XLI7, XLI8, XLI9, XLI12, XLI1M
 XX1, XX3, XX5, XX6, XX7, XX8, XX9, XX12, XX1M
 YL1, YL12, YL13, YL16, YL17, YL1Z, YL1S, YMI, YMS, YMH (5000), YHI, YHIV, YRIZ,
 U (5000), Z25, Z26, Z27, Z28, Z29, Z310
 COMMON / IN / IA, IBOT1, IFACE, IP2, ISLOPE, ISTEP, IW2, N, NA, NBOT, NN1,
 NSTEP, NSTEP1, NSVF, NNHAX, NXLFS, IR
 COMMON / REAL / ALPHA, AT (5000), BETA1, BETA2, BR (101), BZ (101), CO
 CSVP (101), C2, CHAT (5000), DR, DRA, DRIVL, DMMAX, FZ, FRC, FDR, FZ,
 R1, R11, FA2, RH01, RHAX, ZR, ZS, ZSVP (101), ZAEIYA,
 RY11, Y6E, WDR, ZLYR2, ZLYR1, ZLYR2, ZR, ZS, ZSVP (101), ZAEIYA,
 PIFD
 COMMON / CPLX / A (5000), A2, C (5000, 4), CR (5000), CTWO (5000),
 EYE, XLI, XLI2, XLI3, XLI6, XLI7, XLI8, XLI9, XLI12, XLI1M, XRI, XRIZ,
 XX1, XX3, XX5, XX6, XX7, XX8, XX9, XX12, XX1M (5000)
 YL1, YL12, YL13, YL16, YL17, YL1Z, YL1S, YMI, YMS, YMH (5000), YHI, YHIV, YRIZ,
 U (5000), Z25, Z26, Z27, Z28, Z29, Z310
 LATA MPOUT/55/

*** PRINT RANGE 1398.0) - CR - (RA2 - GT. 2002.0) GC TO 30
 IF (RA2 - GT. 2102.0) - GO TO 30

IFD15270
 IFD15280
 IFD15290
 IFD15300
 IFD15310
 IFD15320
 IFD15330
 IFD15340
 IFD15350
 IFD15360
 IFD15370
 IFD15380
 IFD15390
 IFD15400
 IFD15410
 IFD15420
 IFD15430
 IFD15440
 IFD15450
 IFD15460
 IFD15470
 IFD15480
 IFD15490
 IFD15500
 IFD15510
 IFD15520
 IFD15530
 IFD15540
 IFD15550
 IFD15560
 IFD15570
 IFD15580
 IFD15590
 IFD15600
 IFD15610
 IFD15620
 IFD15630
 IFD15640
 IFD15650
 IFD15660
 IFD15670
 IFD15680
 IFD15690
 IFD15700
 IFD15710
 IFD15720
 IFD15730
 IFD15740

```

C      WRITE(NPOUT,900) RA2
C      IF = IE + 1
C      *** COMPUTE AND PRINT PROPAGATION LOSS AT EACH IPZ*TH DEPTH
C      WRITE(NPOUT,901)
C      DC 20 I=IPZ,N,IPZ
C      ZI = I*LI
C      ZL1 = INT(ZLYE1)
C      PL = CABS(U(I))
C      PIP ( PL,IF,0.0 ) GO TO 10
C      GO TO 15
C      PL = -20.0*ALOG10(PL) + 10.0*ALOG10(RA2)
C      PL = 999.9
C      CCNTINUE
C      PRMAG(I) = CABS(U(I)) TO 20
C      IF(ZI .GT. ZLYE1) GO TO 20
C      IF(ZI .GT. 121.0) GO TO 20
C      WRITE(NFCUT,902) ZI, PL, PRMAG(I)
C      II = II + 1
C      DIPD(II,IB) = PL
C      PIPD(II,IB) = PRMAG(I)*100
C      CCNTINUE
C      CCNTINUE
C      IF(RA2.GT.199C.0) WRITE(31,36) (ATT(I),I=1,4000)
C      FCENAT(7F10.5)
C      *** DETERMINE NEXT RANGE AT WHICH TO PRINT SOLUTION
C      XER = XPR+ELR
C      FCENAT(//,5X,'RANGE =',F9.3,' M.',
C      FCENAT(15X,'DEPTH',6X,'LCSS(DB)',14X,'PRMAG(I)',/)
C      FCENAT(10X,F10.2,3X,F10.2,13X,E12.5)
C      RETURN
C      END
C      SUBROUTINE WRITE2
C      (1) THIS SUBROUTINE IS EFFECTIVELY THE CONTINUATION OF
C      SUBROUTINE WRITE1
C      (2) THE SUBROUTINE WRITES RANGE, RECEIVER DEPTH AND U(I)
C      WHEN CALLED. IT THEN UPDATES THE NEXT WRITE RANGE (XWR)
C      (3) THE FILE WRITTEN INTO CORRESPONDS TO UNIT FILE NUMBER:
C      NOU = 54.
  
```

```

IFD15750
IFD15760
IFD15770
IFD15780
IFD15790
IFD15800
IFD15810
IFD15820
IFD15830
IFD15840
IFD15850
IFD15860
IFD15870
IFD15880
IFD15890
IFD15900
IFD15910
IFD15920
IFD15930
IFD15940
IFD15950
IFD15960
IFD15970
IFD15980
IFD15990
IFD16000
IFD16010
IFD16020
IFD16030
IFD16040
IFD16050
IFD16060
IFD16070
IFD16080
IFD16090
IFD16100
IFD16110
IFD16120
IFD16130
IFD16140
IFD16150
IFD16160
IFD16170
IFD16180
IFD16190
IFD16200
IFD16210
IFD16220

```

```

(4) THE FILENAME AND FILETYPE FOR THIS FILE ARE:
IFCUT

```

```

* CCFLEX A A2 C CR CTWC EYE XMS XRI YRIZ XX12 XX1H YRIZ,
* XLI XL2 XL3 XL4 XL5 XL6 XL7 XL8 XL9 XL10 XL11 XL12 XL13 XL14 XL15 XL16 XL17 XL18 XL19 XL20 XL21 XL22 XL23 XL24 XL25 XL26 XL27 XL28 XL29 XL30 XL31 XL32 XL33 XL34 XL35 XL36 XL37 XL38 XL39 XL40 XL41 XL42 XL43 XL44 XL45 XL46 XL47 XL48 XL49 XL50 XL51 XL52 XL53 XL54 XL55 XL56 XL57 XL58 XL59 XL60 XL61 XL62 XL63 XL64 XL65 XL66 XL67 XL68 XL69 XL70 XL71 XL72 XL73 XL74 XL75 XL76 XL77 XL78 XL79 XL80 XL81 XL82 XL83 XL84 XL85 XL86 XL87 XL88 XL89 XL90 XL91 XL92 XL93 XL94 XL95 XL96 XL97 XL98 XL99 XL100 XL101 XL102 XL103 XL104 XL105 XL106 XL107 XL108 XL109 XL110 XL111 XL112 XL113 XL114 XL115 XL116 XL117 XL118 XL119 XL120 XL121 XL122 XL123 XL124 XL125 XL126 XL127 XL128 XL129 XL130 XL131 XL132 XL133 XL134 XL135 XL136 XL137 XL138 XL139 XL140 XL141 XL142 XL143 XL144 XL145 XL146 XL147 XL148 XL149 XL150 XL151 XL152 XL153 XL154 XL155 XL156 XL157 XL158 XL159 XL160 XL161 XL162 XL163 XL164 XL165 XL166 XL167 XL168 XL169 XL170 XL171 XL172 XL173 XL174 XL175 XL176 XL177 XL178 XL179 XL180 XL181 XL182 XL183 XL184 XL185 XL186 XL187 XL188 XL189 XL190 XL191 XL192 XL193 XL194 XL195 XL196 XL197 XL198 XL199 XL200 XL201 XL202 XL203 XL204 XL205 XL206 XL207 XL208 XL209 XL210 XL211 XL212 XL213 XL214 XL215 XL216 XL217 XL218 XL219 XL220 XL221 XL222 XL223 XL224 XL225 XL226 XL227 XL228 XL229 XL230 XL231 XL232 XL233 XL234 XL235 XL236 XL237 XL238 XL239 XL240 XL241 XL242 XL243 XL244 XL245 XL246 XL247 XL248 XL249 XL250 XL251 XL252 XL253 XL254 XL255 XL256 XL257 XL258 XL259 XL260 XL261 XL262 XL263 XL264 XL265 XL266 XL267 XL268 XL269 XL270 XL271 XL272 XL273 XL274 XL275 XL276 XL277 XL278 XL279 XL280 XL281 XL282 XL283 XL284 XL285 XL286 XL287 XL288 XL289 XL290 XL291 XL292 XL293 XL294 XL295 XL296 XL297 XL298 XL299 XL300 XL301 XL302 XL303 XL304 XL305 XL306 XL307 XL308 XL309 XL310 XL311 XL312 XL313 XL314 XL315 XL316 XL317 XL318 XL319 XL320 XL321 XL322 XL323 XL324 XL325 XL326 XL327 XL328 XL329 XL330 XL331 XL332 XL333 XL334 XL335 XL336 XL337 XL338 XL339 XL340 XL341 XL342 XL343 XL344 XL345 XL346 XL347 XL348 XL349 XL350 XL351 XL352 XL353 XL354 XL355 XL356 XL357 XL358 XL359 XL360 XL361 XL362 XL363 XL364 XL365 XL366 XL367 XL368 XL369 XL370 XL371 XL372 XL373 XL374 XL375 XL376 XL377 XL378 XL379 XL380 XL381 XL382 XL383 XL384 XL385 XL386 XL387 XL388 XL389 XL390 XL391 XL392 XL393 XL394 XL395 XL396 XL397 XL398 XL399 XL400 XL401 XL402 XL403 XL404 XL405 XL406 XL407 XL408 XL409 XL410 XL411 XL412 XL413 XL414 XL415 XL416 XL417 XL418 XL419 XL420 XL421 XL422 XL423 XL424 XL425 XL426 XL427 XL428 XL429 XL430 XL431 XL432 XL433 XL434 XL435 XL436 XL437 XL438 XL439 XL440 XL441 XL442 XL443 XL444 XL445 XL446 XL447 XL448 XL449 XL450 XL451 XL452 XL453 XL454 XL455 XL456 XL457 XL458 XL459 XL460 XL461 XL462 XL463 XL464 XL465 XL466 XL467 XL468 XL469 XL470 XL471 XL472 XL473 XL474 XL475 XL476 XL477 XL478 XL479 XL480 XL481 XL482 XL483 XL484 XL485 XL486 XL487 XL488 XL489 XL490 XL491 XL492 XL493 XL494 XL495 XL496 XL497 XL498 XL499 XL500 XL501 XL502 XL503 XL504 XL505 XL506 XL507 XL508 XL509 XL510 XL511 XL512 XL513 XL514 XL515 XL516 XL517 XL518 XL519 XL520 XL521 XL522 XL523 XL524 XL525 XL526 XL527 XL528 XL529 XL530 XL531 XL532 XL533 XL534 XL535 XL536 XL537 XL538 XL539 XL540 XL541 XL542 XL543 XL544 XL545 XL546 XL547 XL548 XL549 XL550 XL551 XL552 XL553 XL554 XL555 XL556 XL557 XL558 XL559 XL560 XL561 XL562 XL563 XL564 XL565 XL566 XL567 XL568 XL569 XL570 XL571 XL572 XL573 XL574 XL575 XL576 XL577 XL578 XL579 XL580 XL581 XL582 XL583 XL584 XL585 XL586 XL587 XL588 XL589 XL590 XL591 XL592 XL593 XL594 XL595 XL596 XL597 XL598 XL599 XL600 XL601 XL602 XL603 XL604 XL605 XL606 XL607 XL608 XL609 XL610 XL611 XL612 XL613 XL614 XL615 XL616 XL617 XL618 XL619 XL620 XL621 XL622 XL623 XL624 XL625 XL626 XL627 XL628 XL629 XL630 XL631 XL632 XL633 XL634 XL635 XL636 XL637 XL638 XL639 XL640 XL641 XL642 XL643 XL644 XL645 XL646 XL647 XL648 XL649 XL650 XL651 XL652 XL653 XL654 XL655 XL656 XL657 XL658 XL659 XL660 XL661 XL662 XL663 XL664 XL665 XL666 XL667 XL668 XL669 XL670 XL671 XL672 XL673 XL674 XL675 XL676 XL677 XL678 XL679 XL680 XL681 XL682 XL683 XL684 XL685 XL686 XL687 XL688 XL689 XL690 XL691 XL692 XL693 XL694 XL695 XL696 XL697 XL698 XL699 XL700 XL701 XL702 XL703 XL704 XL705 XL706 XL707 XL708 XL709 XL710 XL711 XL712 XL713 XL714 XL715 XL716 XL717 XL718 XL719 XL720 XL721 XL722 XL723 XL724 XL725 XL726 XL727 XL728 XL729 XL730 XL731 XL732 XL733 XL734 XL735 XL736 XL737 XL738 XL739 XL740 XL741 XL742 XL743 XL744 XL745 XL746 XL747 XL748 XL749 XL750 XL751 XL752 XL753 XL754 XL755 XL756 XL757 XL758 XL759 XL760 XL761 XL762 XL763 XL764 XL765 XL766 XL767 XL768 XL769 XL770 XL771 XL772 XL773 XL774 XL775 XL776 XL777 XL778 XL779 XL780 XL781 XL782 XL783 XL784 XL785 XL786 XL787 XL788 XL789 XL790 XL791 XL792 XL793 XL794 XL795 XL796 XL797 XL798 XL799 XL800 XL801 XL802 XL803 XL804 XL805 XL806 XL807 XL808 XL809 XL810 XL811 XL812 XL813 XL814 XL815 XL816 XL817 XL818 XL819 XL820 XL821 XL822 XL823 XL824 XL825 XL826 XL827 XL828 XL829 XL830 XL831 XL832 XL833 XL834 XL835 XL836 XL837 XL838 XL839 XL840 XL841 XL842 XL843 XL844 XL845 XL846 XL847 XL848 XL849 XL850 XL851 XL852 XL853 XL854 XL855 XL856 XL857 XL858 XL859 XL860 XL861 XL862 XL863 XL864 XL865 XL866 XL867 XL868 XL869 XL870 XL871 XL872 XL873 XL874 XL875 XL876 XL877 XL878 XL879 XL880 XL881 XL882 XL883 XL884 XL885 XL886 XL887 XL888 XL889 XL890 XL891 XL892 XL893 XL894 XL895 XL896 XL897 XL898 XL899 XL900 XL901 XL902 XL903 XL904 XL905 XL906 XL907 XL908 XL909 XL910 XL911 XL912 XL913 XL914 XL915 XL916 XL917 XL918 XL919 XL920 XL921 XL922 XL923 XL924 XL925 XL926 XL927 XL928 XL929 XL930 XL931 XL932 XL933 XL934 XL935 XL936 XL937 XL938 XL939 XL940 XL941 XL942 XL943 XL944 XL945 XL946 XL947 XL948 XL949 XL950 XL951 XL952 XL953 XL954 XL955 XL956 XL957 XL958 XL959 XL960 XL961 XL962 XL963 XL964 XL965 XL966 XL967 XL968 XL969 XL970 XL971 XL972 XL973 XL974 XL975 XL976 XL977 XL978 XL979 XL980 XL981 XL982 XL983 XL984 XL985 XL986 XL987 XL988 XL989 XL990 XL991 XL992 XL993 XL994 XL995 XL996 XL997 XL998 XL999

```

```

*** WRITE RANGE, DEPTH AND U(I)
WRITE(NOU,*) RA2, ZE, U(IWZ)

*** DETERMINE NEXT RANGE AT WHICH TO WRITE SOLUTION
NWR = NWR + NWR

```

```

RETURN
END

```

```

SUBROUTINE ATTENU(U,ATT,IA,NA)
THIS SUBROUTINE APPLIES ARTIFICIAL ATTENUATION TO THE BOTTOM-
MOST NA GRID POINTS AS PER ARESD PE MODEL BY EROCK - NORDA
TECH NOTE 12 - JAN 78
(1) ATTENUATION MATRIX ATT IS CALCULATED IN SUBROUTINE
NEWHA1

```

```

CCREIX U(5000)
DIMENSION ATT(5000)

```

```

DO 10 I=1, NA
U(IA+I) = U(IA+I) * ATT(I)
CCCONTINUE

```

```

10

```


PLO000390
 PLO000400
 PLO000410
 PLO000420
 PLO000430
 PLO000440
 PLO000450
 PLO000460
 PLO000470
 PLO000480
 PLO000490
 PLO000500
 PLO000510
 PLO000520
 PLO000530
 PLO000540
 PLO000550
 PLO000560
 PLO000570
 PLO000580
 PLO000590
 PLO000600
 PLO000610
 PLO000620
 PLO000630
 PLO000640
 PLO000650
 PLO000660
 PLO000670
 PLO000680
 PLO000690
 PLO000700
 PLO000710
 PLO000720
 PLO000730
 PLO000740
 PLO000750
 PLO000760
 PLO000770
 PLO000780
 PLO000790

```

A(I,J) = DATA(I,J)
CCMIXUE
CCNTINUE

PLOT/GRAPHICS ROUTINE.
CALL TEK618
CALL CCMPS
CALL FAGE(1,0,8.5)
CALL FLOWUE(1,0,2)
CALL AREA2L(8,0,0)
CALL FEIGHTI(2)
CALL YNAME(1,1,1)
CALL YNAMEH(1,1,1)
CALL SHCHSH(90,1,0,0,2,1)
CALL FEIGHTI(3,1)
CALL FASALF(1,1)
CALL MIXALF(1,1)
CALL FEADIN(1,1)
CALL FEIGHTI(2)
CALL MESSAGE(1)
CALL MESSAGE(10,1,4,6.40)
CALL YAYANG(0,0)
CALL FEIGHTI(0,0)
CALL RESET(SWISSM)
CALL GRAP(1400,0,100,2000.0,121,-20.0,1.0)
CALL FCOMON(20,0)
CALL FEIGHTI(0,1,25)
CALL CONHAN(A,1,1)
CALL CONLANG(1,1,1)
CALL CCNLANG(96,5)
CALL FASPLN(2,5)
CALL LINEAR
CALL CCNTU(1,1,1)
CALL TOT
CALL GRID(1,1)
CALL ENDPL(1)
CALL LONEP
CALL SICE
ENR
  
```

20
10
C

C

C

C

C

C

C

C

C

C

C

C

C

C

C

C

C

C

C

C

C

APPENDIX C

RUNNING THE CONTOUR PLOT ON THE NPS COMPUTER

A. INTRODUCTION

This Appendix describes a procedure for running the TL contour plot on the NPS computer. Detailed instructions for running the IFD program can be found in Jaeger(1983).

E. COPYING THE FILE FOR USE

Once the TL values have been generated by the IFD program, all that is needed to produce a TL contour plot is the file PICTS FORTRAN. This file is shown in Appendix E and can be copied from a computer account maintained by the Underwater Acoustics Curriculum. To link with this account and obtain a copy of the file, the user should proceed as follows:

- (1) log on terminal.
- (2) Enter: CP LINK 0160P 191 195 RR .
- (3) When prompted for the read password enter: UX .
- (4) Enter: ACC 195 C .
- (5) Enter: COPY PICTS FORTRAN C = = A .

At this point the PICTS FORTRAN file should reside on the user's A disk.

C. RUNNING THE PROGRAM

Before running the program the user must obtain the TL values from the IFD program. These TL values must be sent to

a data disk in order for the FICIS program to be able to use them. This can be done by placing a WRITE statement in the IFD program that sends the values to a data disk. The modified IFD depicted in Appendix A uses this technique and can be used as a guide.

Once the data disk has been created, the user must assign temporary disk space (TDISK) to give the program sufficient room to generate the TL contours. For more information on how to assign temporary disk space, see NPS Technical Note TN-VM-C1 which is available in the computer consultant's office.

With these initial steps completed, all that remains is to compile and run the program. The program can be compiled by:

Enter: FCRTGI PLOTS .

The program must be run at the TEK618 graphics terminal under DISSFIA. This can be done by:

Enter: DISSPLA .

The user will then be prompted for the compiled Fortran program name and the file definitions for the data disk, before the program will run.

APPENDIX D SOURCE DEPTH SENSITIVITY ANALYSIS

During the laboratory experiment, two supplemental sets of measurements were taken to obtain an indication of the sensitivity of the pressure amplitude to changes in the source depth. The first set of measurements was obtained by varying the source depth with the receiver fixed at 1.0X (4.8 cm from the beach), and lowered in depth to the bottom. For the second set of measurements, the receiver was fixed at the third dump distance (14.4 cm from the beach), and measurements were taken with the source fixed at 5, 7, 9, 11, 13, 15, 17, 19, 21, 23, 25, 27, 29, and 31 cm from the surface.

The results of the first analysis are shown in Figure D.1. In the figure, pressure was normalized by dividing by the maximum pressure and depth was normalized by dividing by the depth of the water column. Although theory predicts only one propagating mode at this distance, the results show modal phase interference.

The results of the second analysis are shown in Figure D.2 through Figure D.6. In the figures, each curve represents a set of measurements taken with the source fixed at a specific depth. For convenience, more than one curve is shown on a given figure. All pressure values were normalized by dividing by the maximum pressure in the field. The depth values were normalized by dividing by the maximum water depth.

In general, at 3.0X there appears to be modal phase interference which is influenced by source depth. Given the roughness of this analysis, the details of this interference are obscure. However, the modal interference does not appear

to be inconsistent with either the placement of the source
or with the previous experimental measurements.

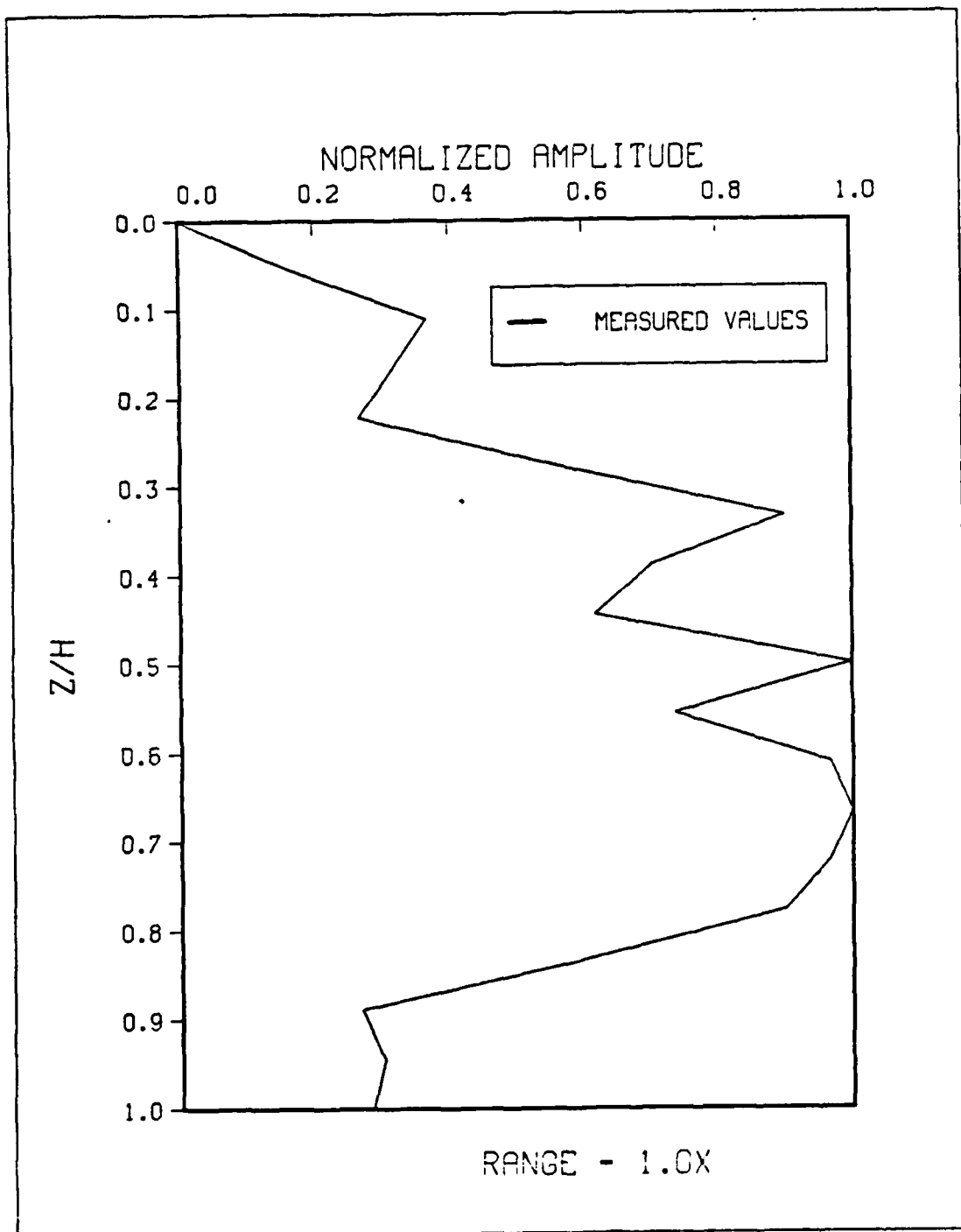


Figure D.1 Source Sensitivity Analysis at 1.0X.

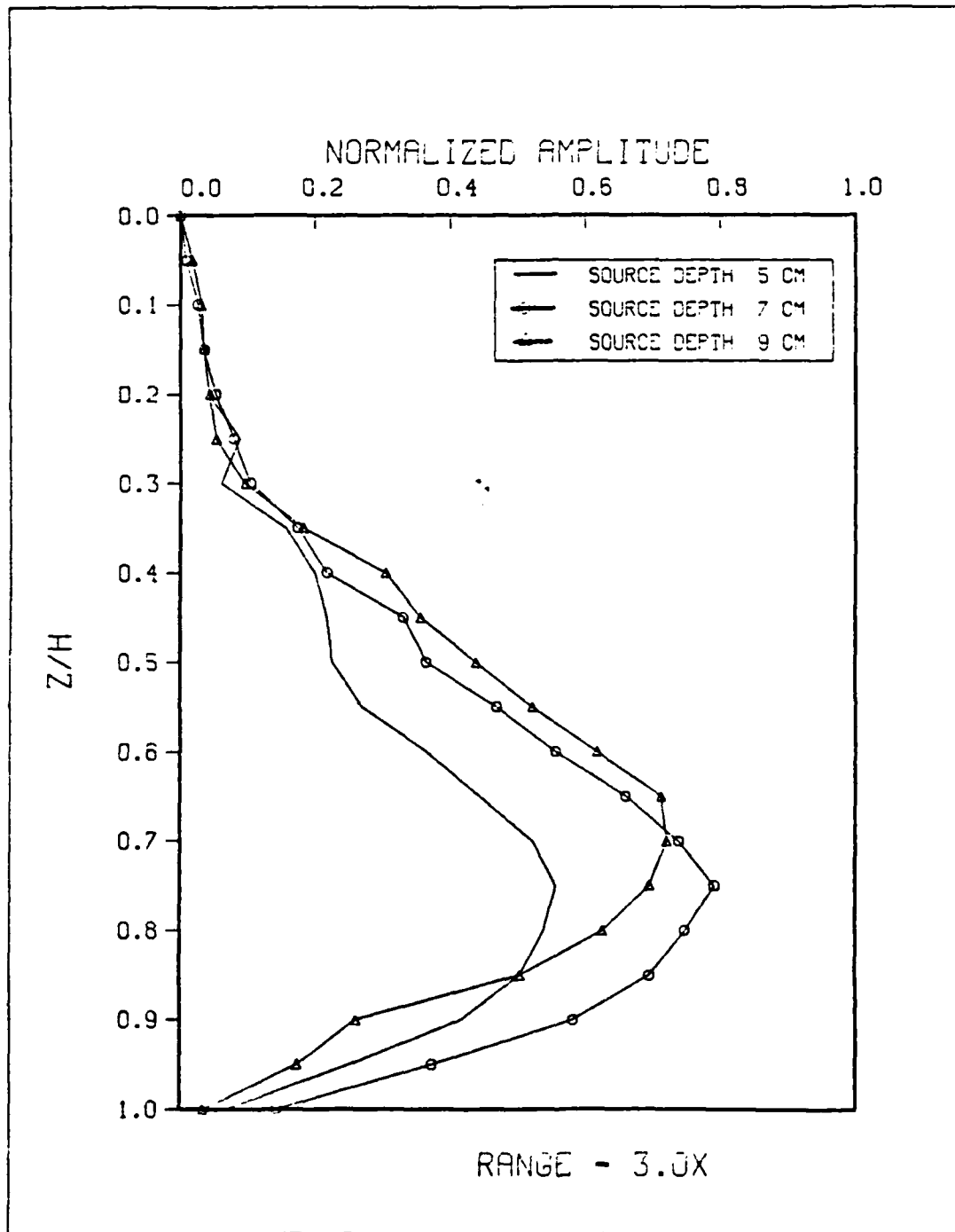


Figure D.2 Measurements with Source Depth of 5, 7, and 9 Cm.

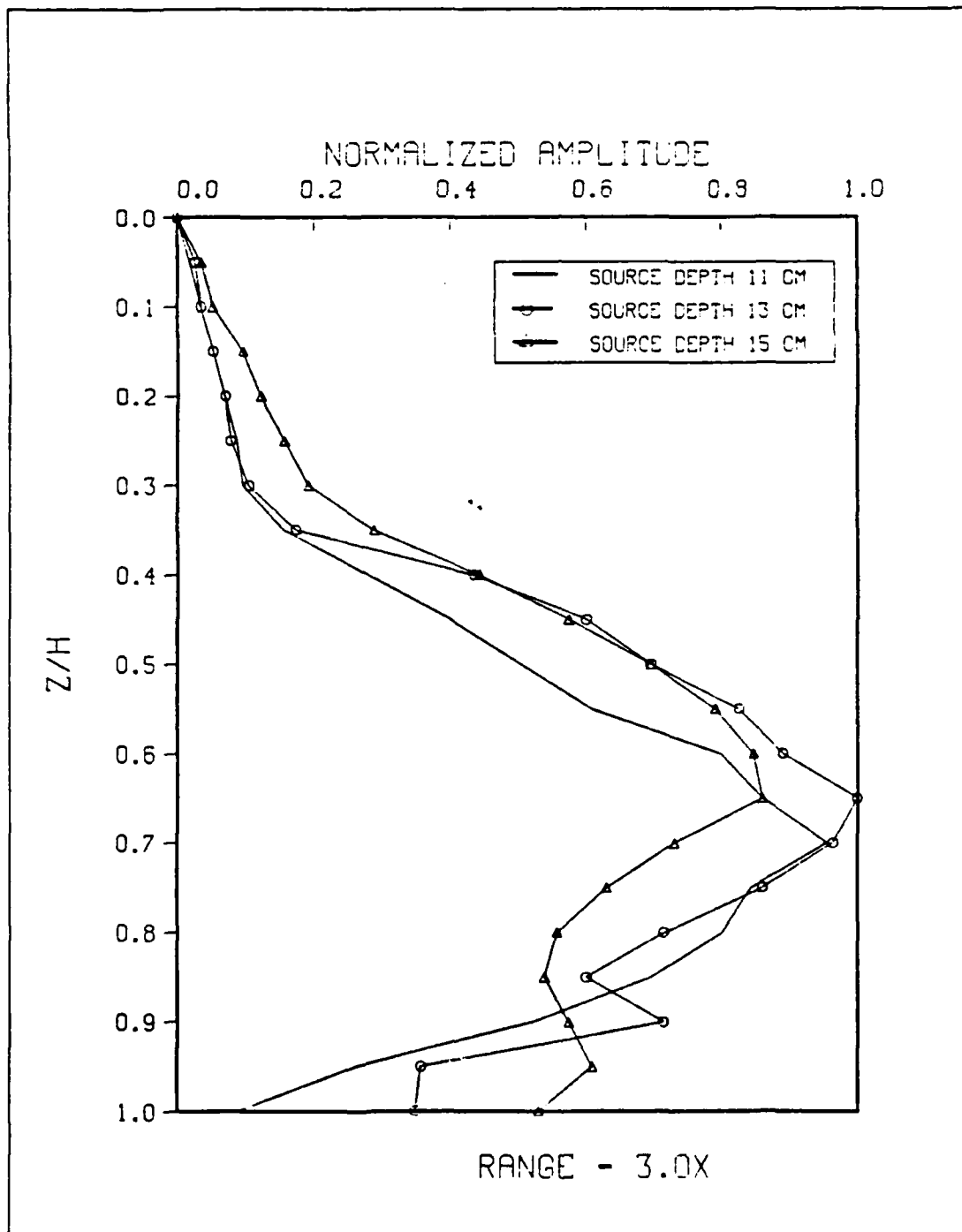


Figure D.3 Measurements with Source Depth of 11, 13, and 15 cm.

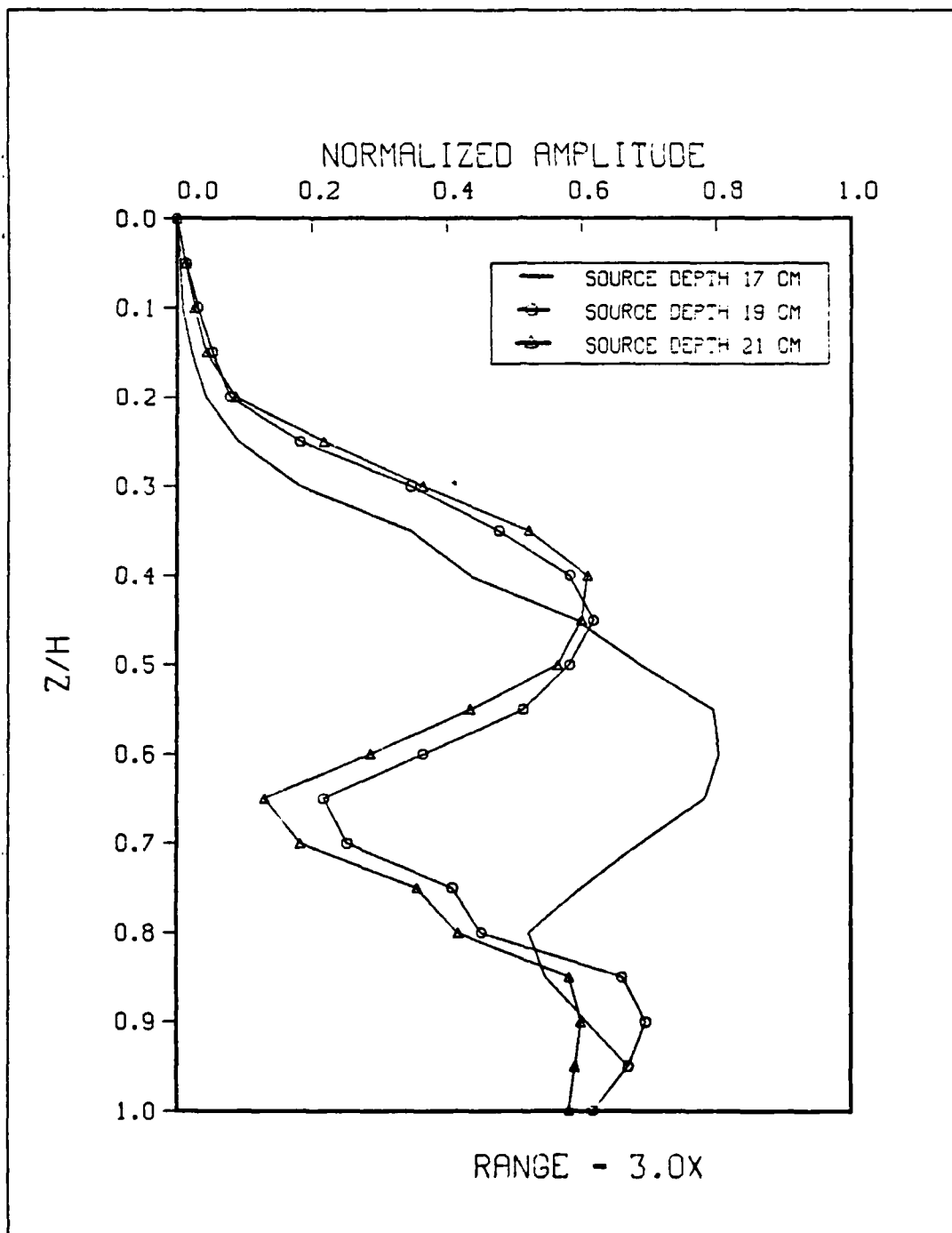


Figure D.4 Measurements with Source Depth of 17, 19, and 21 Cm.

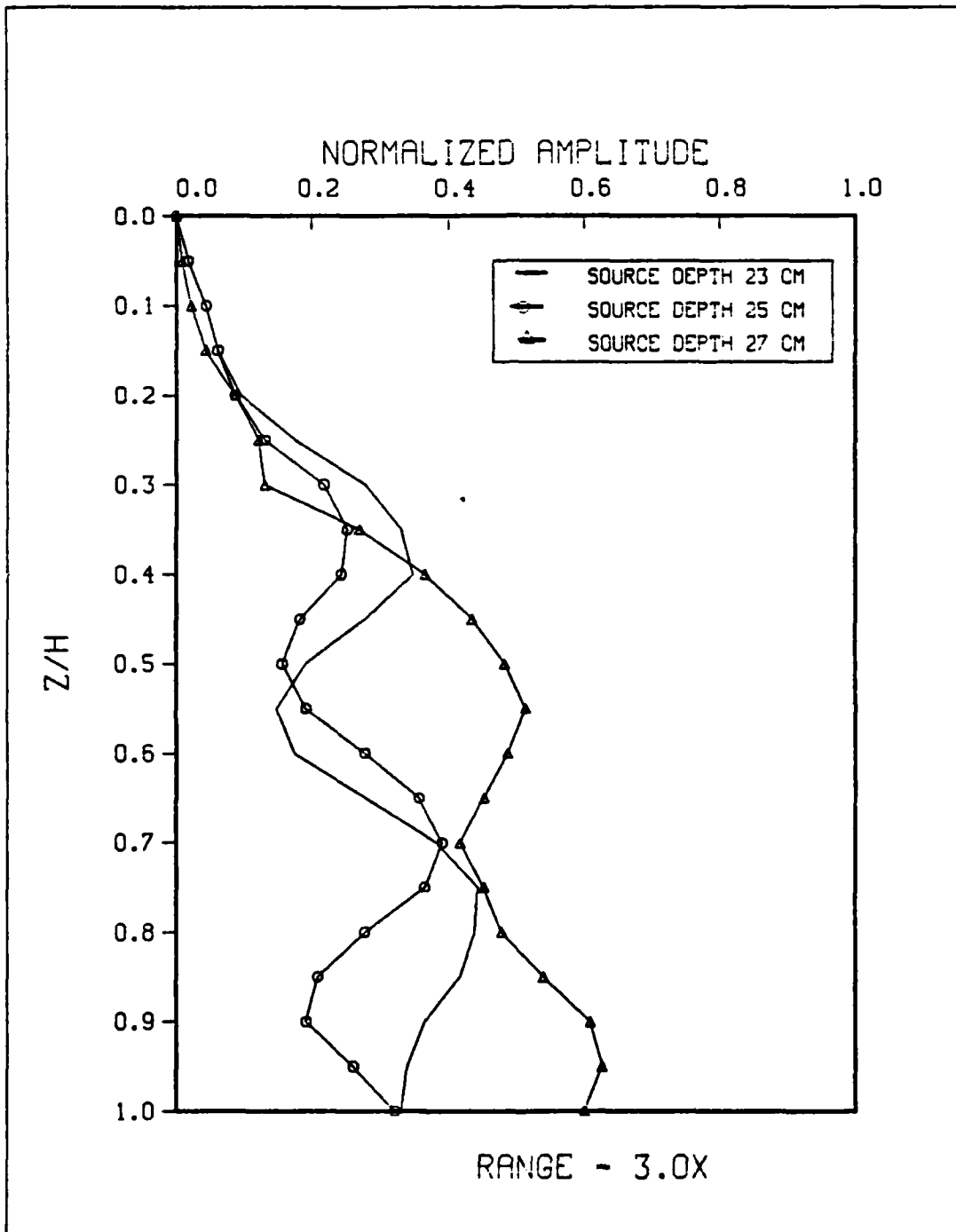


Figure D.5 Measurements with Source Depth of 23, 25, and 27 Cm.

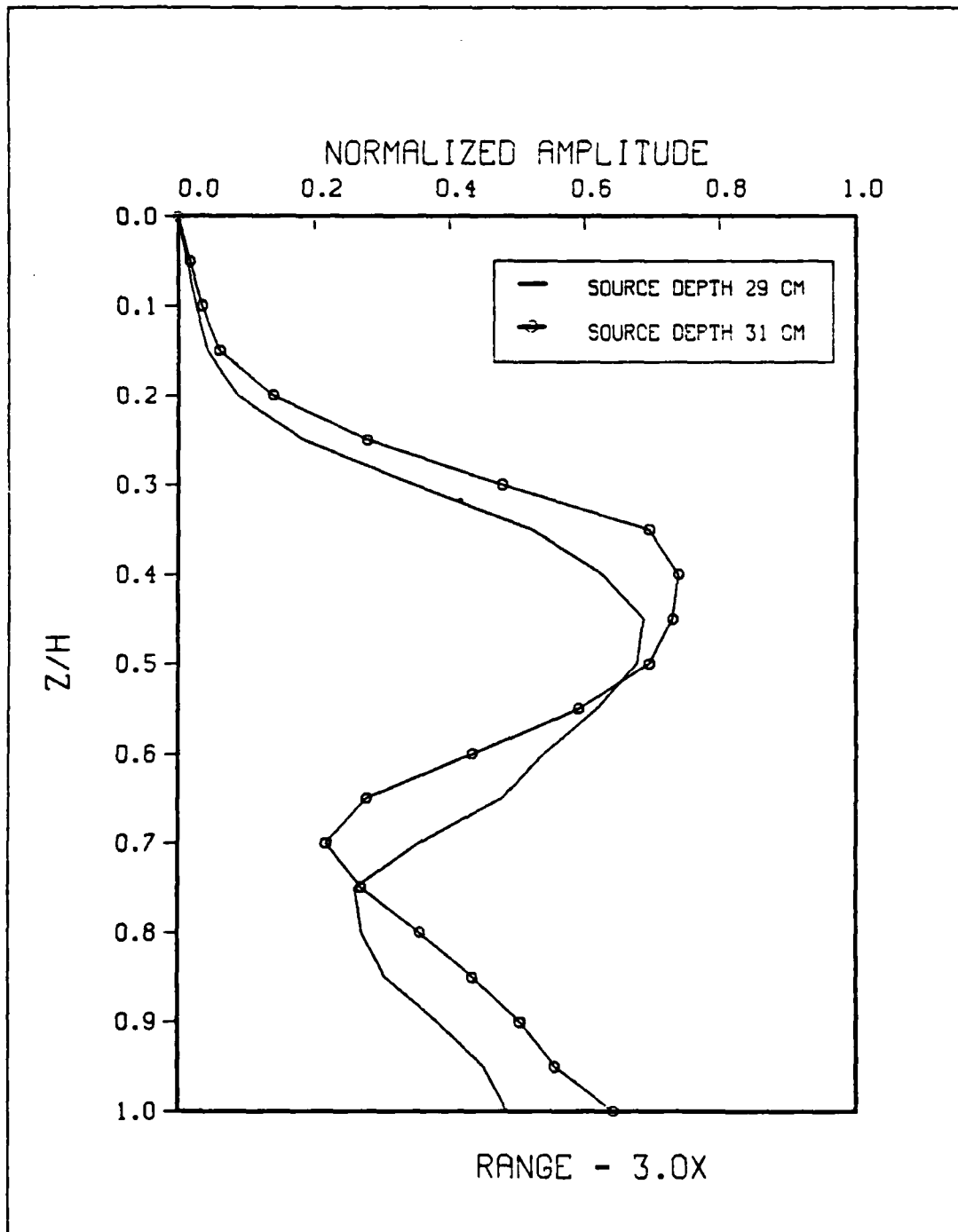


Figure D.6 Measurements with Source Depth of 29 and 31 Cm.

BIBLIOGRAPHY

Anderson, C.L., and Liebermann, R.C., "Sound Velocities In Rocks And Minerals," Physical Acoustics, IV-B, Edited by K.P. Mason, Academic Press, 1968.

Paek, C.K., The Acoustic Pressure In A Wedge-Shaped Water Layer Overlying A Fast Fluid Bottom, Master's Thesis, Naval Postgraduate School, March, 1984.

Eradstow, J.A., Laboratory Study Of Sound Propagation Into A Fast Fluid Medium, Master's Thesis, Naval Postgraduate School, June, 1981.

Erock, H.K., The AESD Parabolic Equation Model, NCEA Technical Note 12, January, 1978.

Coppens, A.E., Humphries, and Sanders, J.V., "Propagation Of Sound Out Of A Fluid Wedge Into An Underlying Fluid Substrate Of Greater Sound Speed", Accepted for Publication by JASA, May 1984.

Coppens, A.E., and Sanders, J.V., "Propagation Of Sound From A Fluid Wedge Into A Fast Bottom," PLENUM, 1980.

Coppens, A.E., Sanders, J.V., Icanou, G.I., and Kawamura, M., Two Computer Programs For The Evaluation Of The Acoustic Pressure Amplitude And Phase At The Bottom Of A Wedge Shaped Fluid Layer Overlying A Fast Fluid Half Space, Naval Postgraduate School Technical Report NPS 81-79-002, December, 1978.

Graves, R.F., Nagel, A., Uberall, H., and Zauer, G.I., "Range Dependent Normal Modes In Underwater Sound Propagation: Application To A Wedge Shaped Ocean," JASA, Vol. 58, December 1975.

Hardin, R.H., and Tarrert, F.D., "Applications Of The Split Step Fourier Method To The Numerical Solution Of Nonlinear And Variable Coefficient Wave Equations," SIAM Review, Vol. 15, 1973.

Jaeger, L.F., A Computer Program For Solving The Parabolic Equation Using An Implicit Finite-Difference Solution Method Incorporating Exact Interface Conditions, Master's Thesis, Naval Postgraduate School, September, 1983.

Jensen, F.E., and Kuperman W.A., Environmental Acoustical Modeling At SACLANTCEN, SACLANTCEN Report SR-34, November, 1979.

Jensen, F.E., and Kuperman, W.A., "Sound Propagation In A Wedge-Shaped Ocean With A Penetrable Bottom," JASA, Vol. 67, May, 1980.

Jensen, F.E., and Krol, H., The Use Of The Parabolic Equation Method In Sound Propagation Modeling, SACLANTCEN Memorandum SM-72, August, 1975.

Kawamura, M., and Icanou, I., Pressure On The Interface Between A Converging Fluid Wedge And A Fast Fluid Bottom, Master's Thesis, Naval Postgraduate School, December, 1978.

Kinsler, L.E., Frey, A.R., Correns, A.B., AND Sanders, J.V., Fundamentals Of Acoustics, Third Edition, John Wiley and Sons, 1982.

Lee, I., and Botseas, G., IFD: An Implicit Finite-Difference Computer Model For Solving The Parabolic Equation, NTSC Technical Report 6659, May, 1982.

Lee, I., Botseas, G., and Papadakis, J.S., "Finite-Difference Solution To The Parabolic Equation," JASA, Vol. 70, September, 1981.

Lee, I., and McDaniel, S.T., "A Finite-Difference Treatment Of Interface Conditions For The Parabolic Equation: The Irregular Interface," JASA, Vol. 73, May, 1983.

Lee, I., and Papadakis, J.S., Numerical Solutions Of Underwater Acoustic Wave Propagation Problems, NTSC Technical Report 5929, February, 1979.

LeSesre, E., Personal Communication, 11 May 1984.

McDaniel, S.T., and Lee, I., "A Finite-Difference Treatment Of Interface Conditions For The Parabolic Equation: The Horizontal Interface," JASA, Vol. 71, April, 1982.

INITIAL DISTRIBUTION LIST

	No. Copies
1. Defense Technical Information Center Cameron Station Alexandria, Virginia 22314	2
2. Library, Code 0142 Naval Postgraduate School Monterey, California 93943	2
3. Commanding Officer ATTN: IT Mark E. Kosnik SWCSCGICOM SWC Dept HD Class 85, CLCVN 1 OCT 84 Newport, Rhode Island 02841	2
4. Superintendent ATTN: Lt. J.V. Sanders, Code 61 Sd Naval Postgraduate School Monterey, California 93943	8
5. Superintendent ATTN: Lt. A.B. Coppens, Code 61 Cz Naval Postgraduate School Monterey, California 93943	2
6. Superintendent ATTN: ICDB C.R. Lunlap, USN (Ret), Code 68 D1 Naval Postgraduate School Monterey, California 93943	3
7. Superintendent ATTN: Lt. C.K. McCoers, Code 68 Mr Chairman, Department of Oceanography Naval Postgraduate School Monterey, California 93943	1
8. Chief of Naval Research ATTN: Lt. Michael McKissick 800 N. Quincy St. Arlington, Va 22217	1
9. Eugene W. Brown NAVCCEANO Code 7300 Fay St. Louis, Ms 39522	1
10. Commanding Officer ATTN: Lt. James Andrews Naval Ocean Research and Development Activity NSTI Station Fay St. Louis, Ms 39522	1
11. Commanding Officer ATTN: Mr. T.N. Lawrence, Code 323 Naval Ocean Research and Development Activity NSTI Station Fay St. Louis, Ms 39522	1

12. Commanding Officer
ATTN: Lt. Robert Gardner
Naval Ocean Research and Development Activity
NSTI Station
Bay St. Louis, Ms 39522

1

END

FILMED

3-85

DTIC